Università
Ca'Foscari
Venezia

Corso di Dottorato di Ricerca in Economia

Ciclo XXXVI

Tesi di Ricerca

Three Essays in Bayesian Financial Econometrics

SSD: ECON-05/A

Coordinatore di Dottorato
Prof. Pietro Dindo

Supervisori
Prof. Roberto Casarin
Prof. Monica Billio

Dottorando
Andrea Trovato
Matricola 956606

L'attività formativa e di ricerca si è svolta in collaborazione con l'impresa Eurizon Capital SGR S.p.A nell'ambito di un percorso di Dottorato innovativo a caratterizzazione intersettoriale.

to ALFI,

to my grandfathers,

to my precious friends Carlo, Eugenio and Angelo,

to brilliant professors and co-authors Roberto Casarin and Davide Raggi,

to Gianni Amisano,

to myself.

Acknowledgements

I owe a debt of gratitude to many people for helping me bring this project to a successful conclusion: teachers, referees, friends and colleagues who provided, without exception, valuable feedback to my work. I would like to express my gratitude to my supervisor, Professor Roberto Casarin, for inspiring me at each step of this journey and to Professor Davide Raggi, patient co-author with Roberto, for precious comments and suggestions. I would like to show my appreciation to my supervisor Professor Monica Billio and to professors Pietro Dindo, Giacomo Pasini and Margherita Gerolimetto for constant advice and useful discussions. I'm grateful to my company, Eurizon Capital Asset Management, in particular to Marco Avoledo, Nicola Doninelli, Silvio Rostagno and Viviana Zicca for supporting me over the entire PhD program. I have a special appreciation for my team manager, Paolo Bernardelli, and the amazing colleagues within the Fixed Income department for valuable advice, suggestions and significant feedbacks. On this, my deep gratitude goes to Maria Luisa Matarrelli, for encouraging and supporting each step of my research. A lovely thought to my old friends Davide, Luca and Paolo for constant support over ups and downs and to PG for keeping the spirit of 'Vallevento' alive through the passage of time. This work is also in memory of my father and of my uncle and friend Piero. My deep and special gratitude goes to Gianni Amisano, for inspiring my research since our first encounter. To conclude, I'm infinitely indebted to my family: Irene, Ludo and Coco, in the order they have come into my life.

Contents

List of Figures

List of Tables

Introduction

Motivation and Contribution

Tactical asset allocation (TAA) plays an important role in investment management. In determining portfolio performance attribution, asset allocation policy is shown to be the dominating factor. Well Fargo Asset Management was considered to be the first to introduce TAA products in the 1970s, with an innovative approach to implement dynamic shifts between stock and bond in a systematic way arising from quantitative tools. Since performance of TAA depends on volatility, managing switches in returns variability and modelling volatility spillovers emerge as fundamental steps for a rewarding dynamic portfolio allocation.

Instead of the traditional max-likelihood procedure, in this work I follow a Bayesian approach to make inference about model parameters. Bayesian inference (e.g., see Zellner, 1971; Robert et al., 1993; Koop, 2003; Robert, 2007) yields great popularity in economic applications since this approach integrates priors about parameters into model estimate. In a Bayesian framework, inference is therefore a learning process based not only on data but also on extra-sample information. The combination of these two sources of inputs is efficient since it accounts for the degree of uncertainty about data and priors. I follow a data-augmentation approach and a Markov Chain Monte Carlo (MCMC) procedure for posterior approximation (e.g., see Hastings, 1970; Carlin and Chib, 1995; Robert and Casella, 2004). I propose a new and efficient Gibbs Sampling algorithm following, for instance, Geman and Geman (1984),

Gelfand and Smith (1990) and Casella and George (1992).

The augmentation and Bayesian inference allow for generating projections of different market scenarios based on a simulation process arising from posterior distributions. In this work I provide an application of this scheme by evaluating the coherence of the portfolio allocation with the predominant macroeconomic regime implied in the market yield curve.

Outline of the Thesis

The following essay includes three original chapters. **Chapter 1** provides an early warning method for tactical asset allocation to deal with volatility clustering and fat-tail distributions of financial returns. The early warning signals are given by a two-state Markov switching model with high-volatility and low-volatility states and time-varying transition probabilities. The transition is driven by exogenous factors namely early-warnings. Using Bayesian inference and Gibbs Sampling for posterior approximation, I apply the model to daily returns of the S&P500 Index sampled from December 2000 up to May 2024. The paper suggests that a measure of the gap between implied volatility (VIX Index) and realised volatility has important leading properties in forecasting switches between volatility regimes. The paper argues that trading strategies need to be calibrated on the predominant volatility state. Therefore, trend-following signals deliver significant gains in low volatility, while short-term reversal strategies yield positive performance in the high volatility regime.

In **Chapter 2**, a data-enriched term-structure model for interest rates is presented following a general term-structure architecture based on non-arbitrage arguments. According to the Vasicek's model, the yield curve is completely driven by the unobserved instantaneous spot rate. Nevertheless, many alternative sources of information can be used to estimate it. Our state-space model includes the traditional Vasicek's measurement equation with the spot rate as a state process and it is augmented with further measurement equations on bonds at different maturities. In order to make the evaluation of the yield curve more reactive

to market events, the model incorporates additional exogenous variables related to monetary policy, equity market volatility and macroeconomic fundamentals, such as inflation and output gap. All the measurement equations are driven by the state process and the augmentation allows for improving estimation of the latent spot rate. We propose a Bayesian framework for model inference based on an efficient posterior approximation procedure. The computational efficiency follows from the linearity of the model, which allows for Kalman filtering and smoothing recursions. The paper presents an innovative and interpretable way to estimate the risk premium as a combination of explicit sources of market risk. The model is applied to the US yield curve sampled at a monthly frequency from December 2000 up to May 2024. The augmentation and Bayesian inference allow for generating projections of the yield curve in line with different market scenarios. Such a simulation provides great support to decisions of tactical asset allocation since it allows for evaluating the coherence of the portfolio allocation with the predominant regime implied in the market yield curve.

Chapter 3 presents a flexible way for modelling volatility spillovers. Popular extensions of heterogeneous autoregressive models have been proposed for describing realized volatility. However, they leave substantial information unmodelled in residuals. This paper proposes a methodology for dynamic modelling and forecasting realized variance vectors based on a Time-Varying Bayesian Markov Switching VAR Model. The approach allows for flexible dependence patterns and investigates spillover effects across volatilities of different asset classes. The application of the model to a global portfolio investing in bonds, equities and currencies provides that spillovers follow a regime-based representation, with state transitions driven by the 3-month US T-Bill rate, whose dynamics is strictly connected to market expectations about future monetary policy decisions. In terms of volatility forecasting, a stationary bootstrap hypothesis testing on equal forecasting accuracy shows that the model in the paper tends to dominate the competing generalised heterogeneous autoregressive approach. Arising from estimated regime-based volatility spillovers, a dynamic trading algorithm on the S&P500 Index is provided.

Bibliography

Carlin, B. P. and Chib, S. (1995). Bayesian Model Choice via Markov Chain Monte Carlo. *Journal of the Royal Statistical Society, Series B*, B(57):473–484.

Casella, G. and George, E. I. (1992). Explaining the Gibbs sampler. *The American Statistician*, 46:167–174.

Gelfand, A. E. and Smith, A. F. M. (1990). Sampling-based approaches to calculating marginal densities. *Journal of the American Statistical Association*, 85:398–409.

Geman, S. and Geman, D. (1984). Stochastic relaxation, Gibbs distributions and the Bayesian restoration of images. *IEEE Transactions on Pattern Analysis and Machine Intelligence*, 6:721–740.

Hastings, W. K. (1970). Monte Carlo sampling methods using Markov chains and their application. *Biometrika*, 57:97–109.

Koop, G. (2003). *Bayesian Econometrics*. J. Wiley, New York.

Robert, C. P. (2007). *The Bayesian Choice*. Springer.

Robert, C. P. and Casella, G. (2004). *Monte Carlo Statistical Methods (Second Edition)*. University of Chicago.

Robert, C. P., Celeux, G., and Dielbold, F. X. (1993). Bayesian estimation of hidden Markov models: A stochastic implementation. *Statistics and Probability Letters*, 16:77–83.

Zellner, A. (1971). *An Introduction to Bayesian Inference in Econometrics*. J. Wiley, New York.

Chapter 1

Markov Switching Early Warning Models for Tactical Asset Allocation

1.1 Introduction

Tactical asset allocation (TAA) plays an important role in investment management. In determining portfolio performance attribution, asset allocation policy is shown to be the dominating factor. Well Fargo Asset Management was considered to be the first to introduce TAA products in the 1970s, with an innovative approach to implement dynamic shifts between stock and bond in a systematic way. In general terms, the concept of TAA refers to active strategies which seek to deliver positive returns by systematic shifts in portfolio composition in response to new occurring market opportunities. Notable contributions on TAA include Philips et al. (1996) and Lee (2000).

Since performance of TAA depends on volatility, managing switches in returns variability represents the first step for a rewarding dynamic portfolio allocation. In this paper, early warning signals on volatility changes are given by a two-state Markov switching model with high and low volatility states and time-varying transition probabilities.

Markov Switching (MS) models were first introduced by Hamilton and a considerable amount of research has been produced on this topic. Notable examples include Hamilton (1989), Turner and Nelson (1989) and the real interest rate model of Garcia and Perron (1996). Other relevant references are Kim (1994), Kim and Nelson (1999), Casella and Wells (2000) and Kim et al. (2008). Applications in finance of MS models have been rising in popularity as they exhibit great success in describing the abrupt changes in the behaviour of returns. Notable contributions on this topic include Guidolin and Timmermann (2006), Bollen et al. (2000) and Ang and Bekaert (2002).

In the Hamilton setup, state transitions are governed by a first-order Markov process with constant transition probabilities. The constant state transition incorporates a severe constrain and can be a restrictive assumption in many applications. Empirical evidence and economical considerations suggest the opportunity to deal with time-varying transition probabilities. Key contributions on this topic include Agudze et al. (2022), Billio et al. (2016), Billio and Casarin (2011), Fillardo (2004), Dielbold and Weinbach (1994) and Amisano and

Fagan (2013).

Following the example of Kim and Nelson (1999) and Abiad (2003), in contrast to the standard approach, in this paper transitions probabilities are modelled as stochastic variables, whose behaviour is driven by exogenous factors. Given their leading properties, these factors work as early-warnings in forecasting switches between volatility regimes. This approach leads to a new way of modelling the behaviour of returns and deviates from the standard regime-based framework employed in much of the literature. A milestone on finite mixture distributions and Markov Switching models is provided by Frühwirth-Schnatter (2006).

The paper argues that a measure of the gap between volatility implied in options prices and realised volatility provides a timely warning signal about the risk of a potential shift from a regime of low volatility and positive average returns into a state of high volatility and negative average returns.

Using Bayesian techniques (Zellner (1971), Robert et al. (1993), Koop (2003), Robert (2007)), I apply the model to the S&P500 Index (US Equity Index) for daily data from December 2000 up to May 2024. Markov Chain Monte Carlo (MCMC) procedures (Hastings (1970), Carlin and Chib (1995), Robert and Casella (2004)) are applied for model inference. Precisely, the Gibbs Sampling algorithm is implemented in order to simulate data from full conditional distributions. This method was introduced for the first time by Geman and Geman (1984), but other examples include Gelfand and Smith (1990) and Casella and George (1992).

Bayesian inference yields a great advantage in financial applications since this approach integrates priors about parameters into model estimate. In this framework, inference is a learning process based not only on data but also on personal beliefs about asset returns. The combination between these two sources of information is efficient, in the sense that it accounts for data variability and degree of uncertainty about priors.

Model estimate delivers interesting results. First of all, the *Low Volatility* regime has, on average, ergodic probabilities close to 70 %, therefore it can be set as the normal state of daily returns. Secondly, the posterior distribution of returns under the *Low Volatility* regime

is centered on a positive expected value, while the opposite is true in the complementary state. This outcome confirms the asymmetric behaviour of volatility as it tends to be higher in declining than in rising markets. Finally, a measure of the gap between implied volatility (VIX Index) and realised volatility has important leading properties about switches between volatility regimes. Precisely, a rising gap between these two measures of risk provides an efficient early-warning indicator about a potential regime shift of returns into the *High Volatility* state.

The structure of the paper is organised as follows. Section 2 introduces the theory behind Markov Switching models, with the extension of the transition matrix to the case of stochastic transition probabilities. Section 3 describes the general framework of Bayesian inference with special focus on the Gibbs Sampler. Section 4 discusses properties of a dataset of daily returns for the S&P500 and provides an application of the model.

1.2 Markov-Switching Models

1.2.1 Switching Intercept and Variance

Let y_t be the daily return on an asset and s_t a latent variable with values in {1,...,M}. Denote with $\mathbf{y}_{1:T} = (y_1, \ldots, y_T)$ and $\mathbf{s}_{1:T} = (s_1, \ldots, s_T)$ the collection over time of returns and latent variables. Following a Markov Switching representation, a convenient univariate model for daily returns can be written as

$$y_t = \mu_{s_t} + \epsilon_t, \epsilon_t \sim N(0, \sigma_{s_t}), \tag{1.1}$$

$$\mu_{s_t} = \sum_{j=1}^{M} \mu_j \mathbb{I}(s_t = j), \tag{1.2}$$

$$\sigma_{s_t} = \sum_{j=1}^{M} \sigma_j \mathbb{I}(s_t = j), \tag{1.3}$$

with $\boldsymbol{\mu}_j = (\mu_{j1}, \ldots, \mu_{jm})$ and $\boldsymbol{\sigma}_j = (\sigma_{j1}, \ldots, \sigma_{jm})$.

1.2.2 Transition Probabilities

Following Hamilton (1994), transition probabilities $p_{ij} = \mathbb{P}(s_t = i|s_{t-1} = j)$ are assumed to be time-invariant and properly collected into the transition matrix P

$$P = \begin{pmatrix} p_{11} & \dots & p_{M1} \\ \vdots & \ddots & \vdots \\ p_{1M} & \dots & p_{MM} \end{pmatrix},$$

where $\sum_{j=1}^{M} p_{ij} = 1 \ \forall i$. I denote with $\mathcal{M}_1$ the constant transition model.

In the contest of Early Warning Markov Switching models (EWMS), transition probabilities are set to change over time as they are modelled as stochastic variables. This extension evaluates the ability of exogenous factors to forecast the attitude of the system to switch from one regime to another.

Time-varying transition probabilities may be governed by a Probit model, with early-warnings collected into the vector $\mathbf{x}_{t-1}^{'}$ such that

$$p_{ij,t} = \Phi(\mathbf{x}_{t-1}^{'}\boldsymbol{\gamma}_{ij}), \tag{1.4}$$

with $\Phi(\cdot)$ denoting the Gaussian CDF function and $\boldsymbol{\gamma}_{ij}$ the vector of unknown parameters to be estimated. On this topic, Kim et al. (2008), Amisano and Fagan (2013) and Billio and Casarin (2011), for instance, present a good reference about Markov regime-switching regression models with endogenous switching. Provided that the general setup arising from equation (1.4) allows $\mathbf{x}_t$ and $\boldsymbol{\gamma}_{ij}$ to be k-dimensional vectors, the application of the paper will be focused on 2-dimensional vectors, given a constant and an early-warning factor in the Probit equation. This setup allows for investigating at individual level the leading properties of endogenous variables in forecasting regime shifts. Despite it might be a bit inefficient in terms of statistical parsimony, the univariate analysis yields important advantages in empirical applications and portfolio strategies, as it provides a more direct interpretation of

the forecasting power of each early-warning under investigation. Given this backdrop, the 2-state transition probabilities of the model in the paper are given by

$$p_{11,t} = \Phi(\gamma_{11} + \gamma_{21} x_{t-1}), \tag{1.5}$$

$$p_{12,t} = 1 - p_{11,t}, \tag{1.6}$$

$$p_{21,t} = \Phi(\gamma_{12} + \gamma_{22} x_{t-1}), \tag{1.7}$$

$$p_{22,t} = 1 - p_{21,t}, \tag{1.8}$$

with the transition matrix P_t as formalised in 1.2.2. I denote with $\mathcal{M}_2$ the time-varying transition model.

1.3 Bayesian Inference

1.3.1 Introduction

Denote with $\mathbf{y} = (y_1, \ldots, y_T)$ and $\mathbf{s} = (s_1, \ldots, s_T)$ the collection of observable and latent variables, respectively. A Bayesian statistical model with latent variable is given by a parametric model $f(\mathbf{y}|\boldsymbol{\theta}, \mathbf{s})$ for the observable variable $\mathbf{y}$, a parametric model $f(\mathbf{s}|\boldsymbol{\theta})$ for the latent variable $\mathbf{s}$ and a prior distribution $\pi(\boldsymbol{\theta})$ on the vector of parameters $\boldsymbol{\theta}$.
Inference is then based on the joint distribution of $\boldsymbol{\theta}$ and $\mathbf{s}$ conditional on $\mathbf{y}$ (data), called posterior distribution and defined by

$$\pi(\boldsymbol{\theta}, \mathbf{s}|\mathbf{y}) = \frac{f(\mathbf{y}|\boldsymbol{\theta}, \mathbf{s}) f(\mathbf{s}|\boldsymbol{\theta}) \pi(\boldsymbol{\theta})}{\int f(\mathbf{y}|\boldsymbol{\theta}, \mathbf{s}) f(\mathbf{s}|\boldsymbol{\theta}) \pi(\boldsymbol{\theta}) d\boldsymbol{\theta}}, \tag{1.9}$$

where $f(\mathbf{y}|\boldsymbol{\theta}, \mathbf{s}) f(\mathbf{s}|\boldsymbol{\theta})$ represents the complete-data likelihood. Since the denominator is not a function of $\boldsymbol{\theta}$, it is common to rewrite the posterior distribution in terms of the following proportionality

$$\pi(\boldsymbol{\theta}, \mathbf{s}|\mathbf{y}) \propto f(\mathbf{y}|\boldsymbol{\theta}, \mathbf{s}) f(\mathbf{s}|\boldsymbol{\theta}) \pi(\boldsymbol{\theta}). \tag{1.10}$$

Considering the model of the paper, unknown parameters can be conveniently collected into the vector $\boldsymbol{\theta} = (\boldsymbol{\theta}_1, \ldots, \boldsymbol{\theta}_M)$, with $\boldsymbol{\theta}_j = (\mu_j, h_j, \boldsymbol{\gamma}_j)$ and $\boldsymbol{\gamma}_j = (\boldsymbol{\gamma}_{1,j}, \ldots, \boldsymbol{\gamma}_{M,j})$ following from the equation (1.4). For computational advantages, in Bayesian inference it is common to deal with the precision $h_j = 1/\sigma_j$ rather than with the volatility of the process σ_j.

1.3.2 Prior Distributions

Prior distributions are set to reflect any information the researcher has before seeing the data. It is common to choose particular classes of priors which are easy to interpret and make computations more efficient. Natural coniugate priors typically have both such advantages. A coniugate prior distribution is one which, when combined with the likelihood, yields a posterior distribution which falls in the same class of distributions. In addition, a natural coniugate prior has the additional property of having the same functional form as the likelihood function. It means that the prior can be interpreted as rising from a fictitious data set from the same process which generated the actual data.

Considering the model of this paper, it is convenient to write the prior distribution for μ and h as $p(\mu,h) = p(\mu|h)p(h)$ and think in terms of a prior for $\mu|h$ and a prior for h. Given the likelihood function of the model, natural coniugate priors will involve a Normal distribution for $\mu|h \sim N(\mu_0, \sigma_0^2)$ and a Gamma distribution for $h \sim Ga(v_0, \delta_0)$. Details on these topics are provided for instance by Koop (2003) and Robert (2007).

In order to calibrate priors, a preliminary analysis over the first five years of data is conducted by estimating a traditional two-state MS model via Expectation and Maximization (EM) algorithm. The MS model of the paper is designed to describe returns of different types of assets, within a potential universe ranging from equity indexes to commodities and currencies. Since these assets tend to exhibit a different profile in terms of expected returns and volatility, the EM algorithm may calibrate a reasonable parameter space, that is a set of points, around which priors can be formulated. This procedure iterates 2 alternative steps between performing an expectation step, which evaluates the log-likelihood given the current

parameter estimate, and a maximization step which computes parameters by maximizing the expected log-lokilihood. The EM algorithm was first introduced by Dempster et al. (1977). Given the parameter space identified by the EM algorithm, qualitative beliefs are finally formulated in order to collect the prior setup as reported in Table 1.1. Priors for μ_i and σ_i are expressed in annualised values.

Table 1.1: *Inputs for the Gamma distribution are calibrated given expectations in terms of low and high volatility close to 15% and to 35%, respectively. These values are commonly used by investors as empirical thresholds to identify bull and bear market regimes. Hyper-parameters for γ_{ij} are set to match unconditional expected transitions p_{11} and p_{22} around 0.975.*

Parameter	Distribution	Hyper-parameters
μ_1	$N(\mu_{01}, \sigma_{01}^2)$	$\mu_{01} = 5\%$, $\sigma_{01}^2 = (3\%)^2$
μ_2	$N(\mu_{02}, \sigma_{02}^2)$	$\mu_{02} = -5\%$, $\sigma_{02}^2 = (3\%)^2$
h_1	$Ga(v_{01}, \delta_{01})$	$v_{01} = 15$, $\delta_{01} = 0.001$
h_2	$Ga(v_{02}, \delta_{02})$	$v_{02} = 15$, $\delta_{02} = 0.01$
γ_{11}	$N(\alpha_{011}, \Theta_{011})$	$\alpha_{011} = 2$, $\Theta_{011} = 3^2$
γ_{21}	$N(\alpha_{021}, \Theta_{021})$	$\alpha_{021} = 0$, $\Theta_{021} = 5^2$
γ_{12}	$N(\alpha_{012}, \Theta_{012})$	$\alpha_{012} = -2$, $\Theta_{012} = 3^2$
γ_{22}	$N(\alpha_{022}, \Theta_{022})$	$\alpha_{022} = 0$, $\Theta_{022} = 5^2$

1.3.3 Posteriors Approximation

The posterior density summarises all the information, so both prior and likelihood based, about the unknown parameters of the model. Precisely, that information will be proportional to the likelihood times the prior density.

In this paper, a Bayesian approach is considered in order to make inference on the vector $\boldsymbol{\theta}$ of the unknown parameters. Since the Bayes estimator of $\boldsymbol{\theta}$ is not available in closed form, MCMC techniques are applied. In particular, the Gibbs Sampling algorithm is implemented as simulation method to approximate joint and marginal posterior distributions by sampling from conditional posterior distributions. This method was introduced for the first time by Geman and Geman (1984); moreover Robert and Casella (2004) provide more details about the history of the Gibbs sampler. The algorithm takes advantage of the hierarchical structure

of the model, i.e. when a Bayesian model can be written as

$$\pi(\boldsymbol{\theta}, \mathbf{s}|\mathbf{y}) = \int \pi_1(\boldsymbol{\theta}, \mathbf{s}|\mathbf{y}, \lambda)\pi_2(\lambda|\mathbf{y})d\lambda. \tag{1.11}$$

The idea is to simulate from the joint distribution $\pi_1(\boldsymbol{\theta}, \mathbf{s}|\mathbf{y}, \lambda)\pi_2(\lambda|\mathbf{y})$ to approximate $\pi(\boldsymbol{\theta}, \mathbf{s}|\mathbf{y})$ as the marginal when all the conditional distributions $\pi_1(\boldsymbol{\theta}|\mathbf{y}, \mathbf{s}, \lambda)$, $\pi_2(\mathbf{s}|\boldsymbol{\theta}, \mathbf{y}, \lambda)$ and $\pi_3(\lambda|\mathbf{y}, \mathbf{s})$ are known and can be simulated (e.g., see Koop, 2003; Robert, 2007).

As an extension of the former procedure, the Gibbs sampling algorithm can be generalised for a joint distribution $\pi(\theta_1, \ldots, \theta_p)$ with full conditionals $\pi_1, \ldots, \pi_p$. Given the vector $(\theta_1^{(m)}, \ldots, \theta_p^{(m)})$ at the iteration m, it simulates:

- $\theta_1^{(m+1)}$ from $\pi_1(\theta_1|\theta_2^{(m)}, \theta_3^{(m)}, \ldots, \theta_p^{(m)})$;
- $\theta_2^{(m+1)}$ from $\pi_2(\theta_2|\theta_1^{(m+1)}, \theta_3^{(m)}, \ldots, \theta_p^{(m)})$;

  $\vdots$

- $\theta_p^{(m+1)}$ from $\pi_p(\theta_p|\theta_1^{(m+1)}, \theta_2^{(m+1)}, \ldots, \theta_{p-1}^{(m+1)})$.

The Gibbs sampler has 2 notable advantages: first, it does not require θ_i to be one-dimensional and, secondly, the choice of the order of the decomposition can be entirely based on simulation reasons.

Inference on equation (1.4) applies data augmentation procedure. On this topic, Albert and Chib (1993) suggested that, by introducing latent data into the problem, a Probit model on binary response is connected to a gaussian linear model on the continuous latent data response. This approach has different advantages. In particular, it allows exact inference on binary regression parameters and the Gibbs sampling algorithm requires simulation mainly from standard distributions. Denote with $U_1, \ldots, U_N$, N independent binary random variables, where U_i follows a Bernoulli distribution with probability of success p_i. Such a probability is related to a set of covariates in the form of $p_i = H(\mathbf{x}_i^T\boldsymbol{\gamma})$, with $i = 1, \ldots, N$, $\boldsymbol{\gamma}$ a k-dimensional vector of unknown parameters and $H()$ a known cdf connecting the probability

p_i to the linear structure $(\mathbf{x}_i^T\boldsymbol{\gamma})$. In the case of Probit model, $H()$ is the standard Gaussian cdf $\Phi(\cdot)$. Denote with $Z_1,\ldots,Z_N$, N independent latent variables with $Z_i \sim N(\mathbf{x}_i^T\boldsymbol{\gamma},1)$ and let $U_i = 1$ if $Z_i > 0$ and $U_i = 0$ otherwise. It can be proved that U_i are independent Bernoulli variables with $p_i = P(U_i = 1) = \Phi(\mathbf{x}_i^T\boldsymbol{\gamma})$. After introducing latent data, the Gibbs sampling can be applied to make inference on the Probit model. Using standard linear model results, the posterior distribution of $\boldsymbol{\gamma}$ given $\boldsymbol{Z}$ is a multivariate normal distribution, therefore $(\boldsymbol{\gamma}|\boldsymbol{U},\boldsymbol{Z}) \sim N(\alpha,\boldsymbol{\Theta})$, while $Z_1,\ldots,Z_N$ are independent with $(Z_i|\gamma) \sim N(\mathbf{x}_i^T\boldsymbol{\gamma},1)$ truncated at the left by 0 if $U_i = 1$ or at the right by 0 if $U_i = 0$. This general data augmentation procedure is now applied to equation (1.4). Let $\boldsymbol{u}_{ij} = (u_{ij,1},\ldots,u_{ij,T})$ be a vector of binary variables with $u_{ij,t} = 1$ if $(s_t = i \cap s_{t-1} = j)$ and $u_{ij,t} = 0$ otherwise; moreover, define the vector $\boldsymbol{z}_{ij} = (z_{ij,1},\ldots,z_{ij,T})$ of independent latent data response variables $z_{ij,1},\ldots,z_{ij,T}$, with $u_{ij,t} = 1$ if $z_{ij,t} > 0$ and $u_{ij,t} = 0$ if $z_{ij,t} < 0$. Therefore, a 5-block Gibbs sampler may be applied to make inference on the model of the paper. Given the starting point $\boldsymbol{\theta}^0 = (\boldsymbol{\mu}^{(0)},\boldsymbol{h}^{(0)},\mathbf{s}^{(0)},\boldsymbol{\gamma}_{ij}^{(0)})$, at the $m-$th iteration the Gibbs sampler draws recursively:

1. the latent state vector $\mathbf{s}$:
   $(\mathbf{s}^{(m)}|\mathbf{y},\boldsymbol{\mu}^{(m-1)},\boldsymbol{h}^{(m-1)},\boldsymbol{P}^{(m-1)}) \sim FFBS$;

2. the latent data response vector $\boldsymbol{z}_{ij}$:
   $(\boldsymbol{z}_{ij,t}^{(m)}|u_{ij,t}^{(m)} = 1,\boldsymbol{\gamma}_{ij}^{(m-1)}) \sim N(\mathbf{x}_{t-1}^{'}\boldsymbol{\gamma}_{ij},1)$ truncated at the left by 0,
   $(\boldsymbol{z}_{ij,t}^{(m)}|u_{ij,t}^{(m)} = 0,\boldsymbol{\gamma}_{ij}^{(m-1)}) \sim N(\mathbf{x}_{t-1}^{'}\boldsymbol{\gamma}_{ij},1)$ truncated at the right by 0;

3. the vector $\boldsymbol{\gamma}_{ij}$:
   $(\boldsymbol{\gamma}_{ij}^{(m)}|\boldsymbol{u}_{ij}^{(m)},\boldsymbol{z}_{ij}^{(m)}) \sim N(\alpha_{ij1},\boldsymbol{\Theta}_{ij1})$;

4. the vector $\boldsymbol{h}$:
   $(\boldsymbol{h}^{(m)}|\mathbf{y},\mathbf{s}^{(m)},\boldsymbol{\mu}^{(m-1)}) \sim Ga(v_1,\delta_1)$,
   $v_1 = v_0 + T, \delta_1 = \delta_0 + \hat{\epsilon}^{'}\hat{\epsilon}$;

5. the vector $\boldsymbol{\mu}$:
   $(\boldsymbol{\mu}^{(m)}|\mathbf{y},\mathbf{s}^{(m)},\boldsymbol{h}^{(m)}) \sim N(\mu_1,\sigma_1^2)$,

$$\sigma_1^2 = (\sigma_0^{-2} + h^{-1}\mathbf{i}'\mathbf{i})^{-1},$$
$$\mu_1 = (\sigma_0^{-2} + h^{-1}\mathbf{i}'\mathbf{i})^{-1}(\sigma_0^{-2}\mu_0 + h^{-1}\mathbf{i}'\mathbf{i}\bar{\mu}).$$

Since the Gibbs sampler works in terms of full conditional distributions, the smoothed state probabilities $Pr(s_t|I_T)$ are computed, as preliminary step before drawing the latent vector $\mathbf{s}$. Precisely, the Forward Filtering Backward Sampling (FFBS) method applies the Hamilton Filter and the Kim-Nelson smoothing algorithm to compute $Pr(s_t|I_T)$ as

$$Pr(s_t = i|I_T) = \sum_{i=1}^{M} Pr(s_t = i, s_{t+1} = j|I_T), \quad t = T, T-1, \ldots, 1, \tag{1.12}$$

where $I_T = \{\mathbf{y}_1, \ldots, \mathbf{y}_T\}$. See Hamilton (1994) and Kim and Nelson (1999) for a detailed account of the procedure.

1.4 Empirical Results

1.4.1 Data Description

Given a daily dataset for the S&P500 Index from December 2000 up to May 2024, a preliminary analysis highlights that daily returns are affected by heteroskedasticity and fat-tailed distribution. In particular, volatility clustering looks evident and significant over the entire sample of data.

In order to investigate this issue more closely, a GJR-GARCH (1,1,1) model is estimated. Notable references for this class of models are Bollerslev (1986) and Glosten et al. (1993). Specifically, the GARCH parameter regarding the volatility leverage effect is positive and statistically significant. This outcome confirms the asymmetric profile of volatility as negative returns tend to push it higher more than positive returns.

1.4.2 Model Estimates

The two-state EWMS model is now applied to a dataset from December 2000 up to May 2024. In this application, a measure of the gap between implied (VIX Index) and realised volatility works in terms of early-warning for regime shifts. Model estimate suggests that such a measure of risk has important leading properties in forecasting switches between volatility regimes. Before converging to this choice in terms of early-warning, an exploratory analysis on other variables has been conducted. For instance, the slope of the yield curve rather than default spreads have been selected as potential candidates, however regime shifts exhibited just a marginal sensitivity to dynamics of these factors. Such a result was not completely a surprise since the yield curve and default spreads were heavily affected by the synchronised zero-rate monetary policy adopted by central banks around the world, in response to permanent recessionary conditions over a decade, since the collapse of the US banking system in 2008 and reinforced by the COVID-19 pandemic. In such a context of extremely low interest rates, the yield curve and default spreads lost their traditional forecasting property about macroeconomic data and market sentiment. Consistently with this backdrop, in the paper I went to select early-warnings with no direct connection to interest rates.

After running the Gibbs Sampler with 100,000 iterations, model estimate is summarised in Table 1.2, with $\hat{\mu}_i$ and $\hat{\sigma}_i$ expressed in annualised values. The 95% credible interval is reported in the last column.

Under a traditional nomenclature, the *State 1* can be conveniently defined as the *Bull Market* regime as returns tend to exhibit low volatility and positive average values. On the other hand, the *State 2* identifies the *Bear Market* regime, with returns moving around a negative mean in a context of high volatility.

Figure 1.1 shows the estimated mixture of normal distributions for daily returns of the S&P500 Index under the two regimes, with μ_i and σ_i given in Table 1.2. In line with the GJR-GARCH (1,1,1) model previously estimated, the chart confirms the tendency of equity market volatility to be higher in declining than in rising markets. In the case of the S&P500,

Table 1.2: *Under the Bull Market Regime, daily returns are normally distributed as* $(y_t|S_t = 1) \sim N(\hat{\mu}_1 = 15.60\%, \hat{\sigma}_1^2 = (11.72\%)^2)$ *with the transition probability* $\hat{p}_{11,t} = \Phi[2.80 - 12.31(\textit{Implied Vol - Realized Vol})]$. *Similarly, under the Bear Market Regime,* $(y_t|S_t = 2) \sim N(\hat{\mu}_2 = -18.90\%, \hat{\sigma}_2^2 = (32.65\%)^2)$ *with the transition probability* $\hat{p}_{21,t} = \Phi[-1.80 + 1.08(\textit{Implied Vol - Realized Vol})]$.

Parameters	Posterior estimate	C. I.
$\hat{\mu}_1$	15.60%	[13.15%, 18.23%]
$\hat{\mu}_2$	-18.90%	[-30.11%, -8.47%]
$\hat{\sigma}_1$	11.72%	[10.08%, 13.05%]
$\hat{\sigma}_2$	32.65%	[30.04%, 34.75%]
$\hat{\gamma}_{11}$	2.80	[2.64%, 3.05%]
$\hat{\gamma}_{21}$	12.31	[8.04%, 16.67%]
$\hat{\gamma}_{12}$	-1.80	[-1.96%, -1.73%]
$\hat{\gamma}_{22}$	1.08	[0.45%, 1.72%]

volatility in the *Bear Market* regime is three times higher than that in the *Bull Market* regime. Moreover, estimated parameters of the Probit model point out that transition probabilities change over time. In particular, $\hat{p}_{11,t}$ provides that a measure of the gap between implied and realised volatility has a huge negative relationship with the likelihood of returns to remain in the *Low Volatility* regime. Precisely, as such a measure of risk moves higher, the probability of returns to remain in the *Low Volatility* regime decreases and, contextually, the risk of a switching into the *Bear Market* state becomes more consistent. In addition, $\hat{p}_{21,t}$ indicates that rising values of the early warning factor produce considerable effects also on the attitude of the market to come back to the *Bull Market* regime when it lies in the state of high volatility. Since the value of $\hat{\gamma}_{12}$ is quite subdued (1.08), a large gap between the two measures of volatility is required to push the transition probability $\hat{p}_{21,t}$ sufficiently higher for a regime shift. This type of condition is achievable in the *Bear Market* regime since implied volatility may rise much more than the realized counterpart when the degree of pessimism across investors reaches extreme values, driving market sentiment to a capitulation before coming back to normality.

Figure 1.2 reports the example of filtered probabilities concerning the *Bear Market* regime since January 2021.

Figure 1.1: *Estimated mixture of normal distributions for daily returns of the S&P500 Index under the Bull and the Bear market regime.*

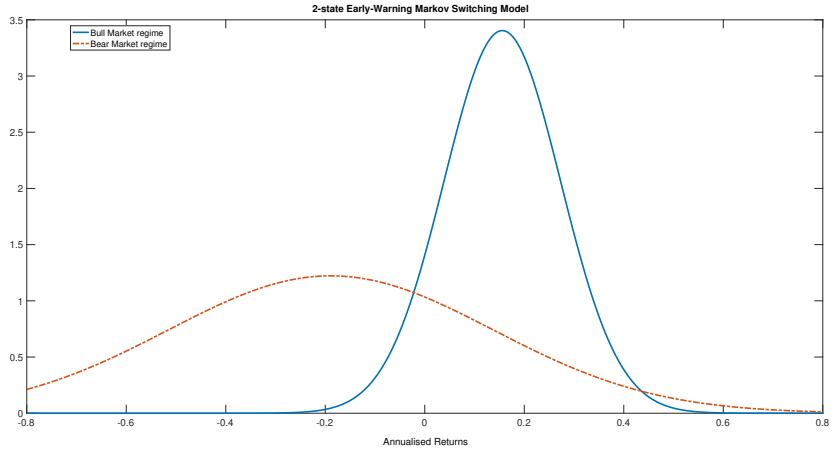

Figure 1.2: *Filtered probabilities of the Bear Market regime* ($S_t = 2$).

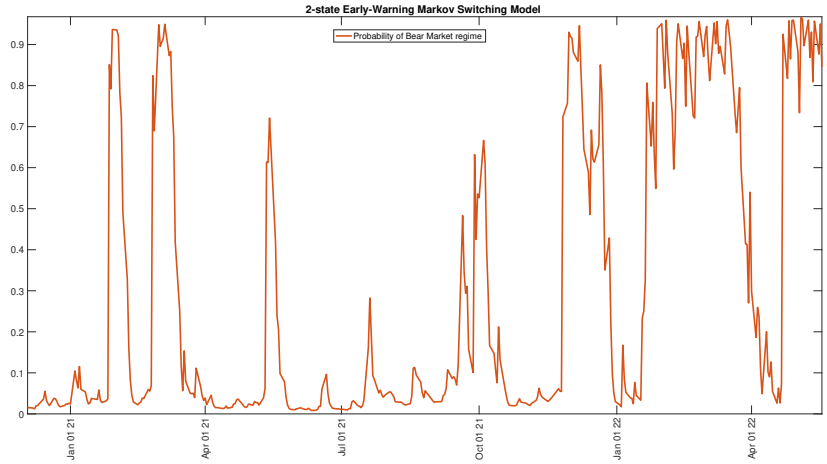

The model of the paper allows for comparing a measure of long-term to short-term volatility. The first one is a function of the ergodic probabilities of the MS process; specifically, given estimate of the time-varying transition matrix at each time t, whose evolution is driven by dynamics of the early-warning factor $\boldsymbol{x}_t$, a measure of long-run volatility is computed by weighting the state-dependent volatilities $\hat{\sigma}_1$ and $\hat{\sigma}_2$ with the dynamic ergodic probabilities given by $\hat{\pi}_{1t} = (1 - \hat{p}_{22,t})/(2 - \hat{p}_{11,t} - \hat{p}_{22,t})$ and $\hat{\pi}_{2t} = (1 - \hat{p}_{11,t})/(2 - \hat{p}_{11,t} - \hat{p}_{22,t})$. On the other hand, the short-term volatility is based on the smoothed probabilities obtained by iterating the Kim-Nelson algorithm. Under this perspective, the long-term volatility may be

interpreted as a proxy of fair value volatility at each time t, while the short-run counterpart should be thought as a measure of returns variability given the most recent market events and data points.

Estimate of $\mathcal{M}_1$ is shown in Table 1.3, with $\hat{\mu}_i$ and $\hat{\sigma}_i$ expressed in annualised values. While

Table 1.3: *Model estimate for* $\mathcal{M}_1$.

Parameters	Posterior estimate
$\hat{\mu}_1$	3.50%
$\hat{\mu}_2$	-6.60%
$\hat{\sigma}_1$	14.50%
$\hat{\sigma}_2$	25.65%
$\hat{p}_{11}$	0.982
$\hat{p}_{22}$	0.972

the regime-specific variances are quite similar across models, the state-specific means are very different between the two specifications. Figure 1.3 might provide a possible explanation behind this result. It compares the two measures of volatility under both model settings, therefore $\mathcal{M}_1$ and $\mathcal{M}_2$, when in 2021 and 2022 the equity market collapsed into a risk-off environment, driven by expectations the FED was to announce the decision of rising interest rates, in response to increasing inflation data. Empirical evidence suggests that FED announcements about changes in the monetary policy stance are not short-lived events, rather they fuel market expectations on inflation dynamics, with great impact on asset pricing. Blue and red dotted lines refer to the long-term volatility for $\mathcal{M}_1$ and $\mathcal{M}_2$, respectively, while the solide lines represent the short-term volatility for the two specifications. According to the picture, the time-varying transition model gains relevant advantages to remark here. First, $\mathcal{M}_2$ allows the short-term volatility to move within a wider range than $\mathcal{M}_1$, with boundaries more in line with empirical evidence and volatility measures deriving from options prices. Second, the more flexible time-varying setup brings the short-term volatility in $\mathcal{M}_2$ to be significantly more reactive than in $\mathcal{M}_1$; such a result is confirmed not only when volatility climbs into the *Bear Market Regime*, but also when it converges to normality (black rectangles for instance). Third, since the time-varying architecture has impact even on the ergodic

Figure 1.3: *Long-term and short-term volatility under* $\mathcal{M}_1$ *and* $\mathcal{M}_2$.

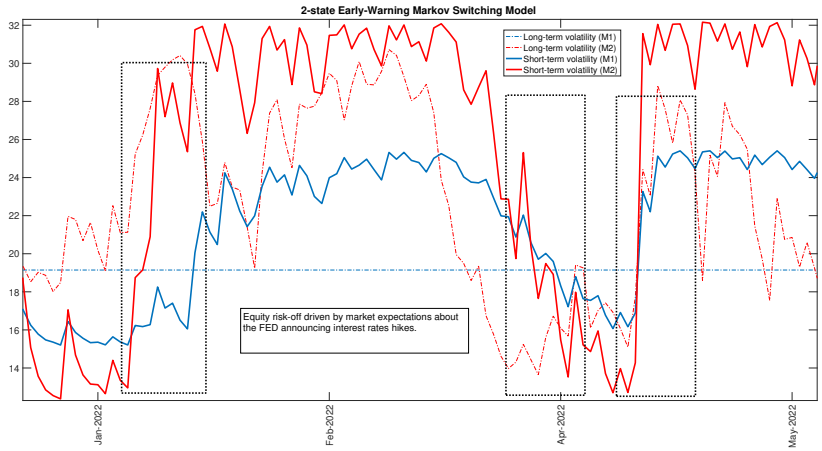

probabilities, among other parameters, the $\mathcal{M}_2$ model delivers a dynamic measure also of the long-term volatility, while it is set to remain constant in $\mathcal{M}_1$, unless model re-estimate. Given this flexibility, $\mathcal{M}_2$ interpreted the market risk-off in 2021 and 2022 in terms of structural change towards the *Bear Market Regime* as the predominant state, with both short-term and long-term volatilities moving higher. This is in contrast to $\mathcal{M}_1$, which estimated that market turmoil as a temporary deviation from the *Bull Market Regime*, given the spike exclusively of the short-term volatility. It follows that the state allocation scheme in $\mathcal{M}_1$ tends to overestimate the duration of the *Bull Market Regime* during periods of negative market returns. This outcome could explain why $\mathcal{M}_1$ estimates a more smoothed difference between the state-specific means, with an higher offsetting volatility for the *Bull Market* state.

Therefore, the gap between long-term and short-term volatility may be relevant even in supporting decisions of asset allocation. A brutal spike in the short-term volatility, in contrast to the long-run counterpart remaining quite stable, may be interpreted as a signal of market overreaction and, therefore, an aggressive tactical trading strategy may be applied. On the other hand, if short-term and long-term volatilities simultaneously move up, a structural change in returns variability appears to be more reasonable than a short-lived overreaction, therefore a defensive portfolio strategy should be recommended here. Given the static estimate of the ergodic probabilities, this allocation scheme can not be applied to $\mathcal{M}_1$, since

spikes of the short-term volatility are generally interpreted as market overreactions. As last step of this model comparison, the (log) marginal likelihood $\log(\Upsilon(\mathbf{Y}|\mathcal{M}_i))$ is finally computed for the two models, with $\log(\Upsilon(\mathbf{Y}|\mathcal{M}_1)) = 2.01e+04$, $\log(\Upsilon(\mathbf{Y}|\mathcal{M}_2)) = 2.08e+04$ and a derived (log) Bayes factor = $\log(\Upsilon(\mathbf{Y}|\mathcal{M}_2))$-$\log(\Upsilon(\mathbf{Y}|\mathcal{M}_1)) \geq 500$. Therefore, also the outcome arising from this exercise puts great emphasis on the incremental value over $\mathcal{M}_1$ introduced by the time-varying transition model $\mathcal{M}_2$.

To conclude, the model doesn't pay special attention to the Covid pandemic; ideally, it is interpreted as a period of high volatility, but a separate regime is not formalised for the event. The notable remark here is that the Covid pandemic wasn't a period of real market turmoil. After an initial short-term risk-off reaction, individual volatilities sharply normalised and risky assets hit new record highs in the following 18 months. This was the result of central banks and governments announcing accommodative and very supportive policies, in response to recessionary conditions potentially arising from the synchronised lockdown imposed by the policy makers around the world.

1.4.3 Tactical Asset Allocation Exercise

Tactical asset allocation (TAA) plays an important role in investment management. In determining portfolio performance attribution, asset allocation policy is shown to be the dominating factor. In general terms, the concept of TAA refers to active strategies which seek to deliver positive returns by systematic shifts in portfolio composition in response to new occurring market opportunities. Notable contributions on TAA include Philips et al. (1996) and Lee (2000).

Different measures may be applied to compare merits of TAA-based models; a first approach is connected to the concept of *Sharpe Ratio* (SR), which measures the risk-adjusted performance of an investment, such as a security or an allocation strategy, compared to a risk-free rate. Specifically, it is defined as the difference between returns of the investment and the risk-free rate, divided by the standard deviation of the investment returns. This ratio ac-

counts for the additional amount of return that an investor receives for an additional unit of risk. Evaluation of the SR generally employs a rolling-window approach, where the ratio is computed over a moving window.

On this topic, there isn't a precise guide about the choice of the length of this window, but a 3-year rolling horizon is generally selected in many empirical applications. Graphical analysis of the rolling SR yields a couple of advantages: first, it investigates the stability of the trading scheme in terms of risk-adjusted returns and, secondly, it evaluates the ability of the strategy to recover from lows after performance drawdowns. Statistical methods may be even applied; thus, for instance, a stochastic bootstrap could be implemented to approximate the SR distribution for hypothesis testing about if TAA results are statistically significant from 0.

A second approach refers to the concept of equity line (EQL), which is a measure of cumulative performance deriving from the implementation of a selected trading rule. In general, an EQL is expressed as investing 100 dollars (or 1 dollar) at the beginning of the evaluation sample and implementing the trading strategy throughout, up to the end of the backtesting period.

In the last part of the section, a daily trading strategy for the US equity market is provided. Precisely, the algorithm calculates the optimal exposure to the S&P500 Index within a range from 0 (neutral stance) to 1 (maximal exposure) by filtering signals on the predominant volatility regime. The TAA exercise is conducted by sequentially re-estimating models with a 3-month frequency.

On this topic, Ang and Bekaert (2004) argue about the importance of implementing a portfolio allocation program which delivers a different composition based on the predominant market regime (bull vs bear market) while Ang and Bekaert (2002) provide a comprehensive framework of asset allocation with regime shifts. Moreira and Muir (2017) present a volatility-timing allocation strategy which increases Sharp ratios over volatility shifts.

First of all, based on the comparison between the two measures of volatility described above,

a first *Buy* signal indicator is defined. More formally, when the short-term volatility moves below its long-run counterpart, a *Buy* trading signal is generated, while a neutral stance is suggested in the opposite case. This first indicator investigates whether the low volatility regime effectively supports a positive allocation in the equity market.

As second step of the exercise, two price-momentum indicators for the S&P500 Index are computed. The first one is obtained as cumulative performance over the last 20 trading days and it works as a proxy of medium-term trend in the path of returns. In particular, it suggests a *Buy* signal when it is positive, otherwise a neutral allocation is implemented. The second indicator is based on the cumulative performance of the last 5 trading days and it provides a measure of mean-reversion of returns towards the medium-term trend. More formally, working as contrarian indicator, it generates a *Buy* trading signal when it assumes negative values, while a *zero-exposure* is recommended in the opposite case. The mean-reversion property delivers important gains under the low-volatility state, since in this environment returns deviate just temporary from their long-run average, therefore they converge to the equilibrium in a relative short period of time. As such, signals from this indicator are implemented only under the low-volatility regime.

Figure 1.4 compares the EQL, therefore the cumulative performance, of the different types of *Buy* signals explained above. In particular, a relevant gap emerges when signals are implemented conditionally on the low rather than on the high-volatility state (blue vs black line). In this last case, indeed, the long-run cumulative performance of the strategy collapses below zero affected by a great amount of volatility. On the other hand, the *Buy* signal implemented in low volatility yields strong and persistent returns over the entire sample. This outcome confirms that volatility is not only a relevant factor for portfolio construction but also a key driver to generate consistent active returns. In addition, the *Buy* signal based on both the medium-term trend and the mean-reversion indicator in low volatility delivers positive performance over the complete backtest (yellow and purple line). Finally, the red line is the result of the global trading signal obtained as a combination of the individual

allocations explained above.

Therefore, results suggest a maximal exposure to the US equity market when all the 3 conditions above are simultaneously verified, that is when returns exhibit a solid positive trend, in combination with a short-term market correction but still in a context of low volatility. Under this perspective, ability of returns to persist in the low volatility regime is crucial for the trading scheme, as it allows to interpret the short-term downtrend as a market overreaction, namely *oversold*, rather than a structural regime shift into a real *Bear Market* state. On the other hand, the model recommends a neutral stance when all the 3 conditions are not satisfied. Finally, intermediate signals are defined depending on the number of holding conditions. For instance, a *Buy* signal of (1/3)-intensity is provided in case of low volatility of returns even though conditions about price momentum don't hold.

Figure 1.4: *Buy signal in low and high volatility states.*

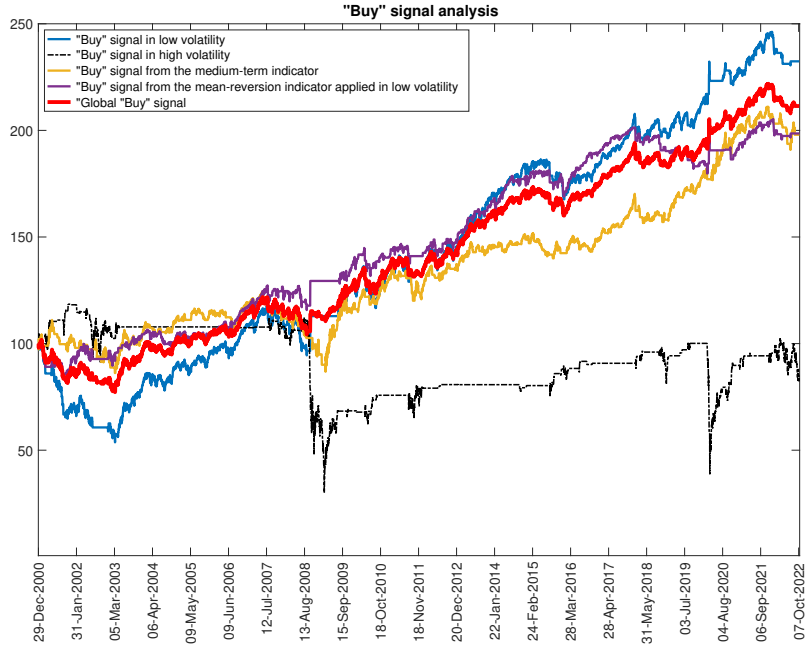

In the last part of the exercise, given the 1-month US T-Bill rate as risk-free rate, a 3-year rolling Sharpe Ratio (SR) is computed, in order to compare the trading scheme of the model with the *Buy&Hold* portfolio. This strategy is as exactly investing 100 dollars in the market at the beginning of the evaluation sample and holding it throughout, up to the end of

Figure 1.5: *3-year rolling Sharpe Ratio (SR).*

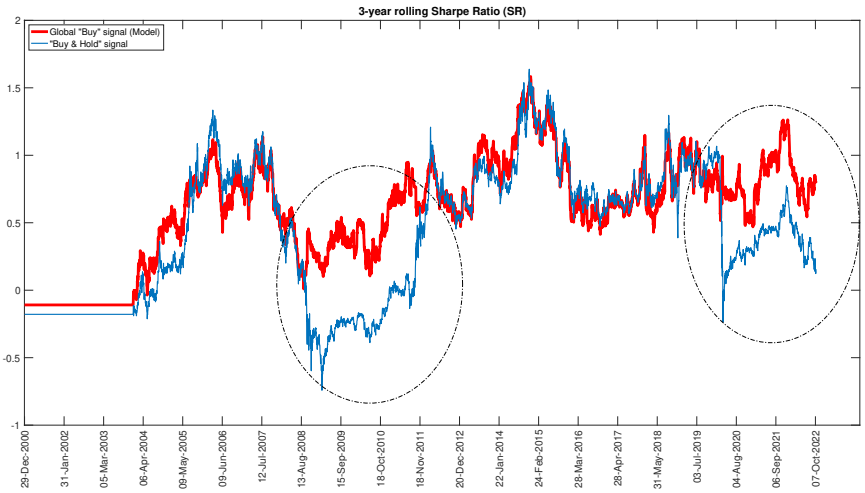

the backtesting period. The *Buy&Hold* portfolio addresses the typical passive allocation scheme of a long-run investor, therefore it is commonly used in empirical applications as a benchmark to evaluate the robustness of tactical asset allocation strategies. Figure 1.5 clearly exhibits that the volatility-filtering exposure to the S&P500 Index provides an efficient control of portfolio drawdowns over the 3 significant risk-off episodes accounted in the backtest (2008-2010, 2021, 2022).

In Figure 1.6, the 95% credible interval for the rolling SR is reported. The chart investigates the ability of the trading strategy to preserve its value over time. Lower and upper bounds of the interval are computed by implementing the strategy at each iteration of the Gibbs sampling. The lower bound moves just marginally below zero only in the occasion of the collapse of the US banking system in September 2008. But since that episode, the overall interval lies definitely in positive territory, even after the market correction generated by the tightening monetary policy announced by the FED in 2021 and 2022.

For a comparison between $\mathcal{M}_1$ and $\mathcal{M}_2$ in terms of risk-adjusted performance, the trading strategy is now applied to the case of MS model with constant transitions ($\mathcal{M}_1$). In Figure 1.7, the 3-year rolling SR is shown for the two alternatives. First of all, $\mathcal{M}_2$ looks globally superior than $\mathcal{M}_1$, as the relative SR is consistently higher over the entire backtesting period. But most importantly, the MS model with time-varying transition probabilities ($\mathcal{M}_2$) deliv-

ers stronger risk-adjusted returns also in the episodes of market risk-off like, for instance, the crush of the US banking system in 2008-2010 or, more recently, when the FED announced the decision of rising aggressively the Fed Funds rates to moderate spiking inflation data.

Figure 1.6: *3-year rolling Sharpe Ratio (SR) with the 95% credible interval.*

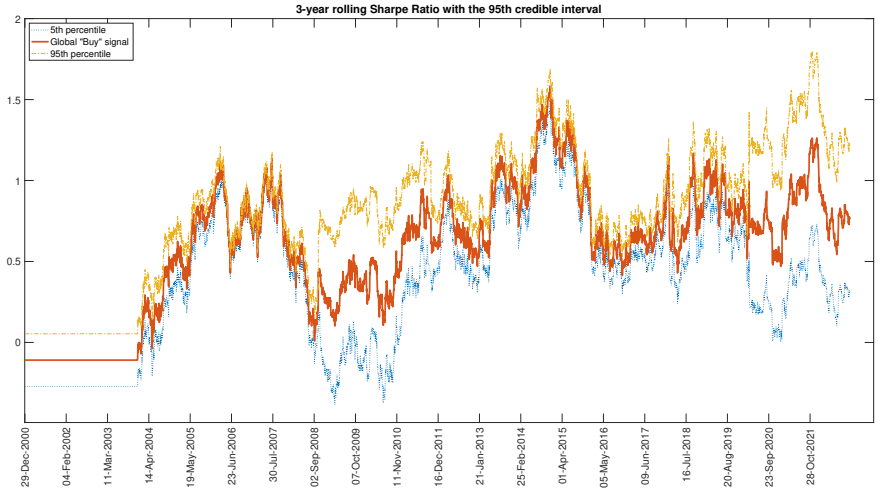

Figure 1.7: *3-year rolling Sharpe Ratio (SR) for $\mathcal{M}_1$ and $\mathcal{M}_2$.*

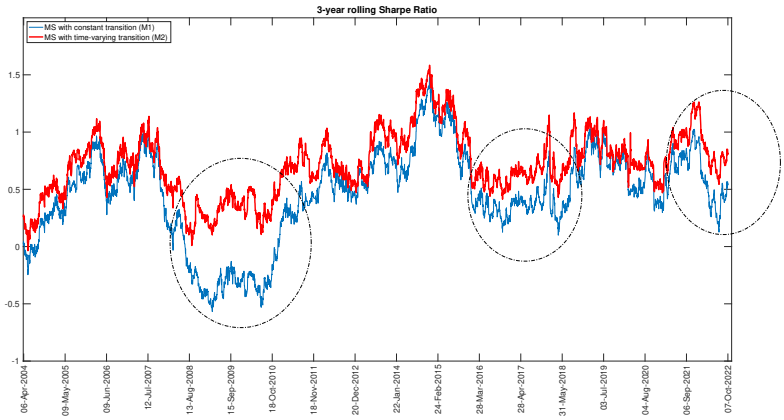

In both occasions, the time-varying setup exhibits a greater ability in switching faster to the high volatility regime, with a timely reduction of the exposure to the US equity market. Following Moreira and Muir (2017), a final comparison between the two competing models is provided in terms of cumulative performance. Precisely, the out of sample exercise in Figure 1.8 shows what would happen if an agent had invested 100 dollars at the beginning of 2004 and then acted following the volatility filtering scheme proposed in the paper under the both

settings in $\mathcal{M}_1$ and $\mathcal{M}_2$. Cumulative returns (equity line) of the time-varying transition model yields a great advantage over the constant transition framework, with an incremental cumulative performance higher than 25% since January 2004.

Figure 1.8: *Model comparison: Equity line since Jan 2004.*

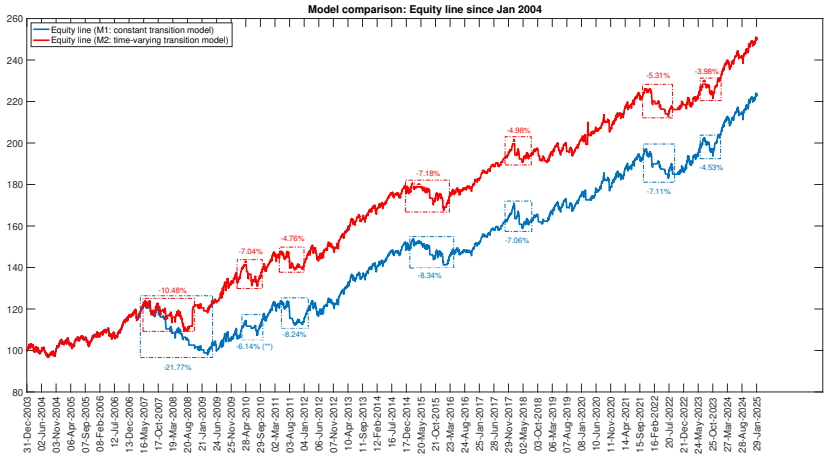

Figure 1.9: *Model comparison: 3-year rolling average returns.*

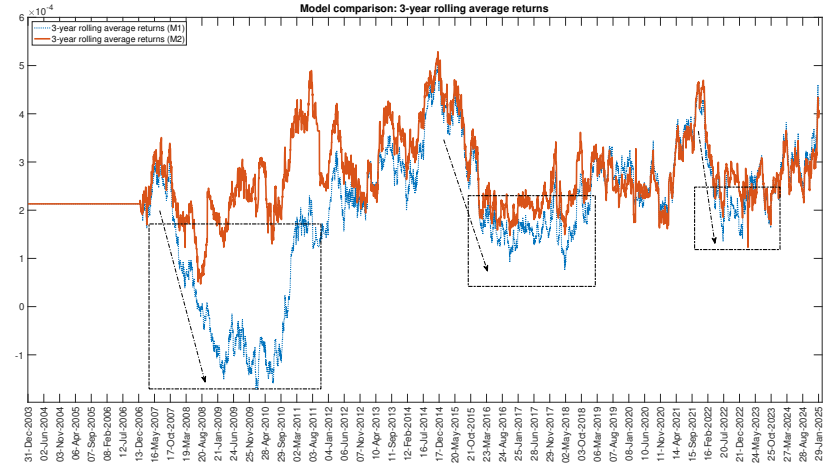

As highlighted by the blue and red dotted rectangles, the most relevant outcome of this comparison is given by the evidence that the time-varying transition setup provides a more efficient mechanism than $\mathcal{M}_1$ in mitigating portfolio drawdowns; according to the figure, this is true not only during the crash of the US banking system in 2008, but also, with high degree of generality, over the other episodes of market selloff. Finally, Figure 1.9 compares

the two models in terms of 3-year rolling average returns. Also under this perspective, the time-varying transition model seems more robust than the competing constant version; in particular, as emphasised by the black dotted rectangles, the volatility filtering scheme in $\mathcal{M}_2$ looks more efficient and reactive than that in $\mathcal{M}_1$ in controlling portfolio drawdowns during periods of market selloff.

1.5 Conclusion

Markov Switching (MS) models were first introduced by Hamilton and a considerable amount of research has been produced on this topic. Applications in finance of MS models have been rising in popularity as they exhibit great success in describing the abrupt changes in the behaviour of returns.

In the Hamilton setup, state transitions are governed by a first-order Markov process with constant transition probabilities. The constant state transition incorporates a severe constrain and can be a restrictive assumption in many applications. Empirical evidence and economical considerations suggest the opportunity to deal with time-varying transition probabilities.

Deviating from the standard setting, in the paper transitions probabilities are modelled as stochastic variables driven by relevant exogenous factors. Given their leading properties, these factors work as early-warnings in forecasting switches between volatility regimes.

Precisely, the paper argues that a measure of the gap between volatility implied in options prices and realised volatility provides a timely warning signal about the risk of a potential shift from a regime of low volatility and positive average returns (bull market) into a state of high volatility and negative average returns (bear market).

The model is applied to the S&P500 Index as it is investigated as a proxy of global equity market. The paper argues that a *Buy* signal in low volatility yields strong and persistent returns over the entire sample. This outcome confirms that volatility is not only a relevant factor for portfolio construction but also a key driver to generate consistent active returns. In addition, trading strategies deliver significant improvements in terms of SR and portfolio drawdowns if signals are calibrated following a volatility-filtering scheme.

To conclude, the exercise investigates the potential added value of a Markov switching model with time-varying transition probabilities with respect to the traditional version with constant transitions. By applying the same trading strategy to both alternatives, the paper shows that the time-varying setup yields consistently a greater advantage in terms of Sharpe

Ratio over the entire backtesting period and, most importantly, it offers a timely portfolio hedging in case of collapse of the market into a bearish scenario.

Bibliography

Abiad, A. G. (2003). Early Warning systems: a survey and a regime-switching approach. *IMF Working Paper*, 3(32).

Agudze, K. M., Billio, M., Casarin, R., and Ravazzolo, F. (2022). Markov switching panel with endogenous synchronization effects. *Journal of Econometrics*, 230:281–298.

Albert, J. and Chib, S. (1993). Bayesian analysis of binary and polychotomous response data. *Journal of the American Statistical Association*, 88:669–679.

Amisano, G. and Fagan, G. (2013). Money growth and inflation: A regime switching approach. *Journal of International Money and Finance*, 33(C):118–145.

Ang, A. and Bekaert, G. (2002). International asset allocation with regime shifts. *Review of Financial Studies*, 15:1137–1187.

Ang, A. and Bekaert, G. (2004). How regimes affect asset allocation. *Financial Analysts Journal*, 60:86–99.

Billio, M. and Casarin, R. (2011). Beta Autoregressive Transition Markov Switching Models for Business Cycle Analysis. *Studies in Nonlinear Dynamics and Econometrics*, 15(4):1–32.

Billio, M., Casarin, R., Ravazzolo, F., and van Dijk, H. (2016). Interconnections between Eurozone and US booms and busts using a Bayesian Panel Markov-switching VAR model. *Journal of Applied Econometrics*, 7(31):1352–1370.

Bollen, N. P. B., Gray, S. F., and Whaley, R. E. (2000). Regime switching in foreign exchange rates: evidence from currency option prices. *Journal of Econometrics*, 94:239–276.

Bollerslev, T. (1986). Generalized Autoregressive Conditional Heteroskedasticity. *Journal of Econometrics*, 31:307–327.

Carlin, B. P. and Chib, S. (1995). Bayesian Model Choice via Markov Chain Monte Carlo. *Journal of the Royal Statistical Society, Series B*, B(57):473–484.

Casella, G. and George, E. I. (1992). Explaining the Gibbs sampler. *The American Statistician*, 46:167–174.

Casella, G., R. C. P. and Wells, M. T. (2000). Mixture models, latent variables and partitioned importance sampling. *CREST, INSEE*, 15.

Dempster, A. P., Laird, N. M., and Rubin, D. B. (1977). Maximum Likelihood from Incomplete Data via the EM Algorithm. *Journal of the Royal Statistical Society, Series B*, 39:1–38.

Dielbold, F. X, L. J. H. and Weinbach, G. (1994). *Nonstationary Time Series Analysis and Cointegration*. Oxford University Press.

Fillardo, A. J. (2004). *Businnes Cycle Phases and Their Transitions*. Springer-Verlag, New Yorks.

Frühwirth-Schnatter, S. (2006). *Finite mixture and Markov switching models*. Springer Science & Business Media.

Garcia, R. and Perron, P. (1996). An Analysis of the Real Interest Rate under Regime Shifts. *The Review of Economics and Statistics*, 1(78):111–125.

Gelfand, A. E. and Smith, A. F. M. (1990). Sampling-based approaches to calculating marginal densities. *Journal of the American Statistical Association*, 85:398–409.

Geman, S. and Geman, D. (1984). Stochastic relaxation, Gibbs distributions and the Bayesian restoration of images. *IEEE Transactions on Pattern Analysis and Machine Intelligence*, 6:721–740.

Glosten, L. R., Jagannathan, R., and Runkle, D. E. (1993). On the Relation between Expected Value and the Nominal Excess Return on Stocks. *Journal of Finance*, 48:1779–1801.

Guidolin, M. and Timmermann, A. (2006). An econometric model for nonlinear dynamics

in the joint distribution of stock and bond retunrs. *Journal of Applied Econometrics*, 21:1–22.

Hamilton, J. D. (1989). A New Approach to the Economic Analysis of Nonstationarity Time Series and the Business. *Econometrica*, 57:357–384.

Hamilton, J. D. (1994). *Time Series Analysis*. Princeton University Press.

Hastings, W. K. (1970). Monte Carlo sampling methods using Markov chains and their application. *Biometrika*, 57:97–109.

Kim, C.-J. (1994). Dynamic Linear Models with Markov-switching. *Journal of Econometrics*, 60:1–22.

Kim, C. J. and Nelson, C. R. (1999). *State-Space Models with Regime Switching: Classical and Gibbs-Sampling Approaches with Application*. MIT Press: Cambridge MA.

Kim, C.-J., Piger, J., and Startz, R. (2008). Estimation of Markov regime-switching regression model with endogenous switching. *Journal of Econometrics*, 2(143):263–273.

Koop, G. (2003). *Bayesian Econometrics*. J. Wiley, New York.

Lee, W. (2000). *Advanced Theory and Methodology of Tactical Asset Allocation*. Wiley.

Moreira, A. and Muir, T. (2017). Volatility-managed portfolios. *The Journal of Finance*, 72:1611–1644.

Philips, T. K., R, G., and Capaldi, R. E. (1996). Tactical Asset Allocation: 1977-1994. *Journal of Portfolio Management*, 23(1):57–64.

Robert, C. P. (2007). *The Bayesian Choice*. Springer.

Robert, C. P. and Casella, G. (2004). *Monte Carlo Statistical Methods (Second Edition)*. University of Chicago.

Robert, C. P., Celeux, G., and Dielbold, F. X. (1993). Bayesian estimation of hidden Markov models: A stochastic implementation. *Statistics and Probability Letters*, 16:77–83.

Turner, C. M., S. R. and Nelson, C. R. (1989). A Markov model of heteroskedasticity, risk and learning in the stock market. *Journal of Financial Economics*, 1(25):3–22.

Zellner, A. (1971). *An Introduction to Bayesian Inference in Econometrics*. J. Wiley, New York.

Chapter 2

A Data-Rich Yield Curve Factor Model [1]

[1] In collaboration with Roberto Casarin and Davide Raggi.

2.1 Introduction

The term structure of interest rates describes the relationship between the yield on a default-free debt security and its maturity. Given the high correlation among bond yields of different maturities, many models use a small number of factors to explain this dependence. The typical econometric approach specifies first a model for short-term interest rates. Then it employs the expectation hypothesis to derive a structural time series model for bond yields over different maturities. Notable contributions to this approach include Hamilton (1987) and Hall et al. (1992).

As different modelling approach, the no-arbitrage assumption is central to a growing literature which assumes that movements in the yield curve can be captured within a no-arbitrage framework, where yields are a linear function of a few unobserved latent factors. Notable contributions on this topic are provided, for instance, by Duffie and Kan (1996), Litterman (1986), Dai and Singleton (2000) and Rudebusch and Wu (2008). The pioneering approach introduced by Vasicek (1977) and Dothan (1978) derives the entire yield curve from the unobserved instantaneous rate r_t. No-arbitrage arguments are then applied to derive a pricing formula for bond yields of different maturities. In this framework the short-term rate works in terms of interconnection between finance and macro-economic perspective. First of all, the short-term rate is a fundamental building block for rates of longer maturities as long yields are formalised in terms of risk-adjusted averages of expected future short-term rates. On the other hand, under the macro-perspective, the short-term rate is the tool under the direct control of central banks, which adjust this rate in order to achieve goals of monetary policy given a sustainable balance between economic growth and inflation expectations.

In the original paper, Vasicek derives the partial differential equation for bond prices and a closed form solution of the pricing problem is provided for the specific case where the latent instantaneous rate follows the stationary Ornstein-Uhlenbeck process. In this setup, since the entire term structure depends on the latent variable r_t, a state-space model for the term structure can be formalised. Under this setting, the stationary Ornstein-Uhlenbeck process

of r_t is the state equation, while yields represent a system of measurement equations. The Kalman Filter is applied to approximate the conditional mean and variance of the system and to evaluate the likelihood. Kim and Nelson (1999) and Commandeur and Koopman (2007) provide a general description of the Kalman Filter and new contributions on state-space models. Given this panel-based representation, the measurement of errors refers to bonds of different maturities.

In the term structure literature, a first attempt to use the Kalman filter for model inference is due to Duan and Simonato (1999); they propose a state-space formulation of the term structure based on a linear Kalman Filter on many yields at different maturities. In the paper, they estimate both the Gaussian and the non-Gaussian case, exploiting the quasi-maximum likelihood principle.

To link the term structure dynamics to macroeconomic fundamentals and eventually expectations, Hördahl et al. (2006), Piazzesi and Swanson (2008) and Rudebusch and Wu (2008) propose an affine term structure dynamic model integrated with macroeconomic variables. Specifically, they assume a multi-factor latent structure which, from a practical perspective, ends up with a model with an enriched set of measurement equations representing mostly inflation and output gap. Rudebusch and Wu (2008), for instance, provide an explicit link of latent factors with the perceived inflation target and cyclical shocks of inflation and output gap.

Frühwirth-Schnatter and Geyer (1998), Duffee (2002), Duffee and Stanton (2012) and Lamoureux and Witte (2002) show that all the variation in the term structure can be explained by the first three principal components, namely the level, slope and curvature of the yield curve, indicating the need for a three-latent factor model. However, the centre of their attention is on demonstrating the feasibility of some particular computational techniques. Rudebusch and Wu (2008) propose a term structure representation based only on two factors, that is the level and the slope. They provide a triangular VAR setup for the latent factors. However, the slope appears to have a negligible impact on the state representation, as residuals of the

relative state equation exhibit a very persistent autocorrelation. Thus, the level remains the predominant factor in their latent structure. Also Kim and Wright (2005) underline that some misspecification problems may occur in the traditional three-factor setup, therefore they suggest a more flexible approach about the number of latent factors. As such, following the approach suggested by Jones (1998), Dai and Singleton (2000) and Polson et al. (2002), the paper written by Sanford and Martin (2005) describes a Bayesian simulation-based method for estimating a single-factor term structure model with the discrete observations on yields augmented by additional high-frequency latent data.

In our paper, we deviate from the previous macro-finance literature by focusing mostly on variables linked to financial markets. Instead of proposing a new equilibrium model, we aim at building a flexible tool that might be used to support decisions of tactical asset allocation. To make the estimate of the yield curve more reactive to market events, we move away from standard models by adding a broader range of variables to model specification. First, we consider the Overnight Index Swap (OIS) rates paid in one year and in three months as a proxy of market expectations about monetary policy decisions. Second, we consider a measure of realized volatility as a link between market sentiment and interest rates. Finally, the Taylor rule is added to connect the yield curve to the macroeconomic activity.

An OIS contract is an over-the-counter trade derivative in which two agents exchange fixed and floating interest rate payments. The floating interest rate is the overnight interbank rate, a measure of the monetary policy stance. In our paper, the term premium implied in OIS rates is proposed as a reasonable proxy of market expectations about the potential path of the FED funds rates. The second factor provides a link between market sentiment and interest rates. As argued in Campbell and Ammer (1993), for instance, high levels of risk-aversion put great pressure on interest rates as investors increase their allocation into defensive assets for hedging their portfolio. Since our model is estimated on monthly data, such a risk factor is extracted in terms of realized volatility from daily returns over a monthly horizon. Finally, as short-term rates are related to macroeconomic fundamentals, the Taylor

rule is introduced as an additional component of the system. This rule allows for reconciling the definition of the instantaneous rate with the potential deviation of inflation and real growth from the relative long-term target. The paper proposes to link the term structure to macroeconomic fundamentals by setting the instantaneous rate r_t equal to the equilibrium nominal rate in the formulation of the Taylor rule.

Following from a general framework based on non-arbitrage arguments, we propose a state-space term structure model which includes the spot rate as a state process and where the measurement equation accounts for yields at different maturities. Instead of focusing on the state process, we deviate from the standard framework by incorporating through data-augmentation additional exogenous variables into the measurement component of the system, where all the measurement equations are driven by the state process and the augmentation allows for improving the estimate of latent spot rate. We apply data-augmentation to connect the diffusive dynamics of r_t to three additional observable factors which approximate explicit sources of market risk: monetary policy decisions, risk-on/risk-off of the equity market and macroeconomic shocks. A new way to estimate the parameter λ, namely the risk premium, is also provided. Instead of looking at λ as an unknown parameter to be estimated, the paper suggests an explicit link between this parameter and well-identified sources of market premium. Such a way of working allows for going ahead of some controversial results achieved within the max-likelihood framework. As highlighted, for instance, by Duan and Simonato (1999), traditional inference may estimate values of λ close to zero or even negative. This outcome is in contrast with the asset pricing theory (see Bekaert et al. (1989), Campbell and Ammer (1993) and Lettau and Watcher (2011)), which supports positive values of λ since it should incorporate a compensation for additional units of risk on holding bonds over the risk-free rate. Thus, in contrast to what suggested in literature, for instance, by Sanford and Martin (2005), we apply data-augmentation on the observable equation instead of the state equation. This new way of working gains relevant advantages when the model is applied for asset allocation purposes. Making the instantaneous rate r_t partially observable yields a

more direct interpretation of the latent factor.

Instead of the traditional max-likelihood procedure, in our paper we follow a Bayesian approach for model inference. By stressing parameters over their credible values, we generate projections of the yield curve consistently with 4 macroeconomic regimes, namely *Expansion*, *Persistent Inflation and Stable Growth*, *Normalising Inflation and Slowdown* and *Recession*. They represent a typical decomposition of the economic cycle, with the economy switching from expansion to recession through shocks in inflation and output gap and connected changes in market sentiment. Given a likelihood-ratio approach, the model finally estimates the probability of each scenario implied in the market yield curve. This type of analysis is of great importance to support investment decisions as it allows to evaluate the coherence of the portfolio allocation with the predominant macroeconomic regime.

We apply the model to the US yield curve sampled at monthly frequency from December 2000 up to May 2024. Implied regime probabilities show interesting and surprising results, for instance, at the end of September 2023. Although world central banks had been implementing aggressive monetary policies since mid 2021, in response to rising inflation data, market rates moved somewhat closely to the yield curve implied by the *Expansion* rather than by the *Persistent Inflation and Stable Growth* regime. That comes as a huge surprise since, in general, hawkish monetary policies tend to push the real economy into a more realistic recessionary environment. From asset allocation perspective, a picture like this one is expected to activate an updating process of the investment choices in favour of a less defensive portfolio, until probabilities of more pessimistic regimes move towards warning values.

Bayesian inference (e.g., see Zellner, 1971; Robert et al., 1993; Koop, 2003; Robert, 2007) yields a great advantage in economic applications as it allows for introducing priors about parameters into the model estimating process. In this framework, inference is a learning process based not only on data but also on extra-sample information. The combination of these two sources of information is efficient because it accounts for data variability and degree of uncertainty about priors. Notable contributions on Bayesian inference for the term struc-

ture are provided, for instance, by Jones (1998), Dai and Singleton (2000) and Polson et al. (2002). It's also worth highlighting the paper written by Sanford and Martin (2005) which describes a Bayesian simulation-based method for estimating a single-factor term structure model with the discrete observations on yields augmented by additional high frequency latent data.

We follow a data-augmentation approach to inference on continous-time models (Eraker, 2001; Elerian et al., 2001; Sanford and Martin, 2005) and a Markov Chain Monte Carlo (MCMC) procedure for posterior approximation (e.g., see Hastings, 1970; Carlin and Chib, 1995; Robert and Casella, 2004). We propose a new and efficient Gibbs Sampling algorithm (e.g., see Geman and Geman, 1984; Gelfand and Smith, 1990; Casella and George, 1992) for our factor-augmented term structure model, where observable factors are included into the diffusion process of the latent instantaneous rate r_t.

The remainder of the paper proceeds as follows. Section 2 introduces both the traditional and the state-space formulation of the Vasicek model. Section 3 describes a general Bayesian inference framework with focus on the Gibbs Sampler. Section 4 presents a monthly dataset from December 2000 up to the present and provides an application of the model.

2.2 The Vasicek Model

2.2.1 Notation and assumptions

Let $P(t, s)$ denote the price at time t of a discount bond maturing at time s, $t \leq s$, with unit maturity value such that $P(s, s) = 1$. The yield to maturity $R(t, T)$ is the rate of return at time t on a bond with maturity date $s = t + T$, that is

$$R(t, T) = \frac{1}{T} \ln P(t, t + T). \tag{2.1}$$

The rate $R(t,T)$ considered as a function of T refers to the term structure at time t. Let $r(t)$ be the instantaneous rate as

$$r(t) = R(t,0) = \lim_{T \to 0} R(t,T). \tag{2.2}$$

In general terms, Vasicek (1977) derives the theoretical form of the term structure of interest rates under three main assumptions. The first one is that the instantaneous rate $r(t)$ follows the Itô's process

$$r(t) = r(0) + \int_0^t f(r(u),u)du + \int_0^t \rho(r(u),u)dZ(u), \tag{2.3}$$

for $t \geq 0$, where $(Z(t))_{t\geq 0}$ is a Wiener process starting at 0, $f(r,u)$ the instantaneous drift and $\rho^2(r,u)$ the diffusion of the process. The second assumption states that the price of a discounted bond depends only on the spot rate over its term. The last assumption is that the market is efficient.

Under these assumptions, it can be shown that the price $P(t,s)$ at time t of a bond with maturity s is a function solely of the instantaneous rate $r(t)$, that is

$$P(t,s) = P(t,s,r(t)). \tag{2.4}$$

In the Vasicek model the price of a discount bond is determined exclusively by the evolution of the instantaneous rate $r(t)$ over the term of the bond, where $r(t)$ is the stochastic risk-free rate of a bond with instantaneous maturity, that is $t = 0$.

2.2.2 Model formulation

The unobserved instantaneous rate $r(t)$ is assumed to be a continuous Markov process, which implies that the probability distribution of $r(u)$ with $u \geq t$ is completely determined by the value of $r(t)$. In the case of the Vasicek model, an explicit assumption is made with respect to

the stochastic process of $r(t)$, as it is assumed to follow the Ornstein-Uhlenbeck specification

$$r(t) = r(0) + \int_0^t k(\theta - r(u))du + \int_0^t \sigma dZ(u), \tag{2.5}$$

where $(Z_t)_{t\geq 0}$ is a Wiener process starting at 0, k the speed of mean-reversion at which the process returns to its long-run mean θ and σ the volatility parameter of the process. Under a few conditions, it can be shown that the yield to maturity $R(r(t), \Psi, \tau)$ with maturity τ can be written as

$$R(r(t), \Psi, \tau) = -\frac{1}{\tau} \ln P(r(t), \Psi, \tau). \tag{2.6}$$

We consider the discrete-time first-order approximation of the continuous time processes following an Euler-Maruyama scheme (Kloeden and Platen (2018)). The approximation is made at the same frequency as the observation frequency. Higher frequency framework can be used to provide a stochastic interpolation and a better approximation of the continuous time process (e.g., see Sanford and Martin, 2005; Eraker, 2001; Elerian et al., 2001). Let $t_n = t_{n-1} + h$, $n = 1, \ldots, N$ be a regular grid with step $h > 0$ such that $t_0 = 0$ and $t_N = T$. For monthly observations, without assuming interpolating latent variables, $h = 1/12$ is the annualizing factor. Define $r_n = r(t_n)$ and $y_{\tau,n} = R(r(t_n), \Psi, \tau)$. The discrete-time observable bond yield process $(y_{\tau,n})_{n\in\mathbb{N}}$ and latent spot-rate process $(r_n)_{n\in\mathbb{N}}$ are

$$\begin{aligned} y_{\tau,n} &= -\frac{1}{\tau} \ln(A(\Psi, \tau)) + \frac{1}{\tau} B(\Psi, \tau) r_n + \varepsilon_n, \quad \varepsilon_n \sim \mathcal{N}(0, \sigma_\tau^2) && (2.7) \\ r_{n+1} &= a(\Psi) + b(\Psi) r_n + \Phi(\Psi)\eta_n, \quad \eta_n \sim \mathcal{N}(0, \sigma^2), && (2.8) \end{aligned}$$

with $n = 1, \ldots, N$. The coefficients are functions of the unknown parameter vector $\Psi = (\theta, \lambda, \sigma_R^2, \sigma^2)$ and of the discretization step h:

$$\begin{aligned} a(\Psi) &= \theta(1 - \exp(-kh)), && (2.9) \\ b(\Psi) &= \exp(-kh)), && (2.10) \end{aligned}$$

$$\Phi(\Psi) = \frac{\sigma^2}{2k}(1-\exp(-2kh)) \tag{2.11}$$

$$A(\Psi,\tau) = \exp\left(\gamma(B(\Psi,\tau)-\tau) - \frac{\sigma^2 B(\Psi,\tau)^2}{4k}\right), \tag{2.12}$$

$$B(\Psi,\tau) = \frac{1}{k}(1-\exp(-k\tau)), \tag{2.13}$$

$$\gamma = \theta + \frac{\sigma\lambda}{k} - \frac{\sigma^2}{2k^2}. \tag{2.14}$$

Details about these formulas are provided by Vasicek (1977) and Duan and Simonato (1999). Given this setup, the Vasicek term structure finally depends on three main factors:

1. **the unobserved instantaneous rate** r_n. It works as the starting point of the yield curve at the shortest maturities;

2. **the long-run mean** θ of the instantaneous rate r_n;

3. **the asymptotic rate over infinite maturities** γ. This parameter represents the rate of return $R_{(t,\infty)}$ at time t of a bond with a very long maturity approaching to infinity. Therefore, it works as the anchor of the yield curve over the longest maturities. Since $\gamma = \theta + \frac{\sigma\lambda}{k} - \frac{\sigma^2}{2k^2}$, the anchor depends on:

   (a) θ, the long-run mean of r_n.

   (b) λ, the risk premium.

   (c) σ, the volatility of r_n.

   (d) k, the speed of mean-reversion of r_n around θ.

With respect to the risk premium λ, in a non-arbitrage framework it identifies a measure of extra-return over r_n for an additional unit of risk. As suggested by the asset pricing theory, a possible source of premium in the bond market refers to the so-called *term premium*, that is a compensation required by investors for holding bonds with longer maturities. A positive value of λ implies a positive premium on bond yields over the term structure.

2.2.3 State-Space formulation

In our paper we consider monthly yields of bonds with maturities $\tau \in \{2, 5, 10, 30\}$. In line with the traditional nomenclature, maturities are expressed in years. Let $\mathbf{y}_n = (y_{2n}, y_{5n}, y_{10n}, y_{30n})$ be a vector of yields over the four maturities. Let $\mathbf{r}_n = (r_{2n}, \ldots, r_{30n})$ be a vector of monthly yields of the instantaneous spot rate over τ. According to the state-space representation, the Vasicek model can be conveniently rewritten in terms of measurement and state equations. The measurement equation is linear in the hidden state process with Gaussian noise

$$\mathbf{y}_n = -\frac{1}{\tau}\ln(\boldsymbol{A}(\Psi, \tau)) + \frac{1}{\tau}\boldsymbol{B}(\Psi, \tau)r_n + \boldsymbol{\varepsilon}_n, \quad \boldsymbol{\varepsilon}_n \sim \mathcal{N}(\mathbf{0}, \boldsymbol{\Sigma}), \tag{2.15}$$

$n = 1, \ldots, N$ i.i.d., where $\boldsymbol{\Sigma}$ is the covariance matrix. On this, we adopt a consolidated specification implemented, for instance, by Duan and Simonato (1999), Rudebusch and Wu (2008) and Sanford and Martin (2005) with

$$\boldsymbol{\Sigma} = \begin{pmatrix} {\sigma^2}_2 & 0 & 0 & 0 \\ 0 & {\sigma^2}_5 & 0 & 0 \\ 0 & 0 & {\sigma^2}_{10} & 0 \\ 0 & 0 & 0 & {\sigma^2}_{30} \end{pmatrix}.$$

The state equation is linear in the state process and has Gaussian noise

$$r_{n+1} = a(\Psi) + b(\Psi)r_n + \Phi(\Psi)\eta_n, \quad \eta_n \sim \mathcal{N}(0, \sigma^2), \tag{2.16}$$

$n = 1, \ldots, N$, with $\mathbb{C}ov(\eta_n, \boldsymbol{\varepsilon}_m) = 0$ for all n, m. The vector of unknown parameters is thus defined as $\Psi = (\theta, \lambda, {\sigma^2}_2, {\sigma^2}_5, {\sigma^2}_{10}, {\sigma^2}_{30}, \sigma^2)$.

2.2.4 Augmented Model

The panel setup proposed in the paper allows for making model inference on observed yields of zero-coupon bonds at different maturities. To make the evaluation of the yield curve more reactive to market events, we deviate from the standard architecture by enriching the specification of the model with a broader range of variables through data-augmentation. In the state-space literature this way of modeling refers to a richer specification of the measurement equation in a state-space system. This generalization has been implemented in Rudebusch and Wu (2008) and Piazzesi and Swanson (2008), among others. More formally, data-augmentation is applied to link the diffusion process of r_t to three additional observable factors connected to market and financial variables.

First of all, let $y_{(ois)n} = ois_{(1y1d)n} - ois_{(3m1d)n}$ be the difference between the Overnight Index Swap (OIS) rates paid, respectively, in 1 year and in 3 months. Let $\mathbf{y}_{(ois)1:N} = (y_{(ois)1}, \ldots, y_{(ois)N})$ be a vector of monthly OIS spreads which will be applied as a proxy of market expectations about monetary policy decisions.

Since their inception, OIS contracts have been growing in popularity and liquidity. An OIS contract is an over-the-counter trade derivative in which two agents exchange fixed and floating interest rate payments. The floating interest rate is the overnight interbank rate, a measure of the monetary policy stance. A burgeoning literature, motivated by Kuttner (2001), Lloyd (2020) and Gürkaynak et al. (2007), argues about advantages of market-based measures in forecasting monetary policy decisions. In our paper, the term premium implied in OIS rates is proposed as a reasonable proxy of market expectations about the potential path of FED funds rates.

The second factor provides a link between market sentiment and interest rates. As argued in Campbell and Ammer (1993), for instance, higher levels of risk-aversion deliver more pressure on interest rates, as investors increase their allocation into defensive assets for hedging their portfolio. Since the model of the paper is estimated on monthly data, a risk factor $\hat{u}_n^2$ is extracted in terms of realized volatility from daily returns r_t on the S&P500 Index, over

a monthly horizon, with $\hat{u}_n^2 = \sum_n r^2{}_n$ and $y_{(e)n} = \ln(\hat{u}_n^2)$. Let $\mathbf{y}_{(e)1:N} = (y_{(e)1}, \ldots, y_{(e)N})$ be the collection over time of this sentiment factor. In this context, the S&P500 Index is reasonably assumed as a proxy of global equity market. An important point emerges here: realized volatility is thought as a proper estimate of market sentiment. This choice seems quite reasonable, since the concept of market sentiment is here interpreted as an indicator about the risk-on/risk-off attitude of investors to hold risky assets in their portfolios. Under this perspective, a rising equity volatility tends to depress market sentiment towards a more defensive stance in the asset allocation.

Third, as short-term rates are related to macroeconomic fundamentals, the Taylor rule (see Taylor (1999)) is introduced as an additional component of the system. This rule allows for reconciling the definition of the instantaneous rate with inflation target and output gap of the economy. A large number of empirical studies has employed some variant of the Taylor rule to approximate the monetary policy reaction function. According to Clarida et al. (2000), Kozicki (1999), Judd and Rudebush (1999) and Rudebusch and Wu (2008), a useful version of the Taylor rule can be written as

$$i_n = r^* + \pi_n^* + g_\pi(\pi_n - \pi_n^*) + g_y c_n + u_n, \tag{2.17}$$

where r^* is the equilibrium real rate, π_n^* the perceived inflation target, π_n the annual inflation rate and c_n a measure of the output gap. In such a version of the Taylor rule, the short-term rate i_n is given by the equilibrium nominal rate $r^* + \pi_n^*$ plus two cyclical adjustments to respond to deviation of inflation and real output from the relative potential target. Given its definition into the Vasicek model, the instantaneous rate r_n can be set equal to the equilibrium nominal rate of i_n. Thus, the following Taylor rule can be specified as

$$i_n = r_n + g_\pi(\pi_n - \pi_n^*) + g_y c_n + u_n, \tag{2.18}$$

where $r_n = r^* + \pi_n^*$ and i_n the yield of a bond maturing in 1 month (common choice in empirical applications). As commonly used in literature and suggested, for instance, by Rudebusch and Wu (2008) and Sanford and Martin (2005), the output gap is defined as the distance between the capacity utilization and its relative long-run trend smoothed by the Hodrick-Prescott's filter. A couple of important remarks are in order here. First, the selected version of Taylor rule allows model setting to deal with a quite simple specification; nevertheless, it lacks an inertial mechanism, that is a lagged interest rate term, which is a significant feature to describe monetary policy dynamics. Second, the measure of output gap selected in the paper might not be the most appropriate, as the cyclical component of consumption is not properly accounted. Given this backdrop, an extension of the paper might employ a different Taylor rule specification to address the two considerations above. The perceived inflation target π_n^* is directly computed by estimating a regime-switching model on the US Core CPI inflation, instead of considering some historical long-run measure. Precisely, the perceived inflation target is given by a two-state Markov switching model with high-inflation and low-inflation states and time-varying transition probabilities. Under this setup, state transitions are driven by volatility of short-term interest rates. More formally, the monthly US Core CPI inflation rate π_t is modelled according to a 2-state MSAR(1) process as

$$\pi_t = \mu_t + \epsilon_t, \epsilon_t \sim (0, R), \tag{2.19}$$

$$\mu_t = c_{s_t} + \phi_{s_t}\mu_{t-1} + \eta_t, \eta_t \sim (0, Q_{s_t}), \tag{2.20}$$

with $s_t = 1, 2$ (low-inflation and high-inflation states). Time-varying transition probabilities are driven by volatility of the 2-year US rate, which works as early-warning in this setting. Inflation is connected to developments of real data, therefore macroeconomic variables might be selected as warning factor. Nevertheless, the choice here converges to short-term rates, since they show an interesting advantage over macro data. Yields and their volatility are

Figure 2.1: *Annualised Perceived Inflation Target.*

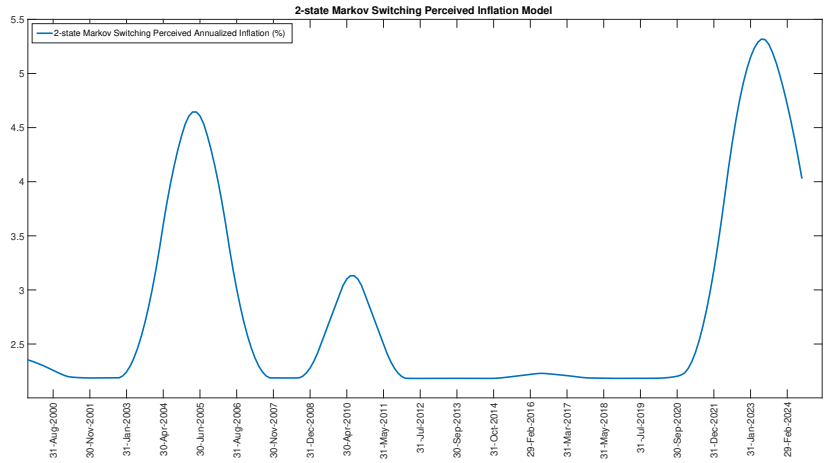

strictly connected to the behaviour of macroeconomic conditions but with the merit to be high-frequency data, therefore the typical delay effect characterising a dataset of macro variables is eliminated. The Kalman Filter is applied to approximate the conditional mean and variance of the process. Given model estimate over a sample from December 2000 up to May 2024, the regime-based unconditional expectation of the monthly inflation rate π_t is given by

$$E(\pi_l) = \bar{\pi}_l = \hat{c}_l/(1-\hat{\phi}_l) = 0.225\%, \tag{2.21}$$

$$E(\pi_h) = \bar{\pi}_h = \hat{c}_h/(1-\hat{\phi}_h) = 0.527\%, \tag{2.22}$$

where l and h refer to low-inflation and high-inflation states, respectively. The perceived inflation target is finally computed as a weighted average of $\bar{\pi}_l$ and $\bar{\pi}_h$, with weights $\bar{w}_l$ and $\bar{w}_h$ given by the estimated ergodic probabilities of the two regimes, that is $\bar{w}_l = (1-\hat{p}_{22,t})/(2-\hat{p}_{11,t}-\hat{p}_{22,t})$ and $\bar{w}_h = (1-\hat{p}_{11,t})/(2-\hat{p}_{11,t}-\hat{p}_{22,t})$. A smoothed version of the perceived inflation target is finally computed by averaging the raw series over a 12-month rolling window, as reported in Figure 2.1

Given the definition of the additional observable factors, the augmented panel-based mea-

surement equations are defined as

$$\mathbf{y}_n = -\frac{1}{\tau}\ln(\boldsymbol{A}(\Psi,\tau)) + \frac{1}{\tau}\boldsymbol{B}(\Psi,\tau)r_n + \boldsymbol{\varepsilon}_n, \tag{2.23}$$

$$y_{n(ois)} = a_2 + b_2 r_n + \varepsilon_{n(ois)}, \tag{2.24}$$

$$y_{n(e)} = a_3 + b_3 r_n + \varepsilon_{n(e)}, \tag{2.25}$$

$$i_n = r_n + g_\pi(\pi_n - \pi_n^*) + g_y c_n + u_n, \tag{2.26}$$

with $\varepsilon_{n(ois)} \sim \mathcal{N}(0, \sigma^2_{ois})$, $\varepsilon_{n(e)} \sim \mathcal{N}(0, \sigma^2_e)$ and $u_n \sim \mathcal{N}(0, \sigma^2_i)$. The system can be extended to include other interbank market rates. Given the data-enriched framework of the model, the new vector of unknown parameters becomes $\boldsymbol{\Psi} = (a_{(\Psi)}, b_{(\Psi)}, \sigma^2{}_2, \sigma^2{}_5, \sigma^2{}_{10}, \sigma^2{}_{30}, \sigma^2, a_2, b_2, \sigma^2_{ois}, a_3, b_3, \sigma^2_e, g_\pi, g_y, \sigma^2_i)$.

In the new vector $\boldsymbol{\Psi}$, the parameter λ disappears, as it is directly derived from equations (20) and (21). More formally, λ is modelled as $\lambda = a_2 - a_3$.

Instead of considering λ in terms of unknown parameter to be estimated, as generally proposed in literature (see Duan and Simonato (1999) for instance), in our paper we suggest an innovative and more intuitive way to estimate the market bond premium λ as explicitly connected to specific sources of risk premium:

1. a_2: the *term premium* connected to expectations about monetary policy decisions. Christensen and Rudebusch (2012), Woodford (2012) and Piazzesi and Swanson (2008) recognise in their studies the efficacy of OIS contracts as leading indicators about future Central Bank rates.

2. a_3: the *market premium* connected to the equity market volatility. According to the asset pricing theory, the anchor γ of the yield curve should be positive related to the risk premium λ, since investors are expected to require a compensation for holding bonds over longer maturities as they have more risk than a short-term rate. Given this, higher equity market volatility and thus a rising level of risk-aversion tends to

generate a downside pressure on yields at longer maturities, as investors increase their allocation into safe assets to hedge their portfolio. Therefore, a_3 implies a negative impact on λ. Bekaert et al. (1989), Campbell and Ammer (1993) and Lettau and Watcher (2011), for instance, explicitly introduce the correlation between bond and equity risk premia as an additional element in bond pricing modelling.

The definition of λ proposed in our paper is set to introduce the most relevant sources of premium into the derivation of the shape of the term structure through the anchor γ: the term premium implied in the path of monetary policy and the market premium required by investors for holding risky assets. This new way of estimating λ appears consistent with the asset pricing theory and avoids the controversial results of different applications (for instance, see Duan and Simonato (1999)), where the maximum likelihood approach delivers estimate of λ close to zero or even negative. An interesting remark is in order here; in contrast to Rudebusch and Wu (2008), for instance, where risk premia are time-varying, in the context of this paper the parameter λ is indicated as fixed. This setting addresses the explicit choice of the paper to propose a flexible tool to support decisions of TAA, rather than a new equilibrium model. Under this perspective, the definition of λ as a well-identified combination of premia looks more intuitive than the time-varying alternative when applied to portfolio strategies.

2.3 Bayesian Inference

Denote with $\mathbf{x}_n = (\mathbf{y}_n, y_{n(ois)}, y_n(e), i_n)$ the vector of observable variables and with $\mathbf{x} = (\mathbf{x}_1, \ldots, \mathbf{x}_N)$ and $\mathbf{r} = (r_1, \ldots, r_N)$ the collections of observable and latent variables, respectively. A Bayesian statistical model with latent variable is given by a parametric model $f(\mathbf{x}|\boldsymbol{\theta}, \mathbf{r})$ for the observable variable $\mathbf{x}$, a parametric model $f(\mathbf{r}|\boldsymbol{\theta})$ for the latent state variable $\mathbf{r}$ and a prior distribution $\pi(\boldsymbol{\theta})$ on the vector of parameters $\boldsymbol{\theta}$.

The inference is then based on the joint distribution of $\boldsymbol{\theta}$ and $\mathbf{r}$ conditional on $\mathbf{x}$ (data),

called posterior distribution and defined by

$$\pi(\boldsymbol{\theta}, \mathbf{r}|\mathbf{x}) = \frac{f(\mathbf{x}|\boldsymbol{\theta}, \mathbf{r}) f(\mathbf{r}|\boldsymbol{\theta}) \pi(\boldsymbol{\theta})}{\int f(\mathbf{x}|\boldsymbol{\theta}, \mathbf{r}) f(\mathbf{r}|\boldsymbol{\theta}) \pi(\boldsymbol{\theta}) d\boldsymbol{\theta}}, \tag{2.27}$$

where $f(\mathbf{x}|\boldsymbol{\theta}, \mathbf{r}) f(\mathbf{r}|\boldsymbol{\theta})$ represents the complete-data likelihood $f(\mathbf{x})$. Since the denominator is not a function of the vector of model parameters $\boldsymbol{\theta}$, it is common to rewrite the posterior distribution in terms of the following proportionality:

$$\pi(\boldsymbol{\theta}, \mathbf{r}|\mathbf{x}) \propto f(\mathbf{x}|\boldsymbol{\theta}, \mathbf{r}) f(\mathbf{r}|\boldsymbol{\theta}) \pi(\boldsymbol{\theta}). \tag{2.28}$$

Considering the model of the paper, parameters can be conveniently collected into the vector $\boldsymbol{\theta} = (\boldsymbol{\theta}_1, \boldsymbol{\theta}_2, \boldsymbol{\theta}_3, \boldsymbol{\theta}_4)$, with $\boldsymbol{\theta}_1 = (\theta, \lambda, \sigma_2^2, \sigma_5^2, \sigma_{10}^2, {\sigma^2}_{30}, \sigma_r^2)$, $\boldsymbol{\theta}_2 = (a_2, b_2, \sigma_{ois}^2)$, $\boldsymbol{\theta}_3 = (a_3, b_3, \sigma_e^2)$ and $\boldsymbol{\theta}_4 = (g_\pi, g_y, \sigma_i^2)$. For computational advantages, in Bayesian inference, it is common to deal with the precision $\gamma_j = 1/\sigma_j$ rather than with the volatility of the process σ_j.

2.3.1 Prior Distributions

Prior distributions reflect any information the researcher has before seeing the data. It is common to choose particular classes of priors which are easy to interpret and make computations more efficient. Natural conjugate priors typically have both such advantages. A conjugate prior distribution is one which, when combined with the likelihood, yields a posterior distribution which falls in the same class of distributions. In addition, a natural conjugate prior has the additional property of having the same functional form as the likelihood function. It means that the prior can be interpreted as rising from a fictitious data set from the same process which generated the actual data.

Since the structure of the panel is based on regressions with Gaussian errors, it is convenient to write the prior distribution of parameters related to the first moment of the distribution μ in terms of conditional Normal distribution $\mu|h \sim \mathcal{N}(\mu_0, \sigma_0^2)$, while a Gamma distribution $h \sim \mathcal{G}a(v_0, \delta_0)$ is applied for the precision h. Notable details on these topics are provided, for

instance, by Koop (2003) and Robert (2007). Table 2.1 summarises the prior setup applied to the model, with numbers expressed in annualised values.

Table 2.1: *Parameters, prior distributions and relative hyper-parameters for the data-enriched model.*

Parameter	Distribution	Hyper-parameters
$a_{(\Psi)}$	$\mathcal{N}(\mu_0, \sigma_0^2)$	$\mu_0 = 0.00015$, $\sigma_0^2 = (0.005/2)^2$
$b_{(\Psi)}$	$\mathcal{N}(\mu_0, \sigma_0^2)$	$\mu_0 = 0.985$, $\sigma_0^2 = (0.005/2)^2$
γ_r	$\mathcal{G}a(v_0, \delta_0)$	$v_0 = 0.01$, $\delta_0 = 1000$
γ_2	$\mathcal{G}a(v_0, \delta_0)$	$v_0 = 0.01$, $\delta_0 = 1000$
γ_5	$\mathcal{G}a(v_0, \delta_0)$	$v_0 = 0.01$, $\delta_0 = 1000$
γ_{10}	$\mathcal{G}a(v_0, \delta_0)$	$v_0 = 0.01$, $\delta_0 = 1000$
γ_{30}	$\mathcal{G}a(v_0, \delta_0)$	$v_0 = 0.01$, $\delta_0 = 1000$
a_2	$\mathcal{N}(\mu_0, \sigma_0^2)$	$\mu_0 = 0.01$, $\sigma_0^2 = (0.05/2)^2$
b_2	$\mathcal{N}(\mu_0, \sigma_0^2)$	$\mu_0 = -0.5$, $\sigma_0^2 = (1)^2$
$\gamma_{\sigma^2_{ois}}$	$\mathcal{G}a(v_0, \delta_0)$	$v_0 = 0.005$, $\delta_0 = 1000$
a_3	$\mathcal{N}(\mu_0, \sigma_0^2)$	$\mu_0 = -0.05$, $\sigma_0^2 = (0.05/2)^2$
b_3	$\mathcal{N}(\mu_0, \sigma_0^2)$	$\mu_0 = 1$, $\sigma_0^2 = (1)^2$
$\gamma_{\sigma^2_e}$	$\mathcal{G}a(v_0, \delta_0)$	$v_0 = 0.05$, $\delta_0 = 1000$
g_π	$\mathcal{N}(\mu_0, \sigma_0^2)$	$\mu_0 = 1$, $\sigma_0^2 = (1/2)^2$
g_y	$\mathcal{N}(\mu_0, \sigma_0^2)$	$\mu_0 = 1$, $\sigma_0^2 = (1/2)^2$
$\gamma_{\sigma_i^2}$	$\mathcal{G}a(v_0, \delta_0)$	$v_0 = 0.005$, $\delta_0 = 1000$

Hyper-parameters for $a_{(\Psi)}$ and $b_{(\Psi)}$ are set given a prior about the unconditional mean of r_t around 1%, which is a reasonable lower bound for the FED funds rates. Inputs for the Gamma distribution are calibrated to achieve expectations in terms of yield volatility close to 1.5%, in line with long-run historical values. Priors for a_2 imply a positive term-premium on bond yields over the term structure, as suggested by the asset pricing theory, while priors for a_3 assume an expected level of equity volatility around 15%, which is a common empirical threshold of normal volatility for risky assets. Finally, priors for g_π and g_y imply a positive relationship between short-term rates and cyclical shocks.

2.3.2 Posteriors Approximation

In general terms, the posterior density summarises all the information, both prior and likelihood-based, about the unknown parameters of the model. Precisely, that informa-

tion will be proportional to the likelihood times the prior density.

In this paper, a Bayesian approach is considered for inference on the vector $\boldsymbol{\theta}$ of unknown parameters. Since the Bayes estimator of $\boldsymbol{\theta}$ is not available in closed form, MCMC techniques are applied. In particular, the Gibbs Sampling algorithm is implemented as simulation method to approximate joint and marginal posterior distributions by sampling from conditional posterior distributions. This method was introduced for the first time by Geman and Geman (1984); moreover Robert and Casella (2004) provide more details about the history of the method. The Gibbs sampler takes advantage of the hierarchical structure of the model, i.e. when a Bayesian model can be written as

$$\pi(\boldsymbol{\theta}, \mathbf{r}|\mathbf{x}) = \int \pi_1(\boldsymbol{\theta}, \mathbf{r}|\mathbf{x}, \lambda)\pi_2(\lambda|\mathbf{x})d\lambda. \tag{2.29}$$

The idea is to simulate from the joint distribution $\pi_1(\boldsymbol{\theta}, \mathbf{r}|\mathbf{x}, \lambda)\pi_2(\lambda|\mathbf{x})$ to approximate $\pi(\boldsymbol{\theta}, \mathbf{r}|\mathbf{x})$ as the marginal when all the conditional distributions $\pi_1(\boldsymbol{\theta}|\mathbf{x}, \mathbf{r}, \lambda)$, $\pi_2(\mathbf{r}|\boldsymbol{\theta}, \mathbf{x}, \lambda)$ and $\pi_3(\lambda|\mathbf{x}, \mathbf{r})$ are known and can be simulated (e.g., see Robert, 2007).

As an extension of the former procedure, the Gibbs sampling algorithm can be generalised for a joint distribution $\pi(\theta_1, \ldots, \theta_p)$ with full conditionals $\pi_1, \ldots, \pi_p$. Given the vector $(\theta_1^{(m)}, \ldots, \theta_p^{(m)})$ at the iteration m, it simulates:

- $\theta_1^{(m+1)}$ from $\pi_1(\theta_1|\theta_2^{(m)}, \theta_3^{(m)}, \ldots, \theta_p^{(m)})$;
- $\theta_2^{(m+1)}$ from $\pi_2(\theta_2|\theta_1^{(m+1)}, \theta_3^{(m)}, \ldots, \theta_p^{(m)})$;

  $\vdots$

- $\theta_p^{(m+1)}$ from $\pi_p(\theta_p|\theta_1^{(m+1)}, \theta_2^{(m+1)}, \ldots, \theta_{p-1}^{(m+1)})$.

Notice that the Gibbs sampler has a couple of advantages: first of all, it does not require the θ_i to be one-dimensional, and, secondly, the choice of the order of the decomposition can be entirely based on simulation reasons. About our model, a multi-block Gibbs sampler is implemented, given $\boldsymbol{\theta} = (\boldsymbol{\theta}_1, \boldsymbol{\theta}_2, \boldsymbol{\theta}_3, \boldsymbol{\theta}_4)$, with $\boldsymbol{\theta}_1 = (r_0, a_{(\Psi)}, b_{(\Psi)}, \sigma^2_{\mathbf{y}_{(2)}}, \sigma^2_{\mathbf{y}_{(5)}}, \sigma^2_{\mathbf{y}_{(10)}}, \sigma^2_{\mathbf{y}_{(30)}}, \sigma^2_r)$,

$\boldsymbol{\theta}_2 = (a_2, b_2, \sigma^2_{ois})$, $\boldsymbol{\theta}_3 = (a_3, b_3, \sigma^2_e)$ and $\boldsymbol{\theta}_4 = (g_\pi, g_y, \sigma^2_i)$. At the $m-$th iteration the Gibbs sampler draws recursively:

i) the latent vector $\mathbf{r}$ of instantaneous rates:
$(\mathbf{r}^{(m)}|\mathbf{y}, \boldsymbol{\theta}_1^{(m-1)})$ via Kalman Filter;

ii) the parameters $a_{(\Psi)}$, $b_{(\Psi)}$ and $h_{\sigma^2_r}$:
$(a^{(m)}_{(\Psi)}|\mathbf{y}, \mathbf{r}^{(m)}, h^{(m-1)}_{\sigma^2_r}) \sim \mathcal{N}(\mu_{1a}, \sigma^2_{1a})$,
$(b^{(m)}_{(\Psi)}|\mathbf{y}, \mathbf{r}^{(m)}, h^{(m-1)}_{\sigma^2_r}) \sim \mathcal{N}(\mu_{1b}, \sigma^2_{1b})$,
$(h^{(m)}_{\sigma^2_r}|\mathbf{y}, \mathbf{r}^{(m)}, a^{(m)}_{(\Psi)}, b^{(m)}_{(\Psi)}) \sim \mathcal{G}a(v_1, \delta_1)$;

iii) the parameters a_2, b_2 and $h_{\sigma^2_{ois}}$:
$(a^{(m)}_2|\mathbf{y}_{(\mathbf{ois})}, \mathbf{r}^{(m)}, h^{(m-1)}_{\sigma^2_{ois}}) \sim \mathcal{N}(\mu_{2a}, \sigma^2_{2a})$,
$(b^{(m)}_2|\mathbf{y}_{(\mathbf{ois})}, \mathbf{r}^{(m)}, h^{(m-1)}_{\sigma^2_{ois}}) \sim \mathcal{N}(\mu_{2b}, \sigma^2_{2b})$,
$(h^{(m)}_{\sigma^2_{ois}}|\mathbf{y}_{(\mathbf{ois})}, \mathbf{r}^{(m)}, a^{(m)}_2, b^{(m)}_2) \sim \mathcal{G}a(v_2, \delta_2)$;

iv) the parameters a_3, b_3 and $h_{\sigma^2_e}$:
$(a^{(m)}_3|\mathbf{y}_{(\mathbf{e})}, \mathbf{r}^{(m)}, h^{(m-1)}_{\sigma^2_e}) \sim \mathcal{N}(\mu_{3a}, \sigma^2_{3a})$,
$(b^{(m)}_3|\mathbf{y}_{(\mathbf{e})}, \mathbf{r}^{(m)}, h^{(m-1)}_{\sigma^2_e}) \sim \mathcal{N}(\mu_{3b}, \sigma^2_{3b})$,
$(h^{(m)}_{\sigma^2_e}|\mathbf{y}_{(\mathbf{e})}, \mathbf{r}^{(m)}, a^{(m)}_3, b^{(m)}_3) \sim \mathcal{G}a(v_3, \delta_3)$;

v) the parameters g_π, g_y and $h_{\sigma^2_i}$:
$(g^{(m)}_\pi|\mathbf{i}, \pi, \pi^*, \mathbf{y}^{\mathbf{og}}, \mathbf{r}^{(m)}, h^{(m-1)}_{\sigma^2_i}) \sim \mathcal{N}(\mu_{4\pi}, \sigma^2_{4\pi})$,
$(g^{(m)}_y|\mathbf{i}, \pi, \pi^*, \mathbf{y}^{\mathbf{op}}, \mathbf{r}^{(m)}, h^{(m-1)}_{\sigma^2_i}) \sim \mathcal{N}(\mu_{4y}, \sigma^2_{4y})$,
$(h^{(m)}_{\sigma^2_i}|\mathbf{i}, \pi, \pi^*, \mathbf{y}^{\mathbf{op}}, \mathbf{r}, g^{(m)}_\pi, g^{(m)}_y) \sim \mathcal{G}a(v_4, \delta_4)$;

vi) the parameters $h_{\sigma^2_{\mathbf{y}_{(2)}}}$, $h_{\sigma^2_{\mathbf{y}_{(5)}}}$, $h_{\sigma^2_{\mathbf{y}_{(10)}}}$, $h_{\sigma^2_{\mathbf{y}_{(30)}}}$:
$(h^{(m)}_{\sigma^2_{\mathbf{y}_{(\tau)}}}|\mathbf{y}, \mathbf{r}, \boldsymbol{A}^{(m)}_{(\Psi,\tau)}, \boldsymbol{B}^{(m)}_{(\Psi,\tau)}) \sim \mathcal{G}a(v_{1h}, \delta_{1h}), \tau = 2, 5, 10, 30.$

Posterior parameters of Normal and Gamma distributions are defined as $\sigma_1^2 = (\sigma_0^{-2} + h^{-1}\mathbf{i}'\mathbf{i})^{-1}$, $\mu_1 = (\sigma_0^{-2} + h^{-1}\mathbf{i}'\mathbf{i})^{-1}(\sigma_0^{-2}\mu_0 + h^{-1}\mathbf{i}'\mathbf{i}\bar{\mu})$, $v_1 = v_0 + T$ and $\delta_1 = \delta_0 + \hat{\epsilon}'\hat{\epsilon}$ with $\bar{\mu}$ the sample parameter estimate.

2.4 Empirical Results

2.4.1 Data Description

The model and inference are applied to a monthly dataset from December 2000 up May 2024, which includes the following series from Bloomberg:

1. US zero-coupon bonds maturing in 2, 5, 10 and 30 years to derive the block of yields collected into the vector $\mathbf{y}_n$.
2. US OIS rates to derive the OIS spread $y_{n(ois)}$.
3. S&P500 daily returns to derive a measure of realized volatility $y_{n(e)}$. The S&P500 index is assumed to be a proxy of the global equity market.
4. US zero-coupon bond maturing in 1 month i_n, US Core CPI inflation π_n and US capacity utilization c_n applied in the Taylor rule.

2.4.2 Model Estimates

Table 2.2 summarises model estimate under 2 different settings: the first one ($\mathcal{M}_1$) as formalised in equations 2.7 and 2.8 and the augmented extension ($\mathcal{M}_2$) over equations 2.8 and from 2.23 to 2.26. Numbers are expressed in annualised values. Given model estimate, Vasicek parameters can be easily computed. On this side, a particular emphasis is put on $\hat{\theta}$ and $\hat{\gamma}$, which are the key drivers of the shape of the entire yield curve.

As for $\mathcal{M}_1$, the long-run mean $\hat{\theta}$ of the instantaneous rate r_n moves around 1.5%, which is a quite depressed number if compared to historical values of FED official rates. Under this perspective, the value of $\hat{\theta}$ around 2% of the augmented model looks more appropriate and consistent with the path of monetary policy implemented by the FED. Castelnuovo et al. (2014) provide a notable reference on monetary policy rules for the United States.

The improvement is connected to the introduction of the equation on OIS rates into the data-enriched version, which explicitly accounts for the impact of monetary policy on the

Table 2.2: *All results are obtained running the Gibbs Sampling with 100,000 iterations, after burning removal and thinning with rate of 20%. Numbers are expressed in annualised values. The column* $\boldsymbol{\Psi}$ *summarises model parameters, while in columns* $\widehat{\boldsymbol{\Psi}}$ *and C. I. parameter estimates and credible intervals are reported for* $\mathcal{M}_1$ *and* $\mathcal{M}_2$*, respectively.*

Model Comparison	Model 1 (Standard Vasicek)		Model 2 (Augmented Vasicek)	
$\boldsymbol{\Psi}$	$\widehat{\boldsymbol{\Psi}}$	C. I.	$\widehat{\boldsymbol{\Psi}}$	C. I.
$\hat{a}_{(\Psi)}$	0.015%	[0.0005%; 0.0306%]	0.025%	[0.015%; 0.035%]
$\hat{b}_{(\Psi)}$	0.989	[0.984%; 0.992%]	0.987	[0.982%; 0.992%]
$\hat{\sigma}$	1.71%	[1.622%; 1.845%]	0.465%	[0.452%; 0.485%]
$\hat{\sigma}_2$	0.842%	[0.811%; 0.897%]	0.262%	[0.195%; 0.355%]
$\hat{\sigma}_5$	0.841%	[0.810%; 0.878%]	0.265%	[0.185%; 0.375%]
$\hat{\sigma}_{10}$	0.844%	[0.818%; 0.892%]	0.264%	[0.182%; 0.382%]
$\hat{\sigma}_{\mathbf{y}_{(30)}}$	0.842%	[0.812%; 0.882%]	0.269%	[0.187%; 0.377%]
$\hat{a}_2$	-	-	0.082	[0.062; 0.105]
$\hat{b}_2$	-	-	−3.615	[−4.510; −2.625]
$\hat{\sigma}^2_{ois}$	-	-	0.185%	[0.178%; 0.197%]
$\hat{a}_3$	-	-	−0.155	[−0.19; −0.13]
$\hat{b}_3$	-	-	3.559	[2.525; 4.655]
$\hat{\sigma}^2_e$	-	-	0.592%	[0.552%; 0.652%]
$\hat{g}_\pi$	-	-	1.035	[0.425; 1.625]
$\hat{g}_y$	-	-	0.514	[0.135; 0.925]
$\hat{\sigma}^2_i$	-	-	0.187%	[0.176%; 0.194%]
$\hat{\theta}$	1.490%	[0.056%; 2.901%]	2.101%	[1.478%; 2.768%]
$\hat{\gamma}$	3.410%	[1.914%; 5.233%]	2.784%	[2.144%; 3.364%]
$\boldsymbol{\Upsilon}(\mathbf{Y}\|\boldsymbol{\Psi})$	3263	-	3776	-

yield curve. Thus, for instance, the hiking cycle started in the summer of 2021, when the FED announced a hawkish monetary policy in response to increasing inflation data, is well integrated into the estimating process of r_n. On the other hand, due to its setup which makes the evaluation of the yield curve less reactive to market dynamics, the estimate of θ under $\mathcal{M}_1$ tends to overweight the impact of the zero-rate monetary policy introduced in September 2008, without putting a proper emphasis on the hawkish tone adopted by the FED since the summer of 2021. Estimate of γ moves around 3.4% in $\mathcal{M}_1$, while it is close to 2.8% in $\mathcal{M}_2$. Also in this case data augmentation yields a great advantage since it estimates the anchor of the yield curve more in line with the natural long-term rate assumed by the FED at 2.5% in targeting its monetary policy. Again, the inability of $\mathcal{M}_1$ to build an explicit

connection between rates and macroeconomic data leads this model to a misleading estimate of the anchor and therefore of the potential steepness of the yield curve.

Estimate of g_π and g_y suggests a positive impact of cyclical shocks on short-term interest rates. In particular, inflation deviating from the equilibrium appears to generate stronger effects on rates than fluctuations of real data around the potential target. Similar results are provided, for instance, by Sanford and Martin (2005).

The parameter λ provides a positive estimate of the risk premium ($\widehat{\lambda} = 0.23$), in line with the asset pricing theory which argues that investors require a compensation for holding bonds over longer maturities. More details on this are provided, for instance, by Campbell and Ammer (1993). Since $\lambda = a_2 - a_3$, a positive value of $\widehat{a}_2$ implies that a positive OIS spread, reflecting a tightening monetary policy, encourages the market to push higher the expected level of future interest rates across maturities and thus the value of the anchor γ. At the same time, a negative value of $\widehat{a}_3$ implies that a steeper yield curve effectively materialises only if market sentiment improves (low equity volatility) on the way of the aggressive stance of the monetary policy. It generally happens when official rates are pushed higher in response to upbeat numbers about the economic growth rather than to mitigate unexpected inflation shocks. On the other hand, the standard model tends to underestimate a bit the value of the risk premium, as $\widehat{\lambda} = 0.17$ under $\mathcal{M}_1$. The lack of an explicit connection to market premia might reconcile this estimate to the one under the augmented model. In any case, the direct interpretation of the risk premium gives $\mathcal{M}_2$ an additional merit when this model is called to support decisions of tactical asset allocation.

As suggested by the (log) marginal likelihood $\Upsilon(\mathbf{Y}|\mathbf{\Psi})$, the augmented version $\mathcal{M}_2$ gains a great advantage over the simpler $\mathcal{M}_1$ setup. Under model inference perspective, such a result puts a great emphasis on the incremental value introduced by the data-rich approach suggested in the paper. Since $\mathcal{M}_2$ has additional variables, the exercise compares the log-data density only for those appearing in both models.

Figure 2.2 compares the market yield curve to the one estimated by the model at the end of

Figure 2.2: *Data-enriched yield curve (red) and market yield curve (blue) at different maturities (horizontal axis). The 95% credible interval is also reported (upper and lower bounds).*

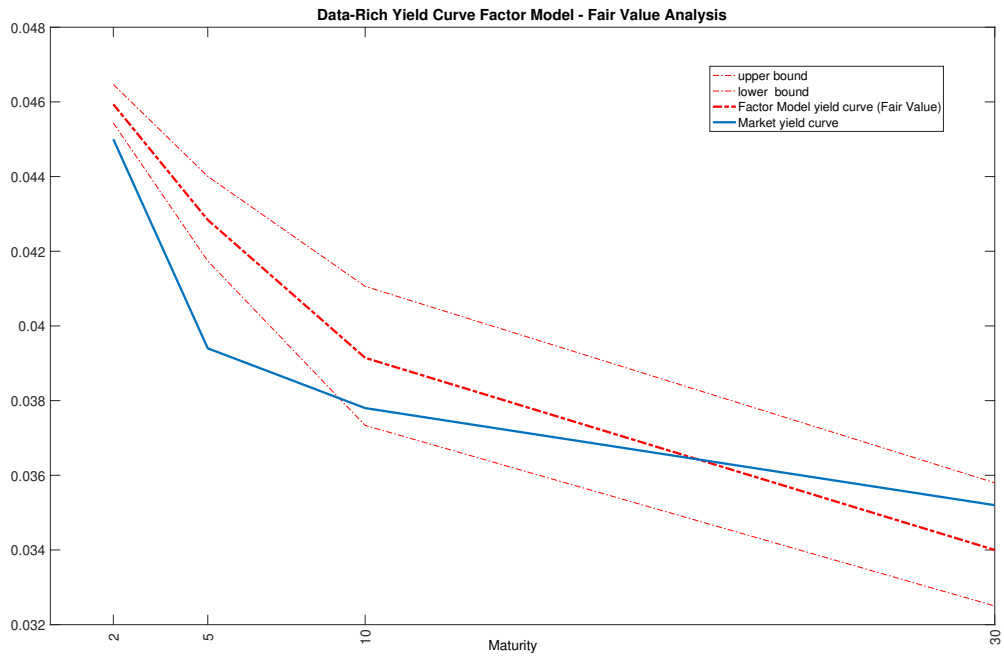

February 2023. Notable considerations may arise as appropriate. The inversion of the market curve looks well justified by model estimate, which confirms the negative slope between rates maturing in 2 and 10 years. Such a negative slope is the result of the aggressive monetary policy adopted by the FED since mid 2021, in order to curb rising inflation data. Since this hawkish tone is in response to inflationary shocks, surprising on the upside, rather than to good news on real growth, market sentiment falls into a risk-off scenario, with investors hedging their portfolio by increasing allocation in the long-term bonds.

A rising demand for safe assets pushes yields down on longer maturities, with a consequent inversion of the curve. This is a typical warning signal of recession. Still in figure 2.2, rates of different maturities are close to the relative fair value, except for the yield paid in 5 years, which is well below the model projection. Such a mis-pricing suggests that investors are aggressively buying bonds at intermediate maturities, in anticipation of lower future rates due to cooling inflation and incoming recessionary conditions (e.g., see Piazzesi and Swanson, 2008; Campbell and Ammer, 1993).

In general terms, a projection like the one in Figure 2.2 would reasonably appear as a signal of less than satisfactory fit. But this is not the case for the example proposed in the chart, as the model remarks here a reasonable mis-pricing in bond yields, following from a generalised risk-off sentiment occurring in the market between February and March 2023. Specifically, in that period few US regional banks announced alarming losses due to their ultra-leveraged exposure to US Treasuries. Given this backdrop, concerns about the real strength of the US banking system pushed investors to sharply change their portfolio strategy by increasing allocation on bonds, as safe asset. Such a climbing demand of defensive yields pushed interest rates down by more than 100 basis points in two weeks. That reaction appeared as driven by an exaggerated risk-off sentiment, given the limited impact of those regional banks on the US credit system. Remarks in Figure 2.2 are exactly in support of this market overreaction, as confirmed by the relevant portion of maturities projected outside the 95% confidence bounds.

The paper doesn't provide an explicit framework on model inference during the Zero Lower Bound (ZLB) periods. This concept refers to that condition in which short-term nominal interest rates are at or close to zero, causing an alarming liquidity trap driven by the inability of central banks to encourage more spending by lowering interest rates. Despite the model in the paper doesn't directly address the question, its data-enriched setup allows to mitigate this emerging lack in a quite satisfactory way. The first 3 charts in Figure 2.3 compare actual and fitted values for the 2, 5 and 10-year rate, respectively, during the 2008-2015 Zero Lower Bound period. To simplify the analysis, the 30-year rate is not considered here, since the longest maturities are marginally affected by the ZLB theme. In very general terms, despite potential autocorrelation in residuals should emerge from the comparison, the underlying dynamics of interest rates (dotted blue lines) appears to be quite well interpreted by the fitted points (orange lines). A possible explanation of this outcome is provided by the last chart in figure, which shows the estimated latent spot rate r_n under 3 different sources of augmentation. Data-enrichment on short-term rates (dotted blue and orange lines) and, in

Figure 2.3: *Model estimate during the 2008-2015 Zero Lower Bound period.*

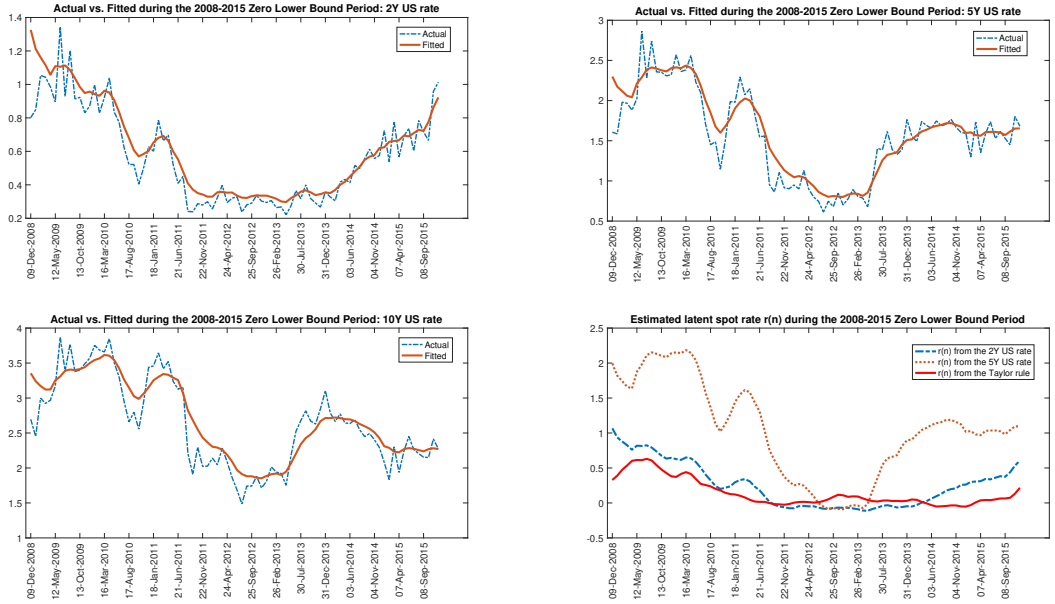

particular, on the Taylor rule (red line) estimates the evolution of the latent spot rate r_n near the zero-boundary over the entire ZLB period. This outcome might allow model inference to partially address the criticalities arising from the ZLB theme.

2.4.3 Predicting the yield curve under different scenarios

MCMC draws may be applied to generate the yield curve under different macroeconomic scenarios, by resampling credible values of model parameters along their posterior distributions. For instance, a recessionary scenario can be simulated by:

i) resampling $\widehat{\theta}$ at the 5^{th} percentile of its posterior distribution since in this environment central banks generally adopt ultra-accommodative monetary policies to support deteriorating real data;

ii) resampling $\widehat{a}_2$ at the 5^{th} percentile of its posterior distribution to simulate a typical downward slope in the OIS curve in anticipation of easing monetary policies;

iii) resampling $\widehat{a}_3$ at the 95^{th} percentile of its posterior distribution to simulate the eq-

Figure 2.4: *Recession scenario yield curve (red) and market yield curve (blue) at different maturities (horizontal axis).*

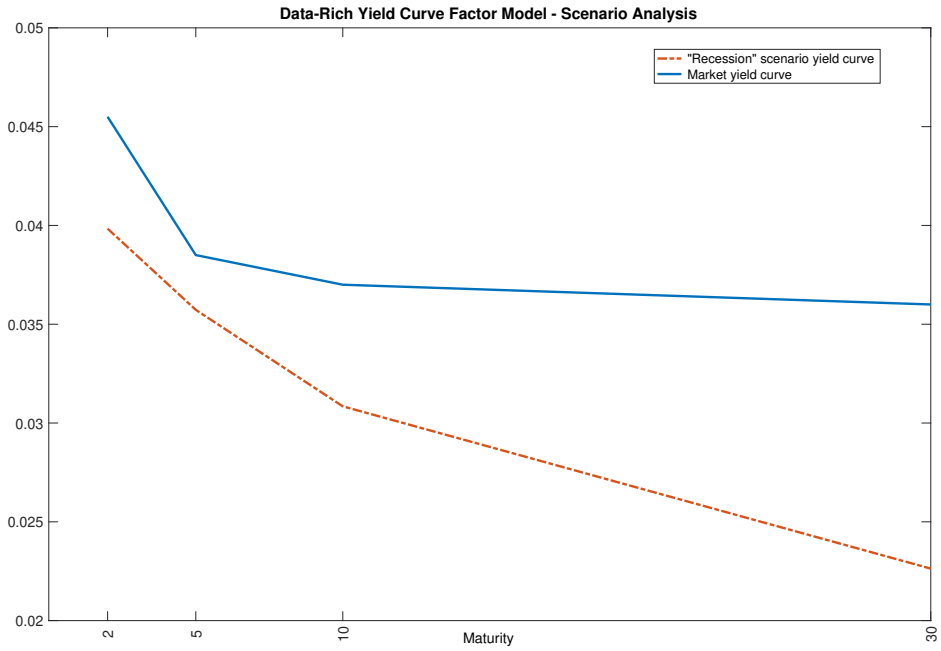

uity market risk-off generated by worsening data on economic growth and company earnings.

Figure 2.4 shows the model projection of the yield curve under the *Recession* scenario. In this environment, the entire term structure is expected to move downward, with longer rates falling quite substantially since investors tend to switch their allocation from risky assets to bonds with longer maturities, in response to market turmoil. In order to further support decisions of asset allocation, we identify 4 different macroeconomic scenarios, namely *Expansion*, *Persistent Inflation and Stable Growth*, *Normalising inflation and Slowdown* and *Recession*. In this scheme, we follow a traditional decomposition of the economic cycle. Macroeconomic shocks are well identified by the Taylor rule as it connects the pattern of short-term rates to deviation of inflation or industrial production to the relative long-term target. Given the equation (2.18) in our $\mathcal{M}_2$ setup, the Taylor rule can be conveniently rearranged as

$$(i_n - r_n) = g_\pi(\pi_n - \pi_n^*) + g_y c_n + u_n, \tag{2.30}$$

Figure 2.5: *Implied regime probabilities at the end of September 2023.*

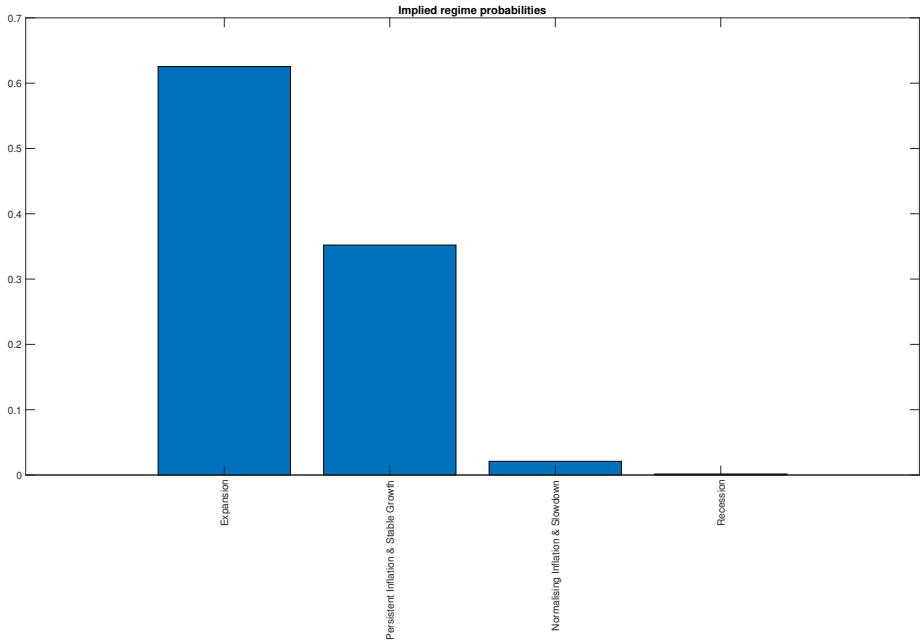

with $u_n \sim \mathcal{N}(0, \sigma_i^2)$ $i.i.d, n = 1, \ldots, T$. Thus, given the assumptions on u_n, the spread between the market rate i_n and r_n follows a normal distribution with expected value given by $g_\pi(\pi_n - \pi_n^*) + g_y c_n$ and variance by σ_i^2. On this, by selecting distressed credible percentiles for g_π and g_y over the relative posterior distributions and by doing the same for $(\pi_n - \pi_n^*)$ and y_n^{OG} along their historical values, we formalise the normal distributions of the gap $(i_n - r_n)$ under the 4 macroeconomic regimes defined above. Thus, for instance, the 95^{th} percentile is chosen to approximate the expected value of $(i_n - r_n)$ under the *Expansion* regime as this scenario identifies extremely positive shocks on both inflation and output gap. We proceed analogously for the other regimes. A likelihood ratio approach is then applied in order to estimate the probability of each regime implied in the market yield curve. Figure 2.5 shows the implied regime probabilities up to the end of September 2023.

Such a picture offers a great support when the model is applied for asset allocation since a mapping of the implied probabilities allows for evaluating the coherence of the portfolio allocation with the predominant regime. For instance, given a picture like the one at the end of September 2023, a portfolio with a particularly defensive stance looks as inappropriate as

it runs the potential risk to anticipate a sharp deterioration of the predominant *Expansion* regime towards more recessionary conditions without intermediate steps. Such a picture should raise questions about the opportunity to update the portfolio allocation in favour of a less defensive tone.

2.4.4 Tactical Asset Allocation Exercise

In order to evaluate the contribution of the augmentation at portfolio strategy level, we identify 2 macro-trading states, namely *Risk-On* and the *Risk-off* regimes. The former is obtained by summing probabilities of *Expansion* and *Persistent Inflation and Stable Growth* scenarios, while the latter by summing probabilities of *Normalising inflation and Slowdown* and *Recession* scenarios. Under the first trading state, a traditional risk-on allocation is recommended by selling the 10-year US rate (defensive asset) and buying the SP500 Index (risky asset), while in the second trading state a complementary risk-off allocation is proposed. Intensity of trading signals is calibrated to reflect the probability of the macro-trading regime.

Implied probabilities of the 4 macroeconomic scenarios are estimated under 2 different frameworks: the data-enriched model proposed in the paper and the standard Taylor rule without augmentation on the state process of r_n. We finally investigate the contribution of the augmentation by implementing the trading strategy under the both settings.

Results of the comparison are reported in figure 2.6 since mid 2022. In terms of strategy performance, the augmented model looks superior than the standard Taylor rule under both the macro-trading regimes and in trading both the asset classes. The reason behind this improvement is connected to the chart at the bottom of the figure, which reports the probability of the risk-off regime estimated under the 2 settings. Due to the lack of an explicit connection to market variables, the standard Taylor rule tends to overestimate the probability of the risk-off regime, despite solid economic conditions, and therefore to recommend a too conservative portfolio allocation. On this, the data-enriched approach shows a greater flexibility

Figure 2.6: *Contribution of the augmentation to portfolio strategy.*

Strategy Perf. Since mid 2022	Risk-On Regime		Risk-Off Regime	
Asset	Sell 10Y rate	Buy SP500	Buy 10Y rate	Sell SP500
Augmented Model	4.93%	13.98%	1.34%	-6.92%
Taylor Rule	4.26%	12.35%	0.82%	-8.10%
Delta	***0.67%***	***1.63%***	***0.52%***	***1.18%***

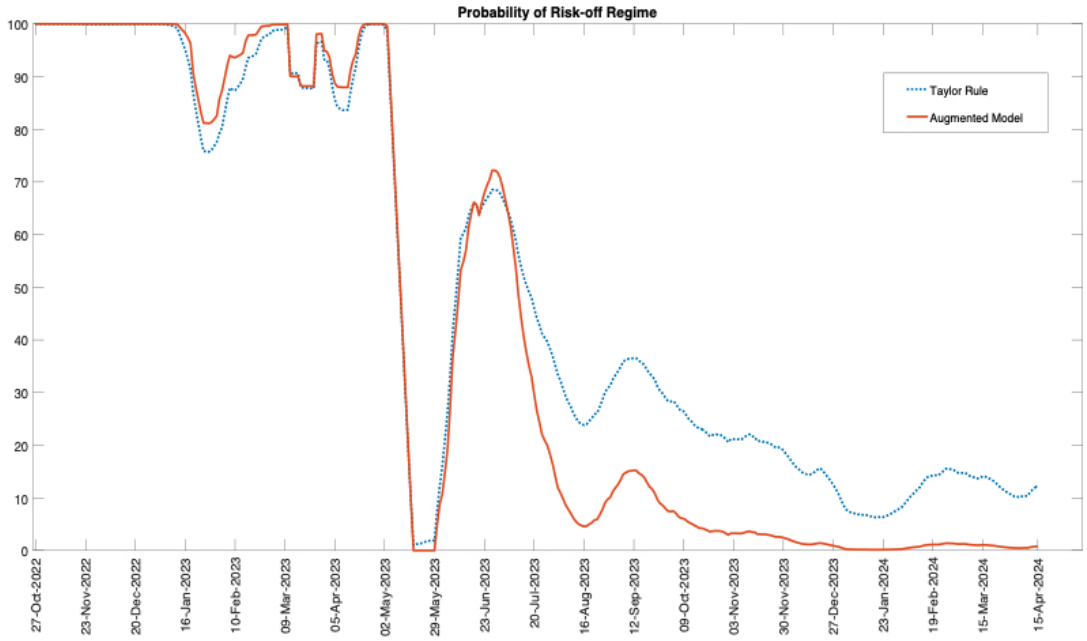

in determining the proper macro-trading scenario, by reducing timely the probability of the risk-off regime, in line with numbers on real data. Consistently with this achievement, the augmentation is able to suggest a more aggressive portfolio allocation which appears strictly coherent with the economic backdrop.

2.5 Conclusions

A data-enriched term-structure model for interest rates is presented following a general term-structure architecture based on non-arbitrage arguments, where yields are a linear function of a few unobserved latent factors. The pioneering approach introduced by Vasicek (1977) and Dothan (1978) derives the entire yield curve from the unobserved instantaneous rate r_t, which works in terms of interconnection between finance and macro-economic perspective. First of all, the short-term rate is a fundamental building block for rates of longer maturities as long yields are formalised in terms of risk-adjusted averages of expected future short-term rates. On the other hand, the short-term rate is the tool under the direct control of central banks to achieve a sustainable balance between economic growth and inflation expectations. In out paper we propose a state-space term structure model which includes the spot rate as a state process and where the measurement equation accounts for yields at different maturities. Instead of focusing on the state process, we deviate from the standard literature by incorporating through data-augmentation additional exogenous variables into the measurement component of the system, where all the measurement equations are driven by the state process and the augmentation allows for improving the estimate of latent spot rate.

In order to make the evaluation of the yield curve more reactive to market events, we apply data-augmentation to connect the diffusive process of the spot rate to monetary policy decisions, risk-on/risk-off of the equity market and macroeconomic shocks. In particular, the Taylor rule is introduced in order reconcile the estimate of the yield curve to macroeconomic variables.

We propose a Bayesian framework for model inference based on an efficient posterior approximation procedure. The computational efficiency follows from the linearity of the model, which allows for Kalman filtering and smoothing recursions. The paper presents an innovative and interpretable way to estimate the risk premium as a combination of explicit sources of market risk. The model is applied to the US yield curve sampled at a monthly frequency from December 2000 up to May 2024. The augmentation and Bayesian inference allow for

generating projections of the yield curve fitting market scenarios connected to the economic cycle. Such a simulation provides great support to decisions of tactical asset allocation since it allows for evaluating the coherence of the portfolio allocation with the predominant macroeconomic regime. Warning divergences should raise questions about the opportunity to revise the asset allocation in a more consistent way.

In the application of the model, a trading strategy is provided. On this, the data-enriched approach shows a greater flexibility than a standard modelling without augmentation in determining the proper macro-trading scenario. Consistently with this achievement, the augmentation is able to suggest a portfolio allocation which appears strictly coherent with the economic backdrop.

Bibliography

Bekaert, G., Engstrom, E., and Grenadier, S. (1989). Stock and Bond Returns with Moody Investors. *Journal of Empirical Finance*, 17:867–894.

Campbell, J. Y. and Ammer, J. (1993). What Moves the Stock and Bond Markets? A Variance Decomposition for Long-Term Asset Returns. *Journal of Finance*, 48:3–37.

Carlin, B. P. and Chib, S. (1995). Bayesian Model Choice via Markov Chain Monte Carlo. *Journal of the Royal Statistical Society, Series B*, B(57):473–484.

Casella, G. and George, E. I. (1992). Explaining the Gibbs sampler. *The American Statistician*, 46:167–174.

Castelnuovo, E., Greco, L., and Raggi, D. (2014). Policy rules, regime switches, and trend inflation: an empirical investigation for the United States. *Macroeconomic Dynamics*, 18:920–942.

Christensen, J. H. E. and Rudebusch, G. D. (2012). The Response of Interest Rates to US and UK Quantitative Easing. *Economic Journal*, 122:F385–F414.

Clarida, R., Galì, J., and Gertler, M. (2000). Monetary Policy Rules and Macroeconomic Stability: Evidence and Some Theory. *Quarterly Journal of Economics*, 115:147–180.

Commandeur, J. F. and Koopman, S. J. (2007). *An Introduction to State Space Time Series Analysis*. Oxford University Press.

Dai, Q. and Singleton, K. J. (2000). Specification Analysis of Affine Term Structure Models. *Journal of Finance*, 55:1943–1978.

Dothan, U. L. (1978). On the Term Structure of Interest Rates. *Journal of Financial Economics*, 6:59–69.

Duan, J. and Simonato, J. (1999). Estimating and Testing Exponential-Affine Term Struc-

ture Models by Kalman Filter. *Review of Quantitative Finance and Accounting*, 13:111–135.

Duffee, G. R. (2002). Term premia and interest rate forecasts in affine models. *The Journal of Finance*, 57(1):405–443.

Duffee, G. R. and Stanton, R. H. (2012). Estimation of dynamic term structure models. *The Quarterly Journal of Finance*, 2(02):1250008.

Duffie, D. and Kan, R. (1996). A Yield-Factor Model of Interest Rates. *Mathematical Finance*, 6:379–406.

Elerian, O., Chib, S., and Shephard, N. (2001). Likelihood inference for discretely observed nonlinear diffusions. *Econometrica*, 69(4):959–993.

Eraker, B. (2001). MCMC analysis of diffusion models with application to finance. *Journal of Business & Economic Statistics*, 19(2):177–191.

Frühwirth-Schnatter, S. and Geyer, A. L. J. (1998). Bayesian estimation of econometric multifactor Cox Ingersoll Ross models of the term structure of interest rates via MCMC methods. *Working Paper, Department of Statistics, Vienna University of Economics and Business Administration.*

Gelfand, A. E. and Smith, A. F. M. (1990). Sampling-based approaches to calculating marginal densities. *Journal of the American Statistical Association*, 85:398–409.

Geman, S. and Geman, D. (1984). Stochastic relaxation, Gibbs distributions and the Bayesian restoration of images. *IEEE Transactions on Pattern Analysis and Machine Intelligence*, 6:721–740.

Gürkaynak, R. S., Sack, B. T., and Swanson, E. P. (2007). Market-Based Measures of Monetary Policy Expectations. *Journal of Business & Economic Statistics*, 25:425–436.

Hall, A. D., Anderson, H. M., and Granger, C. W. J. (1992). A Cointegration Analysis of Treasury Bill Yields. *Review of Economics and Statistics*, 74:116–126.

Hamilton, J. D. (1987). Rational-Expectations Econometric Analysis of Change in Regime. An Investigation of the Term Structure of Interest Rates. *Journal of Economic Dynamics and Controll*, 12:385–423.

Hastings, W. K. (1970). Monte Carlo sampling methods using Markov chains and their application. *Biometrika*, 57:97–109.

Hördahl, P., Tristani, O., and Vestin, D. (2006). A joint econometric model of macroeconomic and term-structure dynamics. *Journal of Econometrics*, 131:405–444.

Jones, C. (1998). Bayesian Estimation of Continuous-Time Finance Models. *Working Paper, Simon School of Business*.

Judd, J. and Rudebush, G. (1999). Taylor's Rules and the Fed: 1970-1997. *Economic Review, Federal Reserve Bank of San Francisco*, 3:3–16.

Kim, C. J. and Nelson, C. R. (1999). *State-Space Models with Regime Switching: Classical and Gibbs-Sampling Approaches with Application*. MIT Press: Cambridge MA.

Kim, H. D. and Wright, J. H. (2005). An Arbitrage-Free Three-Factor Term Structure Model and the Recent Behavior of Long-Term Yields and Distant-Horizon Forward Rates. *Federal Reserve Board, Washinton D.C.*, 33.

Kloeden, P. E. and Platen, E. (2018). Numerical methods for stochastic differential equations. In *Nonlinear dynamics and stochastic mechanics*, pages 437–461. CRC Press.

Koop, G. (2003). *Bayesian Econometrics*. J. Wiley, New York.

Kozicki, S. (1999). How Useful are Taylor Rules for Monetary Policy? *Economic Review, Federal Reserve Bank of Kansas City*, Second Quarter:5–33.

Kuttner, S. P. (2001). Moneatery Policy Surprise and Interest Rates: Evidence from Fed Funds Futures Market. *Journal of Monetary Economics*, 47:523–544.

Lamoureux, C. G. and Witte, M. D. (2002). Empirical analysis of the yield curve: the information in the data viewed through the window of Cox, Ingersoll and Ross. *Journal of Finance*, LVII:1479–1520.

Lettau, M. and Watcher, J. (2011). The Term Structure of Equity and Interest Rates. *Journal of Financial Economics*, 101:90–113.

Litterman, R. B. (1986). Forecasting with Bayesian Vector Autoregressions-Five Years of Experience. *Journal of Business and Economic Statistics*, 4:25–38.

Lloyd, S. P. (2020). Estimating Nominal Interest Rates Expectations: Overnight Indexed Swaps and the Term Structure. *Journal of Banking & Finance*, 119:105915.

Piazzesi, M. and Swanson, E. T. (2008). Futures prices as risk-adjusted forecasts of monetary policy. *Journal of Monetary Economics*, 55:677–691.

Polson, N. G., Muller, J. R., and Muller, P. (2002). Affine state-dependent variance models. *Institute of Statistics and Decision Sciences, Duke University*.

Robert, C. P. (2007). *The Bayesian Choice*. Springer.

Robert, C. P. and Casella, G. (2004). *Monte Carlo Statistical Methods (Second Edition)*. University of Chicago.

Robert, C. P., Celeux, G., and Dielbold, F. X. (1993). Bayesian estimation of hidden Markov models: A stochastic implementation. *Statistics and Probability Letters*, 16:77–83.

Rudebusch, G. D. and Wu, T. (2008). A Macro-Finance Model of the Term Structure, Monetary Policy and the Economy. *The Economic Journal*, 118:906–926.

Sanford, A. D. and Martin, G. M. (2005). Simulation-based Bayesian estimation of an affine term structure model. *Computational Statistics & Data Analysis*, 49(2):527–554.

Taylor, J. B. (1999). *Monetery Policy Rules*. Chicago University Press.

Vasicek, O. (1977). An Equilibrium Characterization of the Term Structure. *Journal of Financial Economics*, 5:177–188.

Woodford, M. (2012). Methods of Policy Accomodation at the Interest-Rate Lower Bound. *Economic Policy Symposium - Jackson Hole*, 1:185–288.

Zellner, A. (1971). *An Introduction to Bayesian Inference in Econometrics*. J. Wiley, New York.

Chapter 3

On Modelling and Forecasting Multivariate Realized Volatility: a Time-varying Bayesian Markov Switching VAR Model

3.1 Introduction

The risk of financial returns is crucial for asset pricing, risk management and portfolio management. Besides individual return volatilities, estimating the covariance structure between assets in portfolio is of great importance to efficiently support decisions of tactical asset allocation.

The traditional approach to estimate the covariance matrix relies on multivariate generalized autoregressive conditional heteroscedasticity models, such as the constant conditional correlation GARCH of Bollerslev (1986), the dynamic conditional correlation GARCH of Engle (2002) or the BEEK extension of Engle and Kroner (1995). Literature on multivariate GARCH models has been advancing towards more flexible specifications which are applicable to portfolios with a large number of assets. These methods have been growing in popularity over last decades, although they still suffer from the curse of dimensionality problem.

Increased availability of high-frequency data in the last decade emerges in development of new non-parametric approaches for modelling volatility in a multivariate setup. While in the GARCH and stochastic volatility framework the volatility process is latent, realized covariance methods employ high-frequency data for modelling the correlative structure of underlying assets, making it effectively observable.

A considerable amount of research has typically focused on univariate volatilities, with the final covariance matrix arising from disjoint models on variance and correlation. A common problem affecting this approach is that the covariance matrix is not guaranteed to be positive definite. In order to deal with the estimate of the entire covariance matrix, Voev (2007) proposed a method where univariate volatilities and correlations are properly combined to produce positive definite matrices. However, the drawback of this framework assumes that the potential volatility spillovers might be negligible.

A pioneer approach for covariance matrix modelling is provided in Barndorff-Nielsen and Shephard (2004), where the theory of realized covariation is introduced. Realized covariance matrices are ex-post measures of covariations on high-frequency data which need to

be further modelled. Notable contributions on this topic are provided, for instance, by the Wishart autoregression model (WAR) of Gouriéroux et al. (2009), followed by numerous extensions presented by Bonato (2009) and Bonato et al. (2013). Under graphical model setting, important references on simulation of inverse Wishart distributions are in Carvalho et al. (2007), Wang and West (2009) and Carvalho and West (2007).

As different modelling approach, Bauer and Vorkink (2011) suggested to estimate market volatility using the matrix-logarithm transformation to guarantee the positive definiteness of the covariance matrix. The Wishart autoregression model, however, is unable to capture the long memory dependence in the correlation structure of returns and is still built on latent processes, whose interpretation remains difficult. The study of Bauer and Vorkink (2011) differs from other contributions since it puts great emphasis primarily on the forecasting power of the model rather than on estimating the entire realized covariance matrix and the connected volatility spillovers.

The realized covariance matrix can be estimated by taking the sum of the outer product of discretely sampled vectors of high-frequency returns over a given horizon. Zhang et al. (2005) proposed an extension to this approach by averaging realized covariations over different non-overlapping subsamples. As shown by Barndorff-Nielsen and Shephard (2004), the realized covariance is a consistent estimator of the covariance matrix but it might be biased and inconsistent if micro-structure noise is present in the data. Sparse sampling might be used to mitigate such inefficiency. In addition, the covariance matrix estimated by realized covariations might not necessarily be positive semi-definite. To overcome these problems, Barndorff-Nielsen et al. (2011) introduced the multivariate realized kernel estimator, which efficiently manages the dependence structure of returns and guarantees the covariance matrix to be positive definite.

In this paper, I contribute to literature by proposing a 2-state Time-Varying Bayesian Markov Switching VAR for modelling state-dependent volatility spillovers across assets in a global portfolio. A milestone on finite mixture distributions and Markov Switching models is pro-

vided by Frühwirth-Schnatter (2006). In this paper regime switches are governed by time-varying transition probabilities, whose stochastic process is driven by exogenous factors, namely early warnings, since they show notable leading properties in forecasting regime changes. The paper provides that market expectations on monetary policy work properly as early-warning signal over the path of the transition probabilities. Such expectations are approximated by changes in the 3-month US T-Bill rate. Following Barndorff-Nielsen et al. (2011), the model is applied to realized volatilities estimated on the multivariate realized kernel method.

In the paper I follow a Bayesian approach to make inference about model parameters. Bayesian inference (e.g., see Zellner, 1971; Robert et al., 1993; Koop, 2003; Robert, 2007) yields great popularity in economic applications as it allows parameters prior information to be integrated in the model estimating process. In a Bayesian framework, inference is therefore a learning process based not only on data but also on extra-sample information. The combination of these two sources of inputs is efficient since it accounts for the degree of uncertainty about data and priors.

I follow a data-augmentation approach and a Markov Chain Monte Carlo (MCMC) procedure for posterior approximation (e.g., see Hastings, 1970; Carlin and Chib, 1995; Robert and Casella, 2004). I propose a new and efficient Gibbs Sampling algorithm following, for instance, Geman and Geman (1984), Gelfand and Smith (1990) and Casella and George (1992). Other notable references on Bayesian Panel Markov-switching VAR models are provided by Agudze et al. (2022) and Billio et al. (2016).

The rest of the paper is structured as follows. Section 2 provides the background about estimate of the realized covariance matrix from daily returns. Section 3 describes VAR models and their extension into a Markov Switching framework. Section 4 talks about Bayesian inference for VAR models in a context of hierarchical priors. Section 5 presents a monthly dataset from December 2000 up to May 2024 and provides an application of the model.

3.2 Estimation of Realized Covariance Matrix from High Frequency data

Let $\mathbf{p}_t$ be a q-dimensional price process which evolves over time according to the following dynamics:

$$d\mathbf{p}_t = \boldsymbol{\mu}_t dt + \boldsymbol{\Sigma}_t d\boldsymbol{W}_t + d\boldsymbol{J}_t, \quad t \in [0, T] \tag{3.1}$$

where $\boldsymbol{\mu}_t$ is a predictable component, $\boldsymbol{\Sigma}_t$ is a $(q \times q)$ volatility process, $\boldsymbol{W}_t$ is a q-dimensional Brownian motion and $\boldsymbol{J}_t$ is a jump process. Given synchronized data, Andersen et al. (2003) and Barndorff-Nielsen and Shephard (2004) suggested to estimate the realized covariance of returns by taking the outer product of the observed high-frequency returns over a defined period. More formally, let $\Delta_k \mathbf{p}_t$ be denoted as a discretely sampled vector of k-th intra-period log-returns in $[t-1, t]$, with N intra-period observations available for each asset j, with $j = 1, 2, \ldots, q$. A simple estimator of realized covariance is defined as

$$\hat{\boldsymbol{\Sigma}}_t^{(RC)} = \sum_{k=1}^{N} (\Delta_k \mathbf{p}_t)(\Delta_k \mathbf{p}_t)'. \tag{3.2}$$

As shown by Barndorff-Nielsen and Shephard (2004), realized covariance is a consistent estimator of integrated covariance and asymptotically mixed normal. However, the estimator is biased and becomes inconsistent if micro-structure noise is present in the data. Sparse sampling might be used to mitigate the problem. On this topic, an interesting contribution is provided by Zhang et al. (2005), whose paper suggested to use efficiently all data by averaging covariance matrices calculated over different subsamples. More formally, given M non-overlapping subsamples, the final realized covariance matrix in given by

$$\hat{\boldsymbol{\Sigma}}_t^{(RCSS)} = \frac{1}{M} \sum_{i=1}^{M} \hat{\boldsymbol{\Sigma}}_{t,i}^{(RC)}, \tag{3.3}$$

where $\hat{\mathbf{\Sigma}}_{t,i}^{(RC)}$ is the covariance matrix calculated over the subsample i. On covariance matrix modelling, Barndorff-Nielsen et al. (2011) introduced the Multivariate Realized Kernel (MRK) estimator, which guaranties the covariance matrix to be positive semi-definite. Moreover, such estimator leads to a consistent estimation of realized covariance also with noise in the data. Thus, following Barndorff-Nielsen et al. (2011), the MRK estimator is defined as

$$\hat{\mathbf{\Sigma}}_t^{(MKR)} = \sum_{h=-N}^{N} k\left(\frac{h}{H}\right)\mathbf{\Gamma}_h, \tag{3.4}$$

where $\mathbf{\Gamma}_h$ is the h-th realized autocovariance, with $\mathbf{\Gamma}_h = \mathbf{\Gamma}'_{-h}$ for $h<0$, and $k(\cdot)$ is a non-stochastic weight function. For empirical implementation of the model, kernel function and bandwidth parameters need to be defined. Following Barndorff-Nielsen et al. (2011), the Parzen kernel is applied, since it satisfies the smoothness conditions and guarantees the matrix $\hat{\mathbf{\Sigma}}_t^{(MKR)}$ to be positive semi-definite. In the application of the paper I apply the optimal bandwidth derived in Barndorff-Nielsen et al. (2011).

3.3 Modelling and Forecasting Multivariate Volatility

Modelling and forecasting a conditional covariance matrix of asset returns is pivotal to asset allocation. In order to develop a valid multivariate framework, one needs to specify a model which produces symmetric and positive semi-definite covariance matrix predictions. On this point, two different types of approach have been recently proposed. The former argues in favour of modelling the Cholesky factorization of the covariance matrix following, for instance, the notable contribution in Chiriac and Voev (2011). The latter arises from direct modelling of the covariance dynamics as proposed, for instance, in Bonato (2009) and in Jin and Maheu (2013).

To ensure positive semi-definite covariance matrices, Chiriac and Voev (2011) proposed to apply the Cholesky decomposition to the covariance matrix. More formally, this approach

is set to model the lower triangular elements of the Cholesky factorization as

$$\mathbf{X}_t = vec(\mathbf{F}_t), \tag{3.5}$$

where $\mathbf{F}_t$ are Cholesky factors given $\mathbf{F}_t'\mathbf{F}_t = \mathbf{\Sigma}_t$ and $\mathbf{X}_t$ is a $(m\times 1)$ vector, with $m = q(q+1)/2$. Forecasts of the covariance matrix are then obtained by reverse transformation.

Heterogeneous autoregression (HAR) models were introduced by Corsi (2009) to approximate the long-memory effect on realized volatility . This approach was specifically designed for a univariate framework. In their original version, HAR models have an autoregressive structure and combine volatilities measured at different frequencies (daily, weekly and monthly). Based on this backdrop, Chiriac and Voev (2011) proposed a Generalized Heterogeneous Autoregression approach (GHAR) as multivariate extension of HAR methods, to model the vector of Cholesky factors $\mathbf{X}_t$ as

$$\mathbf{X}_{t+1}^{(1)} = c + \beta^{(1)}\mathbf{X}_t^{(1)} + \beta^{(5)}\mathbf{X}_t^{(5)} + \beta^{(22)}\mathbf{X}_t^{(22)} + \boldsymbol{\epsilon}_t, \tag{3.6}$$

where 1, 5 and 22 stand for day, week (5 days) and month (22 days) respectively, c is a vector $(m \times 1)$ of constants, $\beta^{(i)}$ are scalar parameters and $\mathbf{X}_t^{(i)}$ are averages of lagged daily Cholesky factors, e.g. $\mathbf{X}_t^{(5)} = \frac{1}{5}\sum_{i=0}^{4}\mathbf{X}_{t-i}$, with $\epsilon_t \sim i.i.d.$, for $t = 1, \ldots, T$. To obtain parameter estimate, Ordinary Least Squared (OLS) is used.

The standard GHAR approach does not take into account the fact that lagged realized covariances are measured with error. Bollerslev et al. (2018) provided an intuitive modification to accomodate this issue in the context of the equation (3.6), by introducing the idea of realized quarticity. They proposed a new dynamic specification for the high-frequency realized covariances, in which they allow parameters of the model to depend linearly on the measurement errors of covariance matrix estimates. The new parametrisation arises from a relatively simple formulation, where individual elements of the covariance matrix are allowed to exhibit distinct dependencies as a function of the measurement errors variances. Hence,

equation (3.6) is updated as

$$\mathbf{X}_{t+1}^{(1)} = c + \boldsymbol{\beta}_t^{(1)} \circ \mathbf{X}_t^{(1)} + \beta^{(5)}\mathbf{X}_t^{(5)} + \beta^{(22)}\mathbf{X}_t^{(22)} + \boldsymbol{\epsilon}_t, \tag{3.7}$$

$$\boldsymbol{\beta}_t^{(1)} = \beta_{(1)}\boldsymbol{i} + \beta_{(1Q)}\boldsymbol{\pi}_{t-1}, \tag{3.8}$$

where $\circ$ denotes the Hadamard product, $\boldsymbol{i}$ is a m-dimensional vector of ones, $\beta_{(1)}$ and $\beta_{(1Q)}$ are scalars and $\boldsymbol{\pi}_{t-1} = \text{diag}(\hat{\boldsymbol{\Sigma}}_t^{(MKR)})^{0.5}$, therefore it collects the vector of asymptotic deviations for each of the individual element of the estimated realized covariance matrix. More general specifications in which $\beta^{(5)}$ and $\beta^{(22)}$ are similarly allowed to depend on measurement errors could be implemented. However, the magnitude of the errors generally decreases with the horizon, thus restricting the attenuation effect to the lagged $\mathbf{X}_t^{(1)}$ only appears to be fairly appropriate. Under a forecasting perspective, the scheme achieves a relevant trade-off between the use of long historical samples for a more accurate estimate of realized covariances, but with a potential forecasting bias, or restricting the estimation to more recent observations to better capture the short-term dynamics, but under the potential risk of increasing forecast errors. See Bollerslev et al. (2018) for a detailed reference on the model.

This modelling strategy has been growing in popularity over the last decade as it proposes an innovative solution to estimate symmetric and positive semi-definite covariance matrices. Nevertheless, it suffers from a few disadvantages deriving from the general setup of the approach.

On this point, the GHAR framework assumes the same structure for all elements of the Cholesky factors in $\mathbf{X}_t$ and this might imply a quite strong assumption in many empirical applications. But much more importantly, a common structure of $\mathbf{X}_t$ leaves a significant amount of information in the error term. Moreover, since the OLS estimate captures the separate dynamics of variances and covariances, the potential dependence between equations remains unmodelled in the residuals. To overcome this problem, following Bonato (2009) and Jin and Maheu (2013) about the idea of directly modelling the covariance dynamics,

in the paper I propose a Bayesian Markov-Switching VAR model on realized log-volatilities. Such model class allows for flexible dependence patters and potential volatility spillovers across assets in portfolio.

3.4 Markov-Switching VAR Models (MSVAR)

Vector autoregressions are linear time-series models designed to capture the joint dynamics of multiple time series. In the reduced-form, VAR models have the following setup:

$$\mathbf{y}_t = \boldsymbol{B}_1\mathbf{y}_{t-1} + \boldsymbol{B}_2\mathbf{y}_{t-2} + \ldots + \boldsymbol{B}_p\mathbf{y}_{t-p} + \boldsymbol{D}\mathbf{z}_t + \boldsymbol{\epsilon}_t, \tag{3.9}$$

where $\mathbf{y}_t$ is a q-dimensional vector, $\mathbf{z}_t$ is a $(d \times 1)$ vector of exogenous variables, $\boldsymbol{B}_j$ and $\boldsymbol{D}$ are $(q \times q)$ and $(q \times d)$ matrices of coefficients and $\boldsymbol{\epsilon}_t$ is a $(q \times 1)$ vector of one-step ahead $i.i.d$ forecast errors with $\boldsymbol{\epsilon}_t \sim \mathcal{N}(\mathbf{0}, \boldsymbol{\Sigma})$, for $t = 1, \ldots, T$.
The VAR model in equation (3.9) can be rearranged as

$$\mathbf{y}_t = \boldsymbol{X}_t\boldsymbol{\beta} + \boldsymbol{\epsilon}_t, \tag{3.10}$$

where $\boldsymbol{X}_t = (\boldsymbol{I}_q \otimes \mathbf{x}_{t-1})$, $\mathbf{x}_{t-1} = (\mathbf{y}_{t-1}^{'}, \ldots, \mathbf{y}_{t-p}^{'}, \mathbf{z}^{'}{}_t)^{'}$ and $\boldsymbol{\beta} = vec(\boldsymbol{B}_1, \boldsymbol{B}_2, \ldots, \boldsymbol{B}_p, \boldsymbol{D})$. More formally, VAR model in equation (3.10) has a SUR representation, with unknown parameters $\boldsymbol{\beta}$ and $\boldsymbol{\Sigma}$.
Back to the paper, let $\mathbf{y}_t$ be a q-dimensional vector of monthly realized log-volatilities based on the multivariate kernel estimator proposed by Barndorff-Nielsen et al. (2011). Moreover, let $\mathbf{s}_t = (s_{1t}, \ldots, s_{mt})$ be a vector of latent variables with values in {1,...,M}. Denote with $\mathbf{y}_{1:T} = (\mathbf{y}_1, \ldots, \mathbf{y}_T)$ and $\mathbf{s}_{1:T} = (\mathbf{s}_1, \ldots, \mathbf{s}_T)$ the collection over time of realized log-volatilities and latent variables. Therefore, a convenient representation of a MSVAR model is given by

$$\mathbf{y}_t = \boldsymbol{X}_t\boldsymbol{\beta}(s_t) + \boldsymbol{\epsilon}_t, \boldsymbol{\epsilon}_t \sim \mathcal{N}(\mathbf{0}, \boldsymbol{\Sigma}(s_t)), \tag{3.11}$$

$$\boldsymbol{\beta}(s_t) = \sum_{j=1}^{M} \boldsymbol{\beta}_j \mathbb{I}(s_t = j), \tag{3.12}$$

$$\boldsymbol{\Sigma}(s_t) = \sum_{j=1}^{M} \Sigma_j \mathbb{I}(s_t = j). \tag{3.13}$$

with $t = 1, \ldots, T$ and $\boldsymbol{\beta}_j = vec(\boldsymbol{B}_{1j}, \boldsymbol{B}_{2j}, \ldots, \boldsymbol{B}_{pj}, \boldsymbol{D}_j)$ are the regime-specific vectors of coefficients.

Following Hamilton (1994), transition probabilities $p_{ij} = \mathbb{P}(s_t = i | s_{t-1} = j)$ are assumed to be time-invariant and properly collected into the transition matrix P

$$P = \begin{pmatrix} p_{11} & \cdots & p_{M1} \\ \vdots & \ddots & \vdots \\ p_{1M} & \cdots & p_{MM} \end{pmatrix},$$

where $\sum_{j=1}^{M} p_{ij} = 1 \ \forall i$.

In the context of Early Warning Markov Switching (EWMS) models, transition probabilities are modelled in terms of stochastic variables, whose process is governed by exogenous factors with leading properties in forecasting regime switches. Notable contributions on this topic are provided by Billio and Casarin (2011), Billio et al. (2016) and Agudze et al. (2022), where Bayesian Markov Switchig VAR are proposed for business cycle modelling.

Time-varying transition probabilities may be assumed as following a Probit model, with early warnings collected into the vector $\mathbf{w}_{t-1}^{'}$. Therefore

$$p_{ij,t} = \Phi(\mathbf{w}_{t-1}^{'} \boldsymbol{\gamma}_{ij}), \tag{3.14}$$

with $\Phi(\cdot)$ denoting the Gaussian CDF function and $\boldsymbol{\gamma}_{ij}$ the vector of unknown parameters to be estimated. Kim et al. (2008) and Amisano and Fagan (2013), for instance, provided relevant references about Markov regime-switching regression models with endogenous switching.

3.5 Bayesian-Inference

3.5.1 Introduction

Denote with $\mathbf{y} = (\mathbf{y}_1, \ldots, \mathbf{y}_T)$ and $\mathbf{s} = (s_1, \ldots, s_T)$ the collection of observable and latent variables, respectively. A Bayesian statistical model with latent variable is given by a parametric model $f(\mathbf{y}|\boldsymbol{\theta}, \mathbf{s})$ for the observable variable $\mathbf{y}$, a parametric model $f(\mathbf{s}|\boldsymbol{\theta})$ for the latent variable $\mathbf{s}$ and a prior distribution $\pi(\boldsymbol{\theta})$ on the vector of parameters $\boldsymbol{\theta}$, where $\boldsymbol{\theta} = (\boldsymbol{B}_{ks_t}, \boldsymbol{D}_{s_t}, \boldsymbol{\Sigma}_{s_t}, \boldsymbol{\gamma}_{ij})$, with $k = 1, \ldots, p$ and $i, j, s_t = 1, \ldots, M$.
The inference is then based on the joint distribution of $\boldsymbol{\theta}$ and $\mathbf{s}$ conditional on $\mathbf{y}$ (data), called posterior distribution and defined by

$$\pi(\boldsymbol{\theta}, \mathbf{s}|\mathbf{y}) = \frac{f(\mathbf{y}|\boldsymbol{\theta}, \mathbf{s}) f(\mathbf{s}|\boldsymbol{\theta}) \pi(\boldsymbol{\theta})}{\int f(\mathbf{y}|\boldsymbol{\theta}, \mathbf{s}) f(\mathbf{s}|\boldsymbol{\theta}) \pi(\boldsymbol{\theta}) d\boldsymbol{\theta}}, \tag{3.15}$$

where $f(\mathbf{y}|\boldsymbol{\theta}, \mathbf{s}) f(\mathbf{s}|\boldsymbol{\theta})$ represents the complete-data likelihood. Since the denominator is not a function of $\boldsymbol{\theta}$, it is common to rewrite the posterior distribution in terms of the following proportionality:

$$\pi(\boldsymbol{\theta}, \mathbf{s}|\mathbf{y}) \propto f(\mathbf{y}|\boldsymbol{\theta}, \mathbf{s}) f(\mathbf{s}|\boldsymbol{\theta}) \pi(\boldsymbol{\theta}). \tag{3.16}$$

3.5.2 Prior Distributions

Prior distributions reflect any information the researcher has before seeing the data. It is common to choose particular classes of priors which are easy to interpret and make computations more efficient. Natural coniugate priors typically have both such advantages. A coniugate prior distribution is one which, when combined with the likelihood, yields a posterior distribution which falls in the same class of distributions. In addition, a natural coniugate prior has the additional property of having the same functional form as the likelihood function. It means that the prior can be interpreted as rising from a fictitious data set from the same process which generated the actual data. Normal and Inverse Wishart

distributions are examples of natural coniugate priors. Notable details on these topics are provided for instance by Koop (2003) and Robert (2007). On Bayesian forecasting and dynamic models, pioneer references are in Harrison and West (1999) and Zhou et al. (2014).

A significant amount of research has been developed on prior distributions for VAR models and different types of prior specification have been provided. For instance, Litterman (1986) proposed the so-called Minnesota prior, which deals with a small number of hyperparameters in a equation-by-equation framework over the VAR specification. Kadiyala and Karlsson (1997) investigated a simulation strategy which applies Gaussian and Inverse-Wishart distributions as natural coniugate priors.

In this paper, I provide a Hierarchical Bayes Estimator by accommodating a VAR into a SUR model, as formalized in equation (3.10). Notable arguments on this topic are introduced by the pioneer paper of Chib and Greenberg (1995). In the hierarchical form, EWMSVAR models have the following structure:

$$\mathbf{y}_t = \boldsymbol{X}_t \boldsymbol{\beta}(s_t) + \boldsymbol{\epsilon}_t, \tag{3.17}$$

$$\boldsymbol{\beta}(s_t) = \sum_{j=1}^{M} \boldsymbol{\beta}_j \mathbb{I}(s_t = j), \tag{3.18}$$

$$\boldsymbol{\beta}_j = \boldsymbol{M_0} \boldsymbol{\psi}_j + \boldsymbol{\zeta}_j, \tag{3.19}$$

$$\boldsymbol{\psi}_j = \boldsymbol{M_1} \boldsymbol{\mu}_j + \boldsymbol{\eta}_j. \tag{3.20}$$

with $j = 1, \ldots, M$, $\boldsymbol{\zeta}_j \sim \mathcal{N}_{qp}(\mathbf{0}, \boldsymbol{D}_{0j})$ and $\boldsymbol{\eta}_j \sim \mathcal{N}_m(\mathbf{0}, \boldsymbol{D}_{1j})$.

According to Chib and Greenberg (1995), the matrices $\boldsymbol{M_0}$ and $\boldsymbol{M_1}$ are assumed to be known, where $\boldsymbol{M_1} = \boldsymbol{I_2}$ and $\boldsymbol{M_0}$ is a $(qp \times 2)$ matrix given by $\boldsymbol{M_0} = vec(\boldsymbol{M_g})$, with

$$\boldsymbol{M_g} = \begin{bmatrix} 0 & 1 \\ \vdots & \vdots \\ 0 & 1 \\ 1 & 0 \\ 0 & 1 \\ \vdots & \vdots \\ 0 & 1 \end{bmatrix},$$

where the ones of the first column and the zeros of the second refer to the g^{th} row of the VAR. Prior setup for model estimate is summarised in Table 3.1. Hyper-parameters on $\boldsymbol{\gamma}_{ij}$ assume a common setting for Markov Switching models where states are generally persistent with few transitions. Priors on $\boldsymbol{\psi_j}$ are set to achieve unconditional annualised volatilities within the range [5%-35%], which follows from reasonable thresholds of price variability in turbulent and in low volatility periods. Quite non-informative priors are applied on modelling $\boldsymbol{\Sigma}_j$ and $\boldsymbol{D}_{0j}$.

Table 3.1: *Parameters, prior distributions and hyper-parameters for the EWMSVAR model.*

Parameter	Distribution	Hyper-parameters
$\boldsymbol{\gamma}_{11}$	$\mathcal{N}(\boldsymbol{\mu}_{\gamma 0}, \boldsymbol{\Sigma}_{\gamma 0})$	$\boldsymbol{\mu}_{\gamma 0} = [2, 1]$, $\boldsymbol{\Sigma}_{\gamma 0} = 10 \times I_2$
$\boldsymbol{\gamma}_{12}$	$\mathcal{N}(\boldsymbol{\mu}_{\gamma 0}, \boldsymbol{\Sigma}_{\gamma 0})$	$\boldsymbol{\mu}_{\gamma 0} = [-2, 1]$, $\boldsymbol{\Sigma}_{\gamma 0} = 10 \times I_2$
$\boldsymbol{\psi}_1$	$\mathcal{N}(\boldsymbol{M}_1\boldsymbol{\mu}_1, \boldsymbol{D}_{11})$	$\boldsymbol{\mu}_1 = [-0.5, 0.5, 0]$, $\boldsymbol{D}_{11} = 0.25 \times I_3$
$\boldsymbol{\psi}_2$	$\mathcal{N}(\boldsymbol{M}_1\boldsymbol{\mu}_2, \boldsymbol{D}_{12})$	$\boldsymbol{\mu}_2 = [-1.5, 0.5, 0]$, $\boldsymbol{D}_{11} = 0.25 \times I_3$
$\boldsymbol{\Sigma}_j$	$i\mathcal{W}(\overline{\boldsymbol{\Sigma}}_j, s)$	$\overline{\boldsymbol{\Sigma}}_j = 10 \times I_q$, $s = q + 1$
$\boldsymbol{D}_{0j}$	$i\mathcal{W}(\overline{\boldsymbol{D}}_{0j}, \rho)$	$\overline{\boldsymbol{D}}_{0j} = 0.5 \times I_{qp}$, $\rho = qp + 1$

3.5.3 Posteriors Approximation

In general terms, the posterior density summarises all the information, so both prior and likelihood based, about the unknown parameters of the model. More formally, that information will be proportional to the likelihood times the prior density.

In this paper, a Bayesian approach is provided to make inference on the vector $\boldsymbol{\theta}$ of unknown parameters. Since the Bayes estimator of $\boldsymbol{\theta}$ is not available in closed form, MCMC techniques are applied. In particular, the Gibbs Sampling algorithm is implemented as simulation method to approximate joint and marginal posterior distributions by sampling from conditional posterior distributions. This method was introduced for the first time by Geman and Geman (1984); Robert and Casella (2004) provided more details about the history of the algorithm. The Gibbs sampler takes advantage of the hierarchical structure of the model, i.e. when a Bayesian model can be written as

$$\pi(\boldsymbol{\theta}, \mathbf{s}|\mathbf{y}) = \int \pi_1(\boldsymbol{\theta}, \mathbf{s}|\mathbf{y}, \lambda)\pi_2(\lambda|\mathbf{y})d\lambda. \tag{3.21}$$

The idea is to simulate from the joint distribution $\pi_1(\boldsymbol{\theta}, \mathbf{s}|\mathbf{y}, \lambda)\pi_2(\lambda|\mathbf{y})$ to approximate $\pi(\boldsymbol{\theta}, \mathbf{s}|\mathbf{y})$ as the marginal when all the conditional distributions $\pi_1(\boldsymbol{\theta}|\mathbf{y}, \mathbf{s}, \lambda)$, $\pi_2(\mathbf{s}|\boldsymbol{\theta}, \mathbf{y}, \lambda)$ and $\pi_3(\lambda|\mathbf{y}, \mathbf{s})$ are known and can be simulated (e.g., see Robert, 2007).

As an extension of the former procedure, the Gibbs sampling algorithm can be generalised for a joint distribution $\pi(\theta_1, \ldots, \theta_p)$ with full conditionals $\pi_1, \ldots, \pi_p$. Given the vector $(\theta_1^{(m)}, \ldots, \theta_p^{(m)})$ at the iteration m, it simulates:

- $\theta_1^{(m+1)}$ from $\pi_1(\theta_1|\theta_2^{(m)}, \theta_3^{(m)}, \ldots, \theta_p^{(m)})$;
- $\theta_2^{(m+1)}$ from $\pi_2(\theta_2|\theta_1^{(m+1)}, \theta_3^{(m)}, \ldots, \theta_p^{(m)})$;

  $\vdots$

- $\theta_p^{(m+1)}$ from $\pi_p(\theta_p|\theta_1^{(m+1)}, \theta_2^{(m+1)} \ldots, \theta_{p-1}^{(m+1)})$.

The Gibbs sampler yields 2 notable advantages: first of all, it does not require θ_i to be one-dimensional, and, secondly, the choice of the order of the decomposition can be entirely based on simulation reasons.

Inference on equation (3.14) applies data augmentation procedure. On this topic, Albert and Chib (1993) suggested that, by introducing latent data into the problem, a Probit

model on binary response is connected to a gaussian linear model on the continuous latent data response. This approach has different advantages. In particular, it allows exact inference on binary regression parameters and the Gibbs sampling algorithm requires simulation mainly from standard distributions. Denote with $U_1, \ldots, U_N$, N independent binary random variables, where U_i follows a Bernoulli distribution with probability of success p_i. Such a probability is related to a set of covariates in the form of $p_i = H(\mathbf{x}_i^T \boldsymbol{\gamma})$, with $i = 1, \ldots, N$, $\boldsymbol{\gamma}$ a k-dimensional vector of unknown parameters and $H()$ a known cdf connecting the probability p_i to the linear structure $(\mathbf{x}_i^T \boldsymbol{\gamma})$. In the case of Probit model, $H()$ is the standard Gaussian cdf $\Phi(\cdot)$. Denote with $Z_1, \ldots, Z_N$, N independent latent variables with $Z_i \sim N(\mathbf{x}_i^T \boldsymbol{\gamma}, 1)$ and let $U_i = 1$ if $Z_i > 0$ and $U_i = 0$ otherwise. It can be proved that U_i are independent Bernoulli variables with $p_i = P(U_i = 1) = \Phi(\mathbf{x}_i^T \boldsymbol{\gamma})$. After introducing latent data, the Gibbs sampling can be applied to make inference on the Probit model. Using standard linear model results, the posterior distribution of $\boldsymbol{\gamma}$ given $\boldsymbol{Z}$ is a multivariate normal distribution, therefore $(\boldsymbol{\gamma}|\boldsymbol{U}, \boldsymbol{Z}) \sim N(\alpha, \boldsymbol{\Theta})$, while $Z_1, \ldots, Z_N$ are independent with $(Z_i|\gamma) \sim N(\mathbf{x}_i^T \boldsymbol{\gamma}, 1)$ truncated at the left by 0 if $U_i = 1$ or at the right by 0 if $U_i = 0$. This general data augmentation procedure is now applied to equation (1.4). Let $\boldsymbol{u}_{ij} = (u_{ij,1}, \ldots, u_{ij,T})$ be a vector of binary variables with $u_{ij,t} = 1$ if $(s_t = i \cap s_{t-1} = j)$ and $u_{ij,t} = 0$ otherwise; moreover, define the vector $\boldsymbol{z}_{ij} = (z_{ij,1}, \ldots, z_{ij,T})$ of independent latent data response variables $z_{ij,1}, \ldots, z_{ij,T}$, with $u_{ij,t} = 1$ if $z_{ij,t} > 0$ and $u_{ij,t} = 0$ if $z_{ij,t} < 0$. A multi-block Gibbs sampler may be applied to make inference on the model of the paper, given $\boldsymbol{\theta} = (\mathbf{s}, \boldsymbol{\gamma}_{ij}, \boldsymbol{\beta}_j, \boldsymbol{\psi}_j, \boldsymbol{\Sigma}_j, \boldsymbol{D}_{0j})$. At the $m-$th iteration, the Gibbs sampler draws recursively:

i) the latent state vector $\mathbf{s}$:
$(\mathbf{s}^{(m)}|\mathbf{Y}, \boldsymbol{\theta}_{-s}^{(m-1)}) \sim FFBS$;

ii) the latent data response vector $\boldsymbol{z}_{ij}$:
$(\boldsymbol{z}_{ij,t}^{(m)}|u_{ij,t}^{(m)} = 1, \boldsymbol{\gamma}_{ij}^{(m-1)}) \sim N(\mathbf{w}_{t-1}' \boldsymbol{\gamma}_{ij}, 1)$ truncated at the left by 0,
$(\boldsymbol{z}_{ij,t}^{(m)}|u_{ij,t}^{(m)} = 0, \boldsymbol{\gamma}_{ij}^{(m-1)}) \sim N(\mathbf{w}_{t-1}' \boldsymbol{\gamma}_{ij}, 1)$ truncated at the right by 0;

iii) the vector $\boldsymbol{\gamma}_{ij}$:

$(\boldsymbol{\gamma}_{ij}^{(m)}|\boldsymbol{u}_{ij}^{(m)}, \boldsymbol{z}_{ij}^{(m)}) \sim N(\alpha_{ij1}, \boldsymbol{\Theta}_{ij1})$;

iv) the vector $\boldsymbol{\beta}_j$:

$(\boldsymbol{\beta}_j^{(m)}|\mathbf{Y}, \boldsymbol{\theta}_{-\beta_j}^{(m-1)}) \sim \mathcal{N}(\tilde{\boldsymbol{\beta}}, \tilde{\boldsymbol{\Omega}})$,

$\tilde{\boldsymbol{\Omega}} = (\boldsymbol{D}_0^{-1} + \sum_t \boldsymbol{X}_t' \boldsymbol{\Sigma}^{-1} \boldsymbol{X}_t)^{-1}$,

$\tilde{\boldsymbol{\beta}} = \tilde{\boldsymbol{\Omega}}(\boldsymbol{D}_0^{-1} \boldsymbol{M}_0 \boldsymbol{\psi} + \sum_t \boldsymbol{X}_t' \boldsymbol{\Sigma}^{-1} \mathbf{y}_t)$;

v) the vector $\boldsymbol{\psi}_j$:

$(\boldsymbol{\psi}_j^{(m)}|\mathbf{Y}, \boldsymbol{\theta}_{-\psi_j}^{(m-1)}) \sim \mathcal{N}(\tilde{\boldsymbol{\psi}}, \tilde{\boldsymbol{\Delta}})$,

$\tilde{\boldsymbol{\Delta}} = (\boldsymbol{D}_1^{-1} + \boldsymbol{M}_0' \boldsymbol{D}_0^{-1} \boldsymbol{M}_0)^{-1}$,

$\tilde{\boldsymbol{\psi}} = \tilde{\boldsymbol{\Delta}}(\boldsymbol{D}_1^{-1} \boldsymbol{M}_1 \boldsymbol{\mu} + \boldsymbol{M}_0' \boldsymbol{D}_0^{-1} \boldsymbol{\beta})$;

vi) the matrix $\boldsymbol{\Sigma}_j$:

$(\boldsymbol{\Sigma}_j|\mathbf{Y}, \boldsymbol{\theta}_{-\Sigma_j}^{(m-1)}) \sim \text{i}\mathcal{W}(\tilde{\boldsymbol{\Sigma}}, s+T)$,

$\tilde{\boldsymbol{\Sigma}} = \overline{\boldsymbol{\Sigma}} + \sum_t (\mathbf{y}_t - \boldsymbol{X}_t \beta)(\mathbf{y}_t - \boldsymbol{X}_t \beta)'$;

vii) the matrix $\boldsymbol{D}_{0j}$:

$(\boldsymbol{D}_{0j}|\mathbf{Y}, \boldsymbol{\theta}_{-D_{0j}}^{(m-1)}) \sim \text{i}\mathcal{W}(\tilde{\boldsymbol{D}}_{0j}, \rho+1)$,

$\tilde{\boldsymbol{D}}_{0j} = \overline{\boldsymbol{D}}_{0j} + (\boldsymbol{\beta} - \boldsymbol{M}_0 \boldsymbol{\psi})(\boldsymbol{\beta} - \boldsymbol{M}_0 \boldsymbol{\psi})'$,

with i$\mathcal{W}$ denoting the Inverse Wishart distribution. Since the Gibbs sampler works in terms of full conditional distributions, smoothed state probabilities $Pr(s_t|I_T)$ are computed, as preliminary step before drawing the latent vector $\mathbf{s}$. Precisely, the Forward Filtering Backward Sampling (FFBS) method applies the Hamilton Filter and the Kim-Nelson smoothing algorithm to compute $Pr(s_t|I_T)$ as

$$Pr(\mathbf{s}_t = i|I_T) = \sum_{i=1}^{M} Pr(\mathbf{s}_t = i, \mathbf{s}_{t+1} = j|I_T), \quad t = T, T-1, \ldots, 1. \tag{3.22}$$

See Hamilton (1994) and Kim and Nelson (1999) for a detailed account of the procedure.

3.6 Empirical Results

3.6.1 Data Description

Model inference is applied to a daily dataset from December 2000 up to May 2024, which includes variables from different markets (Bloomberg as data-provider):

1. Money market: yield to maturity of the 3-month US T-Bill rate.
2. Bond market: returns of future contract on the 2-year and 10-year US Treasury bonds and on the 10-year Bund.
3. Equity market: returns of future contract on S&P500, Nasdaq and EuroStoxx 50 indices.
4. Commodity market: returns of future contract on crude oil and natural resources (Bcom Index).
5. Fx market: returns of forward contract on Euro/Usd, Yen/Usd and Aud/Usd exchange rates.

These assets are selected in order to build a broad-invested portfolio with different sources of risk. Such a portfolio appears as a perfect candidate to investigate volatility spillovers at global portfolio level and it works as reference point to support decisions of tactical asset allocation. The composition of this portfolio follows from the MSCI portfolio classification which provides official benchmarks of various types of allocation. On this, Blitz and van Vliet (2008) investigated the importance of implementing global asset allocation strategies on a broad range of assets rather than on a concentrated portfolio. Innovative examples of portfolio allocation strategies are also presented by Bongaerts et al. (2020), Chan et al. (2000) and Rasmussen (2003), while Ang and Bekaert (2002) provided a comprehensive framework of asset allocation with regime shifts.

3.6.2 Model Estimates

After implementing the MKR estimator for modelling realized covariation, a 2-state Early Warning Markov Switching VAR (EWMSVAR) model is applied to monthly realized volatilities. The first state, namely the *Turbulence* regime, assumes high individual asset volatilities and memory effects which make spillovers somewhat permanent over time. The second state, namely the *Low Volatility* regime, shows low variability in asset pricing and temporary spillovers with rapid decay. Model selection based on AIC and BIC criteria recommends a VAR model of order 2, thus $p = 2$.

The application of the model highlights that changes in the 3-month US T-Bill rate work properly as early-warning factor. Given its short maturity, dynamics of this yield may be reasonably assumed as an efficient proxy of market expectations about forthcoming decisions of monetary policy. Selection of this rate as warning factor emerges from a couple of considerations. The augmented framework in Chapter 2 estimates a positive relationship between equity market volatility and dynamics of the spot risk-free rate r_n, therefore a rising variability in short-term rates appears to be strongly interconnected to equity volatility. Also in terms of asset pricing theory, Bekaert et al. (1989), Campbell and Ammer (1993) and Lettau and Watcher (2011), for instance, argue that the expected return of a risky asset follows a hierarchical premium puzzle structure, with the spot risk-free rate and bond yields at the beginning step, as they compensate investors for the first source of market risk, namely the *term-premium*. In particular, an increasing *term-premium* driven, for instance, by a raising volatility of the spot risk-free rate generally pushes equity prices down, with a consequent spike in their volatility, as investors are forced to require an additional premium for holding high-risky bets in their portfolio. Given this backdrop, dynamics of the spot risk-free rate becomes a significant topic for modelling cross asset volatility. Under the term structure theory, the risk-free rate defines the general level of interest rates, therefore it is strictly connected to decisions of monetary policy. In this context, the 3-month US T-Bill rate arises as a good market proxy of FED funds rates and, therefore, of the risk-free rate

for a couple of reasons: first, its very short maturity properly approximates the concept of risk-free rate and, secondly, it has an efficient pricing, driven by high trading volumes and negligible bid-ask spreads. Under this perspective, the 1-month T-Bill rate, which could be a potential alternative candidate, has a less efficient pricing due to lower trading volumes.

Inference about parameters connected to transitions probabilities and to the hierarchical structure of $\boldsymbol{\beta}_j$ is reported in Table 3.2. Estimate of $\boldsymbol{\gamma}_{12}$ and $\boldsymbol{\gamma}_{22}$ are both positive and this result is made even more consistent by credible intervals far away from zero. Therefore, changes in the 3-month US T-Bill rate have good leading properties in modelling state transitions. Specifically, when this rate climbs suddenly, the probability to persist into the *Turbulence* scenario notably increases; on the other hand, if the system lies in the *Low Volatility* regime, the probability to switch into the *Turbulence* state becomes considerable.

Table 3.2: *All results are obtained running the Gibbs Sampling with 10,000 iterations, after burning removal and thinning with rate of 20%.*

$\boldsymbol{\theta}$	$\widehat{\boldsymbol{\theta}}$	C. I.
$\widehat{\boldsymbol{\gamma}}_{11}$	0.958	$[0.0185; 1.838]$
$\widehat{\boldsymbol{\gamma}}_{12}$	2.701	$[0.689; 5.018]$
$\widehat{\boldsymbol{\gamma}}_{21}$	-1.134	$[-1.473; -0.661]$
$\widehat{\boldsymbol{\gamma}}_{22}$	3.501	$[1.324; 6.008]$
$\widehat{\boldsymbol{\psi}}_{11}$	-0.358	$[-0.458; -0.259]$
$\widehat{\boldsymbol{\psi}}_{12}$	0.515	$[0.407; 0.623]$
$\widehat{\boldsymbol{\psi}}_{21}$	-1.930	$[-2.04; -1.815]$
$\widehat{\boldsymbol{\psi}}_{22}$	0.369	$[0.248; 0.486]$

Under this perspective, announcements of tightening monetary policies in response, for instance, to increasing inflationary pressures, warn about a potential regime shift into a scenario with persistent spillovers and raising individual volatilities.

Estimate of the covariance matrix $\boldsymbol{\Sigma}$ is shown in Table 3.3. Since the number of assets q in portfolio is quite large, the curse of dimensionality problem is mitigated by assuming a state-independent covariance matrix $\boldsymbol{\Sigma}$, with $\boldsymbol{\Sigma}_1 = \boldsymbol{\Sigma}_2$. As highlighted by numbers in Table 3.3, all off-diagonal elements tend to be relative small in absolute terms, thus a VAR of order

2 looks appropriate for this application of the model.

Table 3.3: *Estimate of the covariance matrix* $\mathbf{\Sigma}$ *by running the Gibbs Sampling with 10,000 iterations, after burning removal and thinning with rate of 20%.*

$\mathbf{\Sigma_1 = \Sigma_2}$	2-y US	10-y US	10-y Bund	S&P500	Nasdaq	Stoxx	Oil	NatRes	Euro	Yen	Aud
2-y US	0.085										
10-y US	0.065	0.103									
10-y Bund	0.026	0.038	0.097								
S&P500	0.029	0.032	0.018	0.158							
Nasdaq	0.025	0.023	0.009	0.098	0.138						
Stoxx	0.029	0.027	0.021	0.081	0.062	0.136					
Oil	0.023	0.017	0.007	0.034	0.031	0.027	0.139				
NatRes	0.006	0.009	0.007	0.015	0.012	0.015	0.015	0.099			
Euro	0.019	0.019	0.021	0.022	0.018	0.024	0.013	0.009	0.088		
Yen	0.039	0.032	0.015	0.033	0.032	0.025	0.015	0.012	0.023	0.126	
Aud	0.013	0.019	0.015	0.035	0.032	0.026	0.022	0.019	0.027	0.023	0.094

The curse of dimensionality can be quite challenging even for a model that only has two regimes, and this issue is emphasised further when a global portfolio with many assets is considered. The empirical choice of setting $\Sigma_1 = \Sigma_2$ is one way to go, as it poses a quite reasonable trade-off between flexibility and model specification, which remains fairly simple in this setup. However, the simplification following from a state-independent covariance matrix may be too restrictive in different empirical applications. On this topic, Kastner (2019) addressed a pioneering approach for covariance matrix estimate in many dimensions, which could be incorporated to extend the choice of setting $\Sigma_1 = \Sigma_2$ towards a more innovative and realistic setup. The paper proposed an efficient Bayesian MCMC algorithm for modelling the covariance structure through common latent factors which follow univariate stochastic volatility processes. Moreover, additional sparsity is introduced by applying a hierarchical shrinkage prior, the Normal-Gamma prior, on the factor loadings. Denote with $\mathbf{y}_t = (y_{1t}, \ldots, y_{mt})'$ the m-dimensional return vector, with $t = 1, \ldots, T$, whose conditional distribution is given by $\mathbf{y}_t | \mathbf{\Sigma}_t \sim N_m(\mathbf{0}, \mathbf{\Sigma}_t)$. To reduce dimensionality, the $(m \times m)$ covariance matrix $\mathbf{\Sigma}_t$, with $m(m+1)/2$ free elements, is decomposed into a factor loadings matrix $\mathbf{\Lambda}$ of size $(m \times r)$, with r chosen to be much smaller than m, an r-dimensional diagonal matrix

$\mathbf{V}_t$ and an m-dimensional diagonal matrix $\mathbf{U}_t$ as

$$\mathbf{\Sigma}_t = \mathbf{\Lambda}\mathbf{V}_t\mathbf{\Lambda}^{'} + \mathbf{U}_t. \tag{3.23}$$

Elements of both $\mathbf{V}_t$ and $\mathbf{U}_t$ are allowed to evolve over time according to parametric stochastic volatility models, where

$$\mathbf{U}_t = diag(e^{(h_{1t})}, \ldots, e^{(h_{mt})}), \tag{3.24}$$

$$\mathbf{V}_t = diag(e^{(h_{m+1,t})}, \ldots, e^{(h_{m+r,t})}), \tag{3.25}$$

$$h_{it} \sim N(\mu_i + \phi_i(h_{i,t-1} - \mu_i), \sigma_i^2), \tag{3.26}$$

$$h_{m+j,t} \sim N(\phi_{m+j}h_{m+j,t-1}, \sigma_{m+j}^2), \tag{3.27}$$

with $i = 1, \ldots, m$ and $j = 1, \ldots, r$. More specifically, $\mathbf{U}_t$ describes the idiosyncratic (series-specific) variances while $\mathbf{V}_t$ contains the variances of underlying orthogonal factors $\mathbf{f}_t \sim N(\mathbf{0}, \mathbf{V}_t)$. This setup is commonly written in the hierarchical form as

$$(\mathbf{y}_t|\mathbf{\Lambda}, \mathbf{f}_t, \mathbf{U}_t) \sim N_m(\mathbf{\Lambda}\mathbf{f}_t, \mathbf{U}_t), \tag{3.28}$$

$$(\mathbf{f}_t|\mathbf{V}_t) \sim N_r(\mathbf{0}, \mathbf{V}_t), \tag{3.29}$$

where distributions are assumed to be conditionally independent for all points in time. Model inference is based on an efficient and innovative Bayesian MCMC algorithm which involves a double shrinkage scheme on individual elements of $\mathbf{\Lambda}$, therefore a series-specific shrinkage along rows and a factor-specific shrinkage along columns of $\mathbf{\Lambda}$. Details of the procedure are in Kastner (2019)

3.6.3 Impulse Response Function and Spillover Effects

A VAR model of order p may be conveniently rearranged according to the following companion representation:

$$\mathbf{Y}_t = \boldsymbol{\mu} + \mathbf{B}\boldsymbol{Y}_{t-1} + \mathbf{U}_t, \tag{3.30}$$

where $\mathbf{Y}_t = vec(\mathbf{y}_t, \mathbf{y}_{t-1}, \ldots, \mathbf{y}_{t-p})$, $\boldsymbol{\mu} = vec(\mu, 0, \ldots, 0)$ and $\mathbf{U}_t = vec(\epsilon_t, 0, \ldots, 0)$ are $(qp \times 1)$ vectors and $\mathbf{B}$ is a $(qp \times qp)$ matrix defined as

$$\mathbf{B} = \begin{bmatrix} B_1 & B_2 & \ldots & B_{p-1} & B_p \\ I_q & 0 & \ldots & 0 & 0 \\ 0 & I_q & \ldots & 0 & 0 \\ \vdots & & \ddots & \vdots & \\ 0 & 0 & \ldots & I_q & 0 \end{bmatrix}.$$

Given this setting, solving forward the autoregressive structure implied in (3.30), it can be proved that the expected value h-step ahead of $\mathbf{Y}_t$ is given by

$$E(\mathbf{Y}_{t+h}) = \boldsymbol{C}_{h-1}\mu + \boldsymbol{J}\mathbf{B}^k\boldsymbol{Y}_t, \tag{3.31}$$

where $\boldsymbol{C}_0 = I$ and $\boldsymbol{C}_i = I + \sum_{k=1}^{i} \boldsymbol{B}_k\boldsymbol{C}_{i-k}$, with $\boldsymbol{B}_k = 0$ for $k > p$.

Denote with $\tilde{\boldsymbol{B}}$ the matrix achieved by orthogonalizing each $\boldsymbol{B}_k$ with the Cholesky decomposition factor for $\boldsymbol{\Sigma}$. The matrix $\tilde{\boldsymbol{B}}^h$ is then applied to compute the Orthogonalised Impulse Response Function (OIRF) of each asset class.

In the case of EWMSVAR models, the companion representation and thus the matrix $\mathbf{B}$ follow a regime-based setting as

$$\mathbf{Y}_t = \boldsymbol{\mu}_j + \mathbf{B}_j\boldsymbol{Y}_{t-1} + \mathbf{U}_{jt}, \tag{3.32}$$

with

$$\mathbf{B}_j = \begin{bmatrix} B_{1j} & B_{2j} & \dots & B_{p-1j} & B_{pj} \\ I_q & 0 & \dots & 0 & 0 \\ 0 & I_q & \dots & 0 & 0 \\ \vdots & & \ddots & \vdots & \\ 0 & 0 & \dots & I_q & 0 \end{bmatrix},$$

and $j = \{1, \dots, M\}$. Under this new framework, also the forecasting equation (3.31) assumes the form of conditional expectation on each state j.

Figure 3.1 shows the estimated OIRF for the volatility of the future contract trading the 2-year US rate. According to the picture, volatility of this asset is mainly driven by autoregressive dynamics, with memory effects depending on individual shocks more than on potential spillovers. However, volatility spikes along risky assets like oil or equity, for instance, tend to generate negative contagion effects on volatility of the 2-year US rate. This outcome underlines the attitude of short-term rates to be a defensive asset in market turmoil. During risk-off periods, the rising demand of bonds as portfolio hedging implies lower yields with interest rate volatility normalizing to more compressed levels. This pattern looks quite similar over the 2 regimes, although contagion effects remain somewhat limited under the *Low Volatility* scenario. Figure 3.2 shows the estimated state-dependent OIRF for the volatility of the S&P500 Index, which is generally assumed as a proxy of global equity market. In this second case, impulse functions look significantly different between the 2 states. Under the *Turbulence* scenario, spillovers show significant degree of persistency. On this, volatility of interest rates has a critical impact on equity market volatility. In particular, shocks on the 2-year US rate in response, for instance, to tightening monetary policy tend to generate significant spillovers with a pronounced smoothed decay on volatility of the S&P500 Index. On the other hand, contagions under the *Low Volatility* scenario appear as partially negligible, since volatility of the equity market shows an idiosyncratic profile substantially orthogonal to shocks from other asset classes. On this, rising interest rate volatility may

Figure 3.1: *State-dependent OIRF (vertical axis) for the 2-year US Future and other assets over* $[t+h]$ *periods ahead (horizontal axis).*

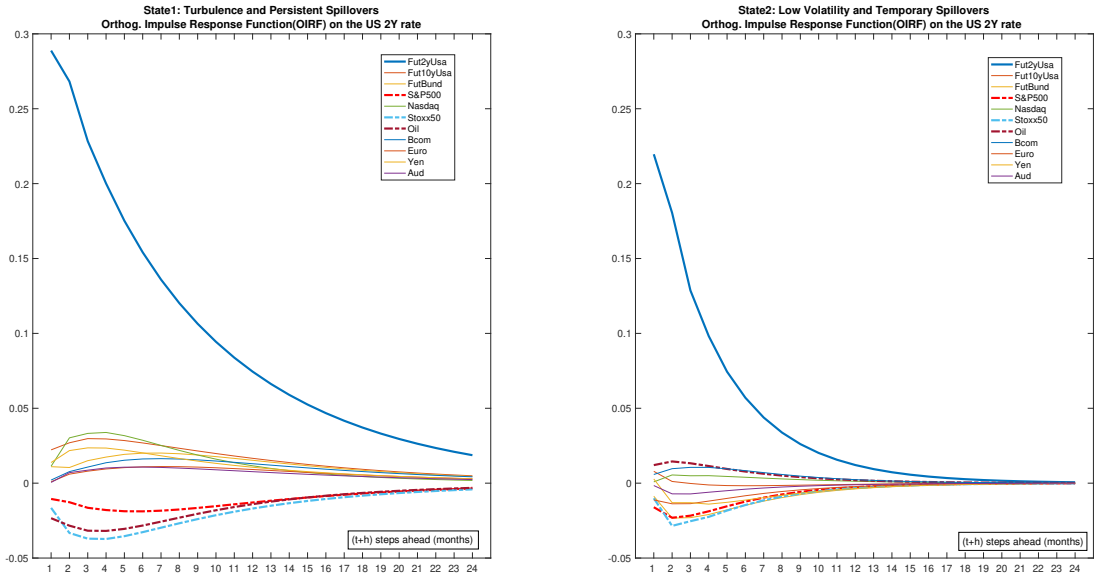

generate a potential contagion to equity variability but it is expected to remain quite limited in terms of intensity and degree of memory. Supported by the contribution of Blitz and van Vliet (2008), who argued to extend the analysis to a broad-invested portfolio, impulse functions are rearranged according to a network-based representation. Such a new perspective aims at underling the degree of interconnection across assets in terms of nodes and edges. More formally, denote with $node_i = \sum_i (OIRF_{ii})$ the cumulative contagion effect on $asset_i$, given a shock on itself, and with $edge_{ij} = \sum_j (OIRF_{ij})$ the marginal cumulative spillover on $asset_i$, given a shock on $asset_j$. Under this new setup, the $node_i$ is a measure of autocorrelation affecting individual volatilities, while the $edge_{ij}$ represents the degree of volatility interconnection between assets i and j.

Figure 3.2: *State-dependent spillovers (vertical axis) for the S&P500 Index and other assets over* $[t+h]$ *periods ahead (horizontal axis).*

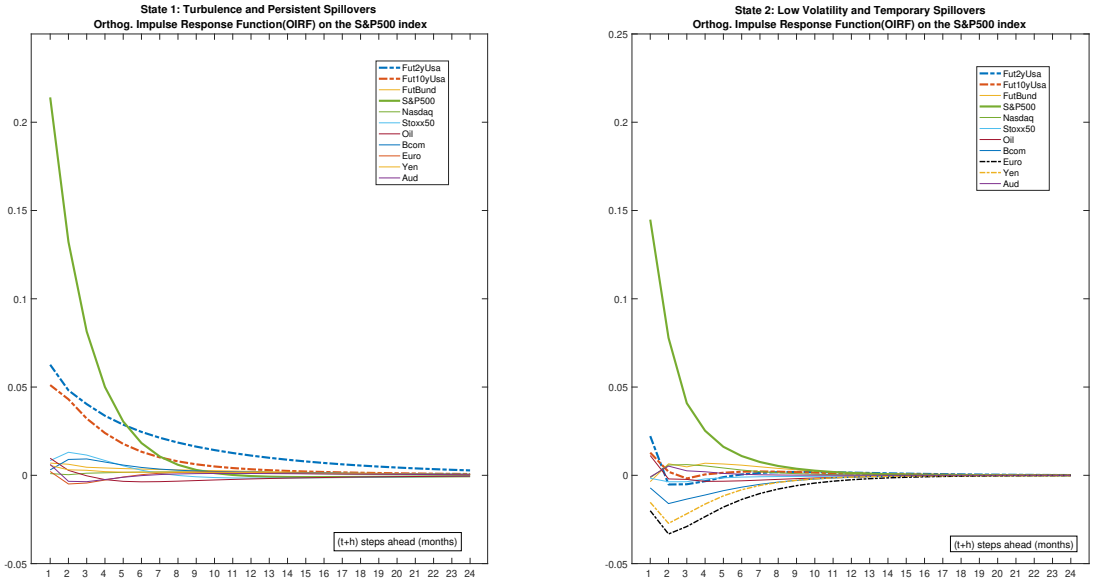

Figure 3.3: *Network representation of state-dependent volatility spillovers.*

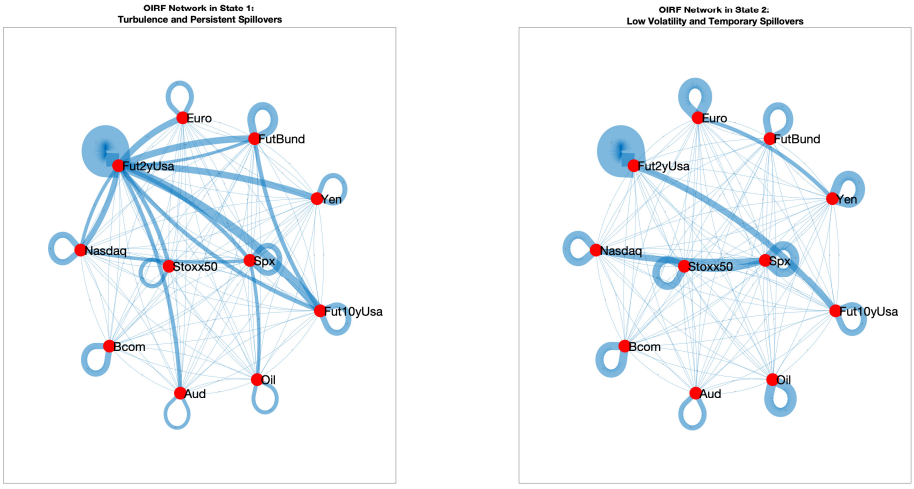

As shown in Figure 3.3, if market behaves in line with the *Turbulence* scenario, shocks on individual volatilities are not expected to remain isolated but, rather, they generate a warning leverage effect on volatility of the entire portfolio. On this, the picture underlines the centrality of the 2-year US rate within the network. Therefore, volatility shocks on short-

term rates make portfolio diversification a challenging task.

The picture is substantially different under the *Low Volatility* scenario since spillovers connect just few nodes. In this environment, volatilities are mainly driven by individual autocorrelation and the leverage effect on portfolio volatility remains quite limited. Diversification and portfolio hedging appear more feasible under this regime.

Finally, the analysis highlights that natural resources (Bcom Index) remain quite indipendent in terms of volatility spillovers with respect to the rest of the portfolio. It implies that being invested in Bcom should help on the way of portfolio diversification also under the *Turbulence* scenario.

3.6.4 A comparison between a hierarchical and a Minnesota prior structure

Since realized volatilities may be highly persistent processes, the section provides a comparison between the hierarchical framework of the paper with a more flexible Minnesota prior structure(see Litterman (1986)). In very general terms, let $\boldsymbol{\beta}_g$ be the $(k\times 1)$ vector containing the parameters of the g^{th} equation of the VAR model, with σ_{gg}^2 the variance of the process of the equation. Litterman assumes that $P(\boldsymbol{\beta}_g) \sim N(\bar{\boldsymbol{\beta}}_g, \bar{\boldsymbol{\Omega}}_g)$, where $\bar{\boldsymbol{\beta}}_g$ and $\bar{\boldsymbol{\Omega}}_g$ denote the prior mean and variance-covariance matrix of $\boldsymbol{\beta}_g$, respectively. By exploiting the SUR representation of a VAR model, with $\mathbf{X}$ the matrix of common regressors equation by equation, it can be shown that the posterior distribution of $\boldsymbol{\beta}_g$, given data $\mathbf{Y}$, is $P(\boldsymbol{\beta}_g|\mathbf{Y}) \sim N(\tilde{\boldsymbol{\beta}}_g, \tilde{\boldsymbol{\Omega}}_g)$ where

$$\tilde{\boldsymbol{\beta}}_g = \tilde{\boldsymbol{\Omega}}_g(\bar{\boldsymbol{\Omega}}_g^{-1}\bar{\boldsymbol{\beta}}_g + \sigma_{gg}^{-2}\mathbf{X}'\mathbf{Y}_g), \tag{3.33}$$

$$\tilde{\boldsymbol{\Omega}}_g = (\bar{\boldsymbol{\Omega}}_g^{-1} + \sigma_{gg}^{-2}\mathbf{X}'\mathbf{X})^{-1}, \tag{3.34}$$

with $\mathbf{Y}_g$ the vector of observed data for the g^{th} equation. Given this backdrop, some remarks are in order here. First, there is prior and posterior independence between equations,

therefore a superior degree of flexibility may be achieved over the hierarchical structure in modelling the memory effect in the process of the realized volatility. Second, $\bar{\boldsymbol{\beta}}_g$ and $\bar{\boldsymbol{\Omega}}_g$ are unknown and specified in terms of few hyper-parameters. Precisely, the mean vector is defined as $\bar{\boldsymbol{\beta}}_g = (0, \ldots, 0, \pi_1, 0, \ldots, 0)$, where π_1 is in the g^{th} position and represents the prior mean of coefficient on the first lag of the endogenous variable in equation g. Moreover, Litterman suggestes to assign numerical values to the hyper-parameters along the diagonal elements of $\bar{\boldsymbol{\Omega}}_g$, according to the following scheme:

$$var(\bar{\boldsymbol{\beta}}_g) = \begin{cases} \pi_2/l^2 \text{ for the } g^{th} \text{ lagged endogenous variable} \\ (\pi_3/l^2)(\sigma_g/\sigma_j) \text{ for the } j^{th} \text{ lagged endogenous variable} \\ \pi_4\sigma_g \text{ for deterministic and exogenous variables} \end{cases}$$

Here, π_2 controls the overall prior tightness or uncertainty on own lags; π_3 controls the tightness of own lags relative to the tightness of lags of the other variables in the equation; π_4 controls the degree of uncertainty on coefficients of the deterministic and exogenous variables; l^2 controls the lag-decay of prior variance, while the factors σ_g and σ_j measure the scale of fluctuations in variables g and j. Consolidated Minnesota rules of thumb suggest to apply small numbers to π_2 and π_3 and large values to π_4. Among others, see Litterman (1986) and Ciccarelli and Rebucci (2003) for a detailed account of the procedure. The section below provides some remarks about the comparison between hierarchical and Minnesota priors applied to short-term interest rates and the US equity market. These assets are selected here for the exercise, as they have a central role in portfolio strategies. Figure 3.4 shows the estimated OIRF for the volatility of the future contract trading the 2-year US rate under both hierarchical and Minnesota priors. In order to highlight the most significant differences between the two settings, the comparison pays particular attention to the behaviour of the impulse functions under the *Turbulence* regime, where spillovers show significant degree of persistency. The picture remains substantially unchanged in terms of relevant volatility

interconnections along the two prior structures, however some remarks emerge here from the comparison. In both settings, short-term rates confirm their attitude to be a difensive asset in market turmoil, as volatility spikes on risky assets tend to generate negative contagion effects to volatility of the 2-year US rate. However, the Minnesota prior setup allows for capturing a significant volatility spillover from Nasdaq and Bcom (natural resources) indices to short-term rates. This outcome appears to be consistent with the empirical evidence. Names trading on the Nasdaq Index are typically high-growth oriented stocks with strong connection to short-term yields, therefore volatility shocks in this market may generate alarming spillovers to volatility of the 2-year US rate. In terms of tactical asset allocation, this picture would encourage the common strategy applied by different fund managers of assuming a short position on the Nasdaq Index to hedge a long strategy on yields. On the other hand, distressed conditions on natural resources are often connected to worsening macroeconomic data, which tend to generate a one-to-one response in terms of interest rate dynamics. Therefore, volatility spikes involving the Bcom Index sound as a warning signal

Figure 3.4: *OIRF on the 2Y US rate under Hierarchical priors and Minnesota priors.*

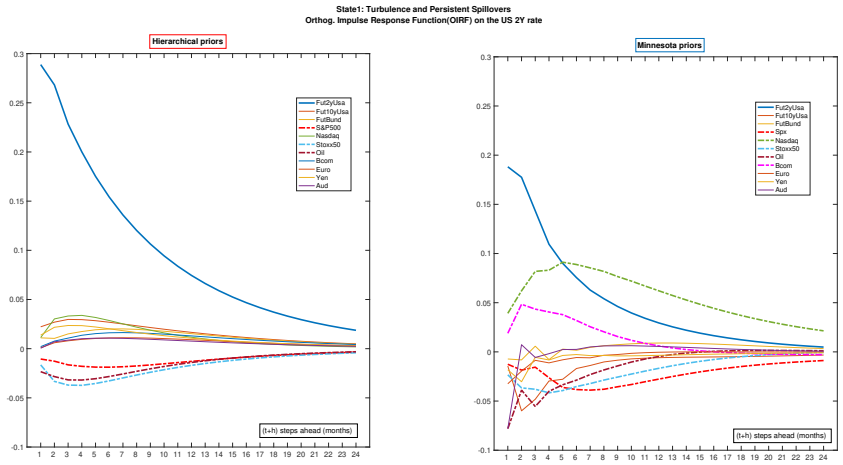

about potential volatility contagion effects spreading to interest rates. Similarly, Figure 3.5 shows the estimated state-dependent OIRF for the volatility of the S&P500 Index under the two prior settings. Again, the general framework of volatility spillovers appears to be quite consolidated along the two structures, with short-term rates confirmed as relevant

Figure 3.5: *OIRF on the S&P500 Index under under Hierarchical priors and Minnesota priors.*

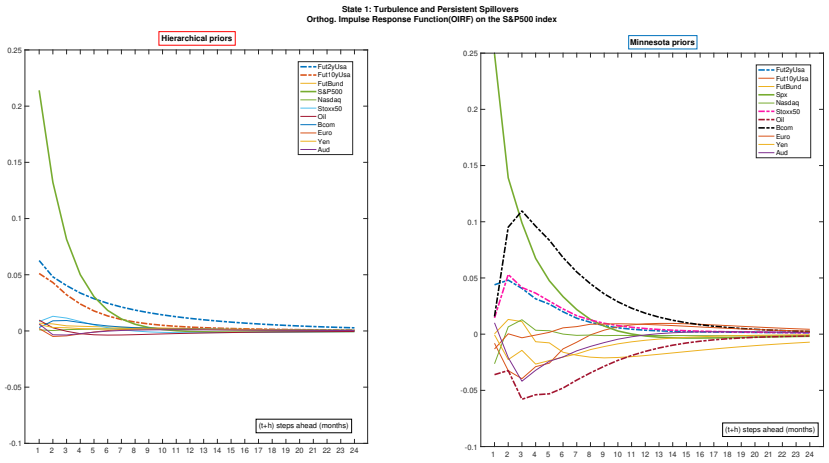

candidate for potential contagion effects to volatility of the US equity market. However, the higher flexibility embedded in the Minnesota setup allows to estimate a noteworthy volatility interconnection between natural resources and equity market; this effect is negligible in the more smoothed prior structure of the hierarchical framework. A joint interpretation of Figure 3.4 and 3.5 would encourage to move one step-ahead with a more exhaustive investigation about the emerging properties of natural resources to be a leading indicator of market sentiment. Under this perspective, the analysis might suggest to apply some volatility measure of the Bcom Index as early-warning in the Probit equation of the model proposed in the paper.

3.6.5 Debate about diversification: the case of the Yen/Usd exchange rate

The Yen/Usd exchange rate is commonly used to hedge portfolio allocation during brutal market selloff. Despite this kind of strategy is implemented in many empirical applications, the real effectiveness of this approach remains an open debate. According to the picture in Figure 3.6, a negative interconnection emerges in terms of volatility spillovers between the cross and risky assets like, for instance, oil and equity indices. This outcome argues in favour

Figure 3.6: *State-dependent spillovers (vertical axis) for the Yen/Usd exchange rate and other assets over* $[t+h]$ *periods ahead (horizontal axis).*

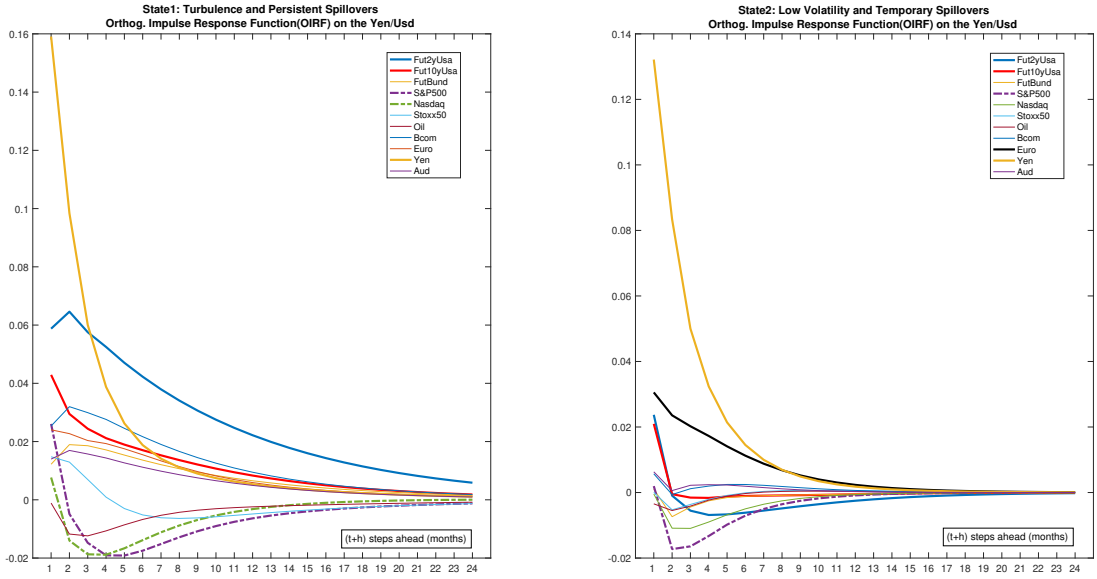

of the ability of the Japanese currency to mitigate portfolio volatility during market turmoil. However, the real consistency of this hedging strategy is compromised, at least partially, by evidence in Figure 3.7 and 3.8, where the estimated realized volatilities are reported for the cross and the S&P500 Index, which is reasonably assumed as a proxy of risky asset. As emphasized by the red lines, volatility of the Japanese currency in the *Turbulence* scenario moves around a much lower fair value than that of the S&P500 Index.

Figure 3.7: *realized volatility of the Yen/Usd exchange rate.*

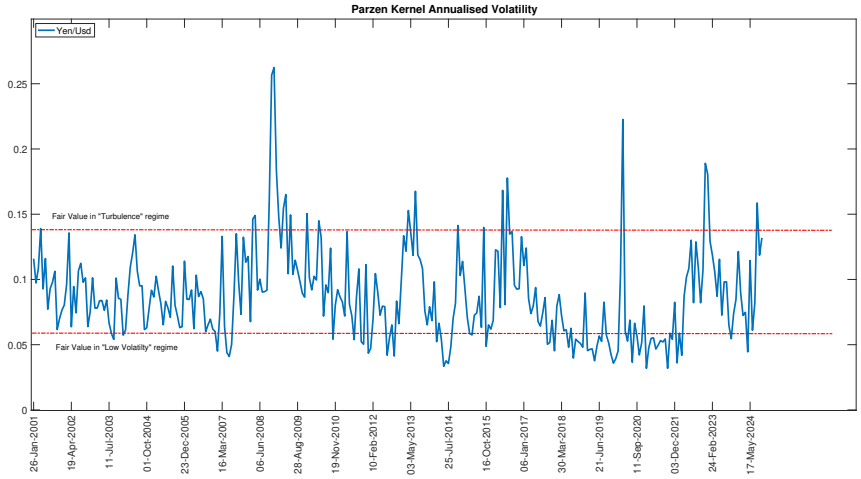

Figure 3.8: *realized volatility of the S&P500 Index.*

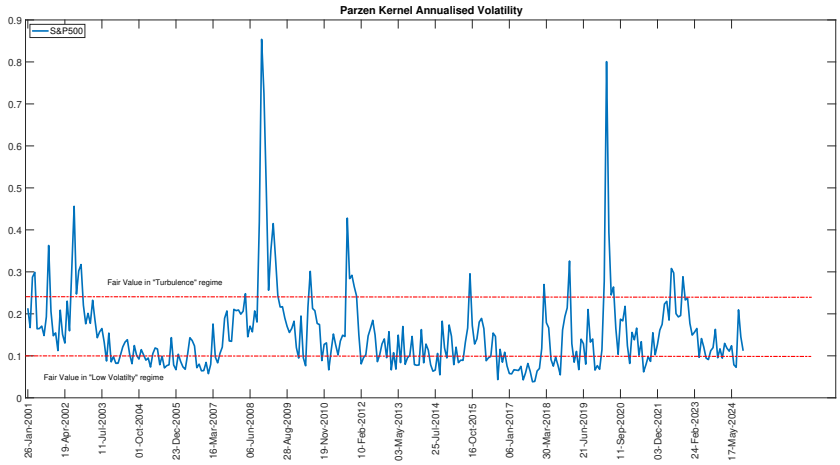

Literature on derivatives and asset pricing argues that the optimal hedging ratio between 2 assets is a function of their correlation and of the ratio between individual volatilities. Exhaustive details on this topic are in Hull (2021). Under hedging strategy perspective, such a volatility gap implies that a notable portion of portfolio should be allocated in the Yen/Usd rate in order to mitigate the exposure to the S&P500 Index. However, in case of high risk-oriented portfolios, this hedging scheme might be unfeasible.

3.6.6 A comparison between orthogonalised and generalised impulse responses

In order to check the robustness of the conclusions emerging from the analysis based on impulse responses, the section provides a comparison between orthogonalised (OIRF) and generalised (GIRF) impulse response functions computed for the model in the paper. Generalised impulse responses are invariant to the reordering of the variables in the VAR, but this is not the case for the orthogonalised version, where shocks modelling depends on how variables are ranked in the Cholesky decomposition of the covariance matrix. Typically many alternative reparametrizations may be employed to compute orthogonalised impulse responses, but there is no clear guidance about which one should be applied. On this is-

sue, the generalised impulse response functions are unique, in contrast to the orthogonalised setup. To make further exposition clearer, the comparison employs the impulse functions only under the *Turbulent* regime, where spillovers exhibit a relevant degree of persistency. Figure 3.9 explores the behaviour of the OIRFs and GIRFs computed for the volatility of

Figure 3.9: *OIRFs and GIRFs for the 2-year US rate under the Turbulent regime.*

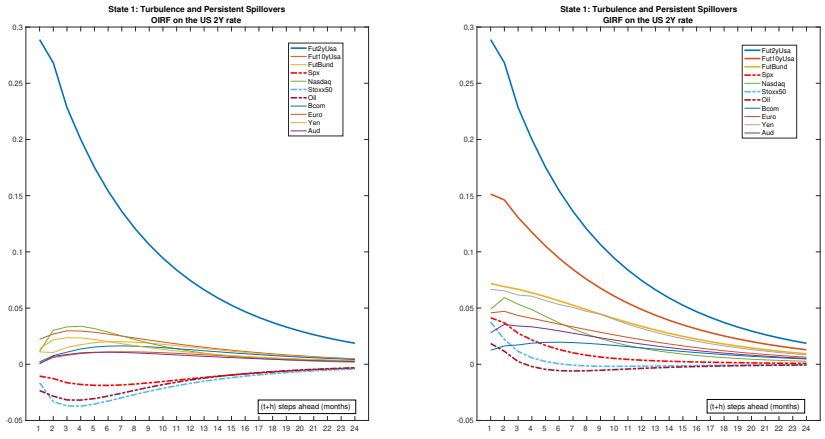

the 2-year US rate. A couple of remarks are in order here. First, the outcome under the GIRF structure confirms that volatility of this asset is mainly driven by the autoregressive dynamics rather than by potential spillovers. However, in contrast to the orthogonalised framework, the generalised setting estimates a stronger interconnection involving yields of different maturities, therefore volatility spikes on long-term rates, therefore 10-year US Treasuries and Bunds, are allowed to generate potential contagion effects on the short-term rate volatility. This outcome doesn't pose a structural change to the overall picture, but it appears to be more realistic in empirical applications. Second, even though the magnitude of the negative relationship with volatility of risky assets looks less pronounced, the attitude of short-term rates to be a difensive asset in market turmoil is confirmed also under the generalised impulse response structure. Figure 3.10 shows the comparison between OIRFs and GIRFs estimated for the volatility of the S&P500 Index. In this case, the generalised setup emphasises a wider range of volatility interconnections between the US equity market and the other assets in portfolio. Under this perspective, there is no surprise in observing a

significant co-movement in individual volatilities across different equity indices. Given this backdrop, an important remark is in order here: also under the GIRF setup, volatility of interest rates tends to generate significant long-memory spillovers on volatility of the S&P500 Index. Therefore, a rising bond yield volatility, for instance in response to market expectations of a forthcoming tightening monetary policy, remains a key warning factor for equity pricing under both settings.

Figure 3.10: *OIRFs and GIRFs for the S&P500 Index under the Turbulent regime.*

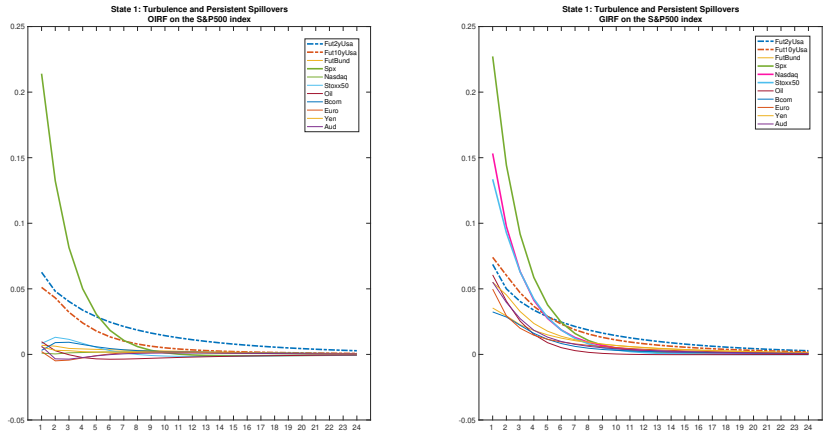

Finally, Figure 3.11 compares the two impulse response structures computed for the Yen/Usd exchange rate. In this case, the overall picture remains substantially unchanged under the two alternatives, with volatility of the 2-year US rate confirmed as the leading factor of potential volatility spillovers; in addition, comments on the hedging scheme, which employs the Japanese currency as defensive asset in market turmoil, remain valid also under the generalised setup. Despite some divergences arise from the comparison, the exercise confirms that volatility of short-term rates has great impact on the volatility contagion scheme of a globally-invested portfolio. Hence, the triangular ordering implied in the orthogonalised framework shows great coherency with the asset pricing theory (see Bekaert et al. (1989), Campbell and Ammer (1993) and Lettau and Watcher (2011)), which argues that the expected return of a risky asset follows a hierarchical premium puzzle structure, with bond yields at the beginning step, as they compensate investors for the first source of market

Figure 3.11: *OIRFs and GIRFs for the Yen/Usd exchange rate under the Turbulent regime.*

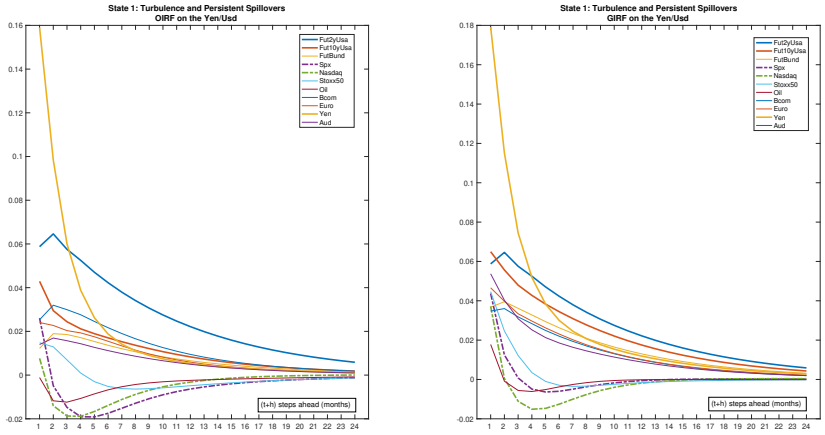

risk, namely the *term-premium*. Therefore, the Cholesky identification scheme proposed in the paper, with rates leading the ordering of variables in the VAR, seems consistent with remarks of this literature.

3.6.7 Forecasting Exercise on realized volatility

To show the contribution of the EWMSVAR model proposed in this paper in terms of volatility forecasting, I compare its prediction to the one delivered by the GHAR method described above. Forecasts of the EWMSVAR model employ the regime-based setup as in equations (3.31) and (3.32).

The prediction scheme is in the spirit of marginal prediction, therefore individual regime-based expectations between time t and $t+1$ are computed using the realization of the exogenous variable at time t and finally combined given the predicted regime probabilities. Equation (3.31) may be applied even for prediction between time t and $t+h$, following a recursive procedure still based on the realization of the exogenous variable at time t. In this second case, prediction of the regime probabilities at time $t+h$ is formulated by employing the time-varying transition matrix in the form of P_t^h. Other forecasting structures may be applied. For instance, expectations of the exogenous variable at time $t+j$ may be recursively

updated given the previous prediction at time $t+j-1$, with j up to h; alternatively, a model for each forecasting horizon can be separately estimated.

For statistical evaluation of volatility prediction, I employ root mean squared error (RMSE) loss functions based on the Frobenius norm. More formally, loss functions are calculated for the $t = \{1, \ldots, T\}$ forecasts as

$$\mathbf{e}_{t,t+1} = \mathbf{\Sigma}_{t+1} - \hat{\mathbf{\Sigma}}_{\boldsymbol{t+1}}, \tag{3.35}$$

$$\Im^{RMSE} = \sqrt{\frac{1}{T-1}\sum_{t=1}^{T-1}\sum_{i=1}^{q}(\mathbf{e}_{ti,i})^2}, \tag{3.36}$$

where $\mathbf{\Sigma}_{t+1}$ and $\hat{\mathbf{\Sigma}}_{t+1}$ are diagonal matrices with volatility proxy and forecast, respectively, on the main diagonal. The exercise assigns equal weights to forecast errors on each volatility; since the model is interpreted as a tool to support decisions of tactical asset allocation, this choice looks quite reasonable, as it provides a measure of the model forecasting properties at portfolio level, where the contribution of a proper prediction is evaluated in a balanced way across assets. Nevertheless, the analysis might be extended to a different scheme where weights are expressed, for instance, as a function of the ordering of variables in the Cholesky decomposition factor.

To evaluate the difference between these 2 competing models under a statistical point of view, I test the null hypothesis of equal forecasting accuracy

$$H_0: \ E[\Im_{ewmsvar} - \Im_{ghar}] = 0,$$

by computing $\Im_{ewmsvar}$ and $\Im_{ghar}$ over 1,000 stationary bootstrap samples, with average block length of 10 months. On this issue, different lengths are investigated to asses the robustness of the result, without any change in the final outcome. As shown in Figure 3.12, the difference $[\Im_{ewmsvar} - \Im_{ghar}]$ over the simulated samples follows a strictly negative-centred distribution. This outcome supports the rejection of the null hypothesis under investigation, as the mean squared error loss function of the EWMSVAR model looks statistically lower

than that of the GHAR approach.

Figure 3.12: *Stationary Bootstrap Analysis of* $H_0 : E[\Im_{ewmsvar} - \Im_{ghar}] = 0$.

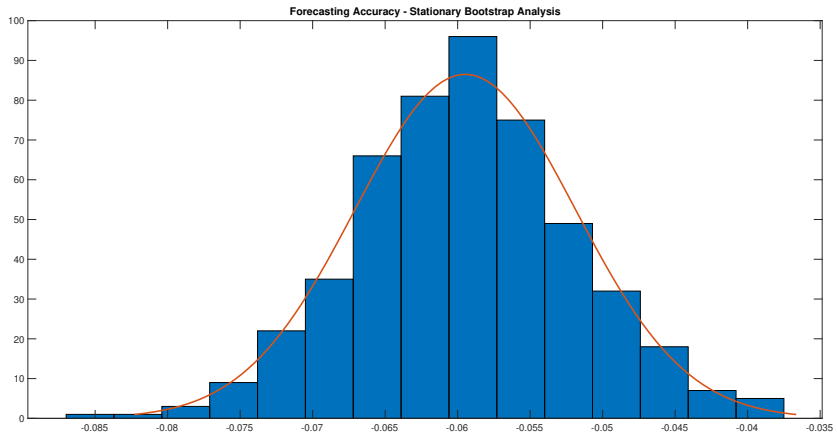

Therefore, according to the statistical framework applied in the exercise, the model in the paper tends to dominate the benchmark proposed by the GHAR approach in terms of volatility forecasting. In order to investigate more in depth the reason behind this outcome, Figure 3.13 compares volatility prediction of the EWMSVAR model (black line) to the one provided by the GHAR framework (green points), during periods of equity market turmoil. In this example, volatility of the S&P500 Index is assumed as a worldwide thermometer of market sentiment. It fits as a common assumption in many empirical applications. Such analysis aims at evaluating the ability of the 2 methods in forecasting volatility shifts when episodes of risk-aversion occur. Under this perspective, the EWMSVAR model tends to dominate the competing approach. On this, the smoothed autoregressive structure leads GHAR projections to be less reactive to volatility spikes, as green points constantly lie below the EWMSVAR prediction. Therefore, the non-linearity implied in the regime-based representation and the explicit modelling of volatility spillovers through the VAR setup bring the EWMSVAR model to achieve consistent advantages in terms of volatility prediction, in particular along volatility regime shifts.

To conclude, Figure 3.14 shows the example of volatility forecast for the S&P500 Index. The chart summarises the general architecture about volatility as implied by the EWMSVAR

Figure 3.13: *Volatility Forecast Comparison*

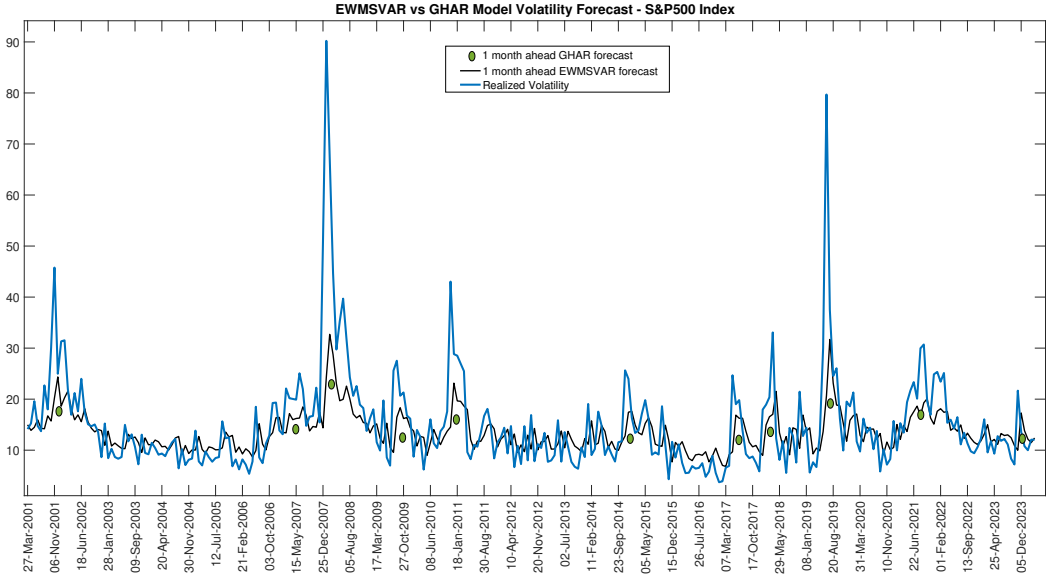

setup. First of all, horizontal lines describe the long-run values for volatility dynamics under *Turbulence* and *Low Volatility* states. They follow from the ergodic probabilities estimated for the 2 regimes. According to the picture, equity volatility moves from a 10% *risk-on floor* to an alarming value close to 26% in case of market selloff. The tightening monetary policy program announced in 2021, for instance, pushed equity market volatility above the estimated risk-off threshold. Arising from equations (3.31) and (3.32), the regime-based 1-month ahead forecast is reported (dashed line). After computing the average prediction error over bootstrap samples, the 90% 1-month ahead forecasting interval is finally provided. Predicting volatility boundaries emerges as particularly significant in order to analyse the market price action. Back to the former example, for instance, after volatility spike in 2021, market sentiment significantly improved as volatility sharply collapsed even below the 10% *risk-on floor* in August 2023. Such a picture appears as an over-reaction of market sentiment and arises questions about the potential sustainability of this upbeat trend. In terms of asset allocation strategy, a de-risking portfolio scheme might be recommended.

To conclude, on the comparison between the EWMSVAR proposed in the paper and the

Figure 3.14: *Realized Volatility Forecast for the S&P500 Index*

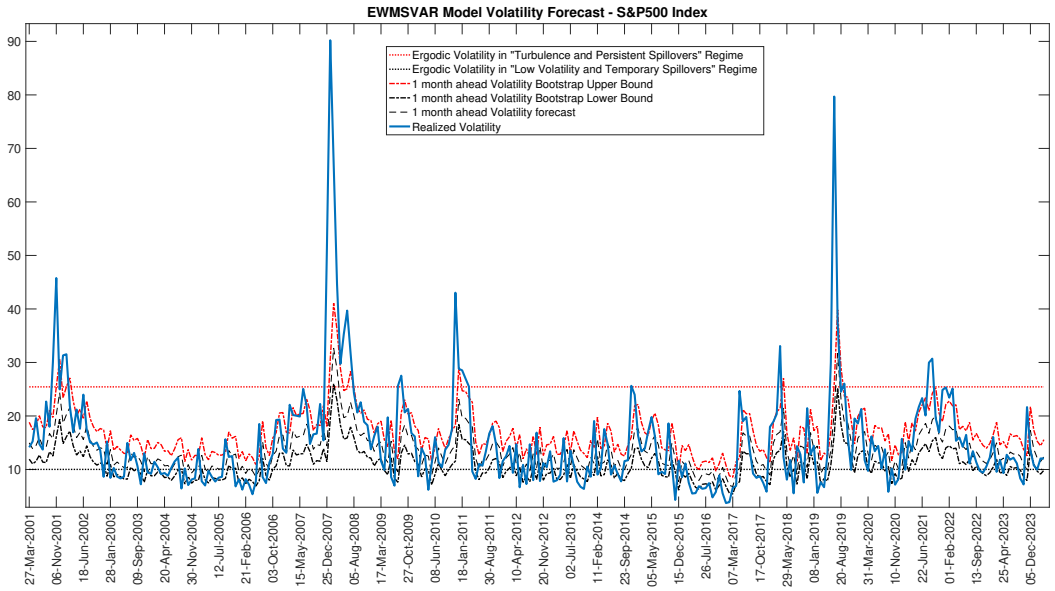

HAR setup, an important remark is in order here: the first approach models the vector y_t of monthly realized log-volatilities and connected volatility spillovers, while the alternative HAR approach extends inference also to realized covariances by modelling the much larger vector X_t, which contains all diagonal and sub-diagonal elements of the Cholesky factor of the estimated realized covariance matrices. Under this perspective, the EWMSVAR model in the paper might be extended to include all the elements of X_t for a more complete comparison.

3.6.8 Asset Allocation Exercise

Tactical asset allocation (TAA) plays an important role in investment management. In determining portfolio performance attribution, asset allocation policy is shown to be the dominating factor. In general terms, the concept of TAA refers to active strategies which seek to deliver positive returns by systematic shifts in portfolio composition in response to new occurring market opportunities. Notable contributions on TAA include Philips et al. (1996) and Lee (2000).

Different measures may be applied to compare merits of TAA-based models; a first approach is connected to the concept of *Sharpe Ratio* (SR), which measures the risk-adjusted performance of an investment, such as a security or an allocation strategy, compared to a risk-free rate. Specifically, it is defined as the difference between returns of the investment and the risk-free rate, divided by the standard deviation of the investment returns. This ratio accounts for the additional amount of return that an investor receives for an additional unit of risk. Evaluation of the SR generally employs a rolling-window approach, where the ratio is computed over a moving window.

On this topic, there isn't a precise guide about the choice of the length of this window, but a 3-year rolling horizon is generally selected in many empirical applications. Graphical analysis of the rolling SR yields a couple of advantages: first, it investigates the stability of the trading scheme in terms of risk-adjusted returns and, secondly, it evaluates the ability of the strategy to recover from lows after performance drawdowns. Statistical methods may be even applied; thus, for instance, a stochastic bootstrap could be implemented to approximate the SR distribution for hypothesis testing about if TAA results are statistically significant from 0.

A second approach refers to the concept of equity line (EQL), which is a measure of cumulative performance deriving from the implementation of a selected trading rule. In general, an EQL is expressed as investing 100 dollars (or 1 dollar) at the beginning of the evaluation sample and implementing the trading strategy throughout, up to the end of the backtesting period.

In order to evaluate the contribution of the model in terms of portfolio allocation, the paper provides a trading strategy on the regime-based representation of volatility spillovers. Precisely, a trading allocation algorithm is proposed for the S&P500 Index, which is reasonably assumed as a proxy of global equity market. The TAA exercise is conducted by sequentially re-estimating models with a 3-month frequency.

On this topic, Ang and Bekaert (2004) argue about the importance of implementing a port-

folio allocation program which delivers a different composition based on the predominant market regime (bull vs bear market) while Ang and Bekaert (2002) provide a comprehensive framework of asset allocation with regime shifts. Moreira and Muir (2017) present a volatility-timing allocation strategy which increases Sharp ratios over volatility shifts.

Figure 3.15: *Smoothed regime probabilities of the 2-state EWMSVAR model.*

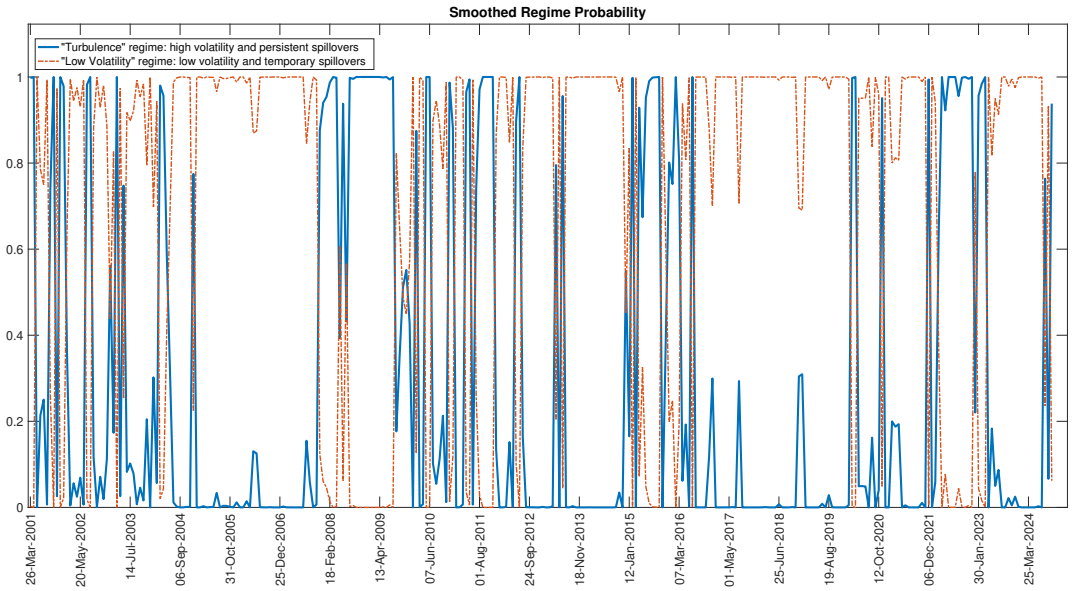

After estimating the 2-state EWMSVAR model, the smoothed regime probabilities are reported in Figure 3.15. In order to support the asset allocation exercise, a 3-month moving average of the *Turbulence* regime probability is computed. This new indicator is expected to provide a smoothed trend about market sentiment. Since it is applied with a lag of 1 month, such indicator works in terms of early-warning signal about potential volatility regime shifts. More formally, the indicator identifies a *Risk-on* environment when it stands below the reasonable threshold of 67% (2/3), otherwise a *Risk-off* regime is activated.

Following, for instance, Moreira and Muir (2017) and Rasmussen (2003), a risk-oriented portfolio is implemented under *Risk-on* conditions, therefore a long stance on the S&P500 Index is applied. Otherwise, if the warning indicator moves above the alarming threshold, the trading scheme provides a more defensive strategy deriving from a combination of

a marginal stance on the S&P500 Index, proportionally to the residual probability of the *Risk-on* scenario, and a prevailing hedging portfolio with a global weight connected to the probability of the *Risk-off* regime. To sum up, under a *Risk-on* environment, characterised by low individual volatilities and temporary spillovers, the trading scheme implements a fully-invested portfolio in the S&P500 Index; on the other hand, under *Risk-off* conditions, the trading strategy recommends a final allocation as a combination of a reduced position on the S&P500 Index and a defensive portfolio, which is explicitly implemented to hedge the allocation on the risky asset.

Following Hull (2021) on the optimal hedging ratio principle, in the algorithm of the paper the traditional correlation is replaced by the marginal cumulative spillover as a measure of interconnection between 2 assets in terms of volatility contagion. In order to achieve a feasible portfolio, the hedging scheme allocates positive weights by selecting few assets with significant negative cumulative spillovers from a shock on the S&P500 Index.

Figure 3.16 shows the performance comparison between a classical $Buy\&Hold$ strategy on the S&P500 Index (blue line) and the trading rule proposed in the paper (red line). Precisely, the chart compares the EQL, therefore the cumulative performance, of the two competing models considered here. On this topic, the so-called $Buy\&Hold$ strategy is as exactly investing 100 dollars in the market at the beginning of the evaluation sample and holding it throughout, up to the end of the backtesting period. The $Buy\&Hold$ portfolio addresses the typical passive allocation scheme of a long-run investor, therefore it is commonly used in empirical applications as a benchmark to evaluate the robustness of tactical asset allocation strategies. The trading algorithm gains relevant advantages over a systematic long position on the US equity market since the early-warning indicator provides significant leading properties in forecasting regime shifts into *Turbulence* scenarios.

As highlighted by the black rectangles in the picture, the scheme proposed in the paper achieves a great mitigation of performance drawdowns over the entire back-testing period. Under this perspective, the algorithm appears as particularly reactive over the collapse of

Figure 3.16: *Model comparison: cumulative trading strategy performance.*

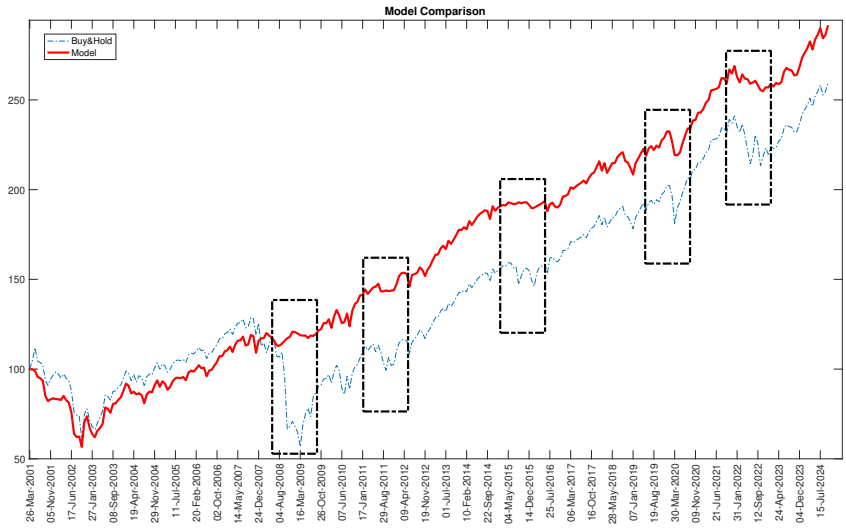

the US banking system in 2008-2009 and, more recently, in 2021-2023 under a widening risk-off sentiment when central banks around the world adopted restrictive monetary policies in response to rising inflation shocks.

In both occasions, the algorithm implements a timely reduction of the exposure to the S&P500 Index in favour of a more defensive hedging portfolio.

Figure 3.17: *Example of portfolio allocation in risk-aversion (January 2023)*

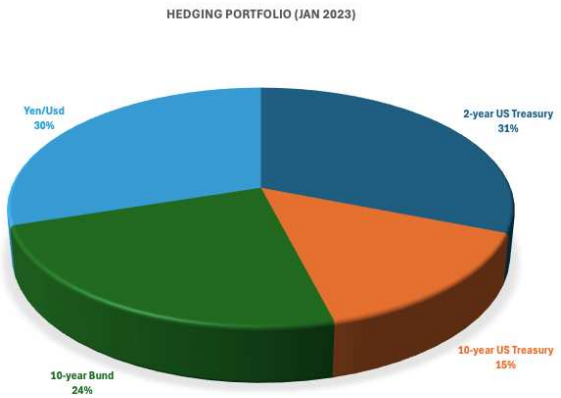

Figure 3.17 reports the hedging allocation proposed by the algorithm in January 2023, when

the probability of the *Risk-off* regime was about 100%. Mainly invested in bonds and in the Japanese currency, this portfolio emerges as a quite typical defensive allocation in a context of significant market risk-aversion.

Finally, Figure 3.18 compares the two models in terms of 3-year rolling Sharpe Ratio. Also under this perspective, the trading rule proposed in the paper seems to be more robust than the *Buy&Hold* strategy; in particular, as emphasised by the black dotted rectangles, the active allocation scheme proposed here looks more reactive than the one in the competing model, as it employs a more efficient control of portfolio drawdowns during periods of market selloff.

Figure 3.18: *3-year rolling Sharpe Ratio (SR) for the 2 competing models.*

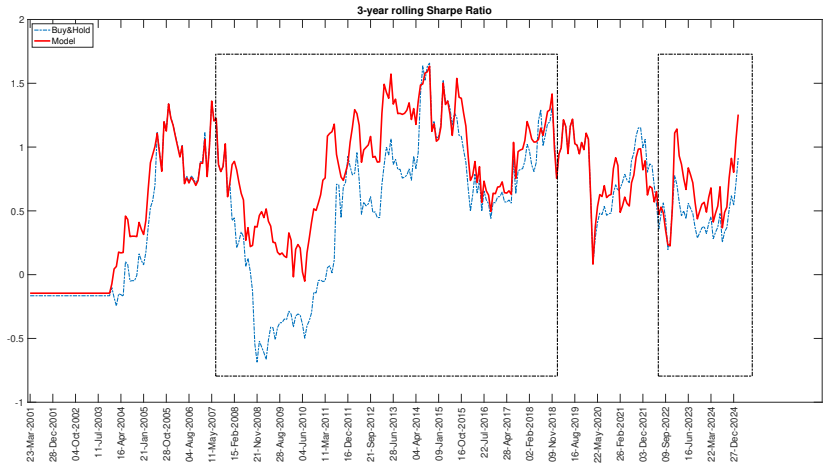

3.7 Conclusions

Popular extensions of heterogeneous autoregressive models have been proposed for describing realized volatility. However, they leave substantial information unmodelled in residuals. Increased availability of high-frequency data in the last decade emerges in development of new non-parametric approaches for modelling volatility in a multivariate setup.

A pioneer approach for covariance matrix modelling is provided by Barndorff-Nielsen and Shephard (2004), who introduced the multivariate realized kernel estimator, which efficiently manages the dependence structure of returns and guaranties the covariance matrix to be positive definite.

This paper contributes to literature by proposing a methodology for dynamic modelling and forecasting realized variance vectors based on a 2-state Early Warning Markov Switching VAR (EWMSVAR) model. The approach allows for flexible dependence patterns and investigates spillover effects across volatilities of different asset classes. The application of the model to a global portfolio investing in bonds, equities and currencies provides that spillovers follow a regime-based representation, with state transitions driven by the 3-month US T-Bill rate, whose dynamics is strictly connected to market expectations about future monetary policy decisions.

Supported by the contribution of Blitz and van Vliet (2008), who argued to extend the analysis to a broad-invested portfolio, impulse functions are rearranged according to a network-based representation. Such a new perspective aims at underling the degree of interconnection across assets in terms of nodes and edges. Under this setup, the $node_i$ is a measure of autocorrelation affecting individual volatilities, while the $edge_{ij}$ represents the degree of volatility interconnection between assets i and j. Under the *Turbulence* scenario, shocks on individual volatilities are not expected to remain isolated but, rather, they generate a warning leverage effect on volatility of the entire portfolio. On this, the paper underlines the centrality of the 2-year US rate within the network. It implies that volatility shocks on short-term yields make the portfolio diversification a challenging task. The picture is substantially different

under the *Low Volatility* scenario since spillovers connect just few nodes. In this environment, volatilities are mainly driven by individual autocorrelation and the leverage effect on portfolio volatility remains quite limited. Diversification and portfolio hedging appear more feasible under this regime.

To show the contribution of the EWMSVAR model proposed in this work in terms of volatility forecasting, the paper compares its prediction to the one delivered by generalised heterogeneous autoregressive (GHAR) methods. A stationary bootstrap hypothesis testing on equal forecasting accuracy shows that the model in the paper tends to dominate the competing approach. This achievement appears as particularly significant in modelling volatility regime shifts.

In order to evaluate the contribution of the model in terms of portfolio allocation, the paper provides a trading strategy on the regime-based representation of volatility spillovers. Precisely, a trading allocation algorithm is proposed for the S&P500 Index, which is reasonably assumed as a proxy of global equity market. The trading scheme gains relevant advantages over a systematic long position on the US equity market since it provides a timely hedging strategy which achieves a great mitigation of performance drawdowns along episodes of market selloff.

Bibliography

Agudze, K., Billio, M., Casarin, R., and Ravazzolo, F. (2022). Markov Switching Panel with Eondogenous Synchronization Effects. *Journal of Econometrics*, 230(2):281–298.

Albert, J. and Chib, S. (1993). Bayesian analysis of binary and polychotomous response data. *Journal of the American Statistical Association*, 88:669–679.

Amisano, G. and Fagan, G. (2013). Money growth and inflation: A regime switching approach. *Journal of International Money and Finance*, 33(C):118–145.

Andersen, T., Bollerslev, T., Diebold, F., and Labys, P. (2003). Modeling and forecasting realized volatility. *Econometrica*, 71(2):579–625.

Ang, A. and Bekaert, G. (2002). International asset allocation with regime shifts. *Review of Financial Studies*, 15:1137–1187.

Ang, A. and Bekaert, G. (2004). How regimes affect asset allocation. *Financial Analysts Journal*, 60:86–99.

Barndorff-Nielsen, O., Hansen, P., Lunde, A., and Shephard, N. (2011). Multivariate realised kernels: consistent positive semi-definite estimators of the covariation of equity prices with noise end non-synchronous trading. *Journal of Econometrics*, 162(2):149–169.

Barndorff-Nielsen, O. and Shephard, N. (2004). Econometric analysis of realized covariation: high frequency based covariance, regression and correlation in financial economics. *Econometrica*, 72(3):885–925.

Bauer, O. and Vorkink, K. (2011). Forecasting multivariate realized stock market volatility. *Journal of Econometrics*, 160(1):93–101.

Bekaert, G., Engstrom, E., and Grenadier, S. (1989). Stock and Bond Returns with Moody Investors. *Journal of Empirical Finance*, 17:867–894.

Billio, M. and Casarin, R. (2011). Beta Autoregressive Transition Markov Switching Models for Business Cycle Analysis. *Studies in Nonlinear Dynamics and Econometrics*, 15(4):1–32.

Billio, M., Casarin, R., Ravazzolo, F., and van Dijk, H. (2016). Iinterconnections between Eurozone and US booms and busts using a Bayesian Panel Markov-Switching VAR models. *Journal of Applied Econometrics*, 31(7):1352–1370.

Blitz, D. and van Vliet, P. (2008). Global tactical cross-asset allocation: Applying value and momentum across asset classes. *Journal of Portfolio Management*, pages 23–28.

Bollerslev, T. (1986). Generalized Autoregressive Conditional Heteroskedasticity. *Journal of Econometrics*, 31:307–327.

Bollerslev, T., Patton, A., and Quaedvlieg, R. (2018). Modeling and forecasting (un)reliable realized covariances for more reliable financial decisions. *Journal of Econometrics*, 207:71–91.

Bonato, M. (2009). Estimating the degrees of freedom of the realized volatility wishart autoregressive model. *SSRN 1357044*.

Bonato, M., Caporin, M., and Ranaldo, A. (2013). Risk spillovers in international equity portfolios. *Journal of Empirical Finance*, 24:121–137.

Bongaerts, D., Kang, X., and van Dijk, M. (2020). Conditional Volatility Targeting. *Financial Analysts Journal*, 76(4):54–71.

Campbell, J. Y. and Ammer, J. (1993). What Moves the Stock and Bond Markets? A Variance Decomposition for Long-Term Asset Returns. *Journal of Finance*, 48:3–37.

Carlin, B. P. and Chib, S. (1995). Bayesian Model Choice via Markov Chain Monte Carlo. *Journal of the Royal Statistical Society, Series B*, B(57):473–484.

Carvalho, C. M., Massam, H., and West, M. (2007). Simulation of hyper-inverse Wishart distributions in graphical models. *Biometrika*, 94(3):647–659.

Carvalho, C. M. and West, M. (2007). Dynamic matrix-variate graphical models. *Bayesian Analysis*, 2(1):69–97.

Casella, G. and George, E. I. (1992). Explaining the Gibbs sampler. *The American Statistician*, 46:167–174.

Chan, K., Hameed, A., and Tong, W. (2000). Profitability of Momentum Strategies in the International Equity Markets. *The Journal of Financial and Quantitative Analysis*, 35(2):153–172.

Chib, S. and Greenberg, E. (1995). Hierarchical analysis of SUR models with extensions to correlated serial errors and time-varying parameter models. *Journal of Econometrics*, 68:339–360.

Chiriac, R. and Voev, V. (2011). Modelling and forecasting multivariate realized volatility. *Journal of Applied Econometrics*, 26(6):922–947.

Ciccarelli, M. and Rebucci, A. (2003). Bayesian VARs: a survey of the recent literature with an application to the European Monetary System. *IMF Working Paper*, pages 2–44.

Corsi, F. (2009). A simple approximate long-memory model of realized volatility. *Journal of Financial Econometrics*, 7(2):174–196.

Engle, R. (2002). Dynamic conditional correlation: a simple class of multivartiate generalized autoregressive conditional heteroskedasticity models. *Journal of Business and Economic Statistics*, 20:339–350.

Engle, R. and Kroner, K. (1995). Multivariate simulataneous generalized arch. *Econometric Theory*, 11:122–150.

Frühwirth-Schnatter, S. (2006). *Finite mixture and Markov switching models*. Springer Science & Business Media.

Gelfand, A. E. and Smith, A. F. M. (1990). Sampling-based approaches to calculating marginal densities. *Journal of the American Statistical Association*, 85:398–409.

Geman, S. and Geman, D. (1984). Stochastic relaxation, Gibbs distributions and the Bayesian restoration of images. *IEEE Transactions on Pattern Analysis and Machine Intelligence*, 6:721–740.

Gouriéroux, C., Jasiak, J., and Sufana, R. (2009). The Wishart autoregressive process of multivariate stochastic volatility. *Journal of Econometrics*, 150(2):167–181.

Hamilton, J. D. (1994). *Time Series Analysis*. Princeton University Press.

Harrison, J. and West, M. (1999). *Bayesian forecasting & dynamic models*. Springer.

Hastings, W. K. (1970). Monte Carlo sampling methods using Markov chains and their application. *Biometrika*, 57:97–109.

Hull, J. (2021). *Options, Futures and other Derivatives*. Pearson.

Jin, X. and Maheu, J. (2013). Modelling realized covariances and returns. *Journal of Financial Econometrics*, 11(2):359–379.

Kadiyala, K. R. and Karlsson, S. (1997). Numerical methods for estimation and inference in Bayesian VAR-Models. *Journal of Applied Econometrics*, 12:99–132.

Kastner, G. (2019). Sparse bayesian time-varying covariance estimation in many dimensions. *Journal of Econometrics*, 210:98–115.

Kim, C. J. and Nelson, C. R. (1999). *State-Space Models with Regime Switching: Classical and Gibbs-Sampling Approaches with Application*. MIT Press: Cambridge MA.

Kim, C.-J., Piger, J., and Startz, R. (2008). Estimation of Markov regime-switching regression model with endogenous switching. *Journal of Econometrics*, 2(143):263–273.

Koop, G. (2003). *Bayesian Econometrics*. J. Wiley, New York.

Lee, W. (2000). *Advanced Theory and Methodology of Tactical Asset Allocation*. Wiley.

Lettau, M. and Watcher, J. (2011). The Term Structure of Equity and Interest Rates. *Journal of Financial Economics*, 101:90–113.

Litterman, R. B. (1986). Forecasting with Bayesian Vector Autoregressions-Five Years of Experience. *Journal of Business and Economic Statistics*, 4:25–38.

Moreira, A. and Muir, T. (2017). Volatility-managed portfolios. *The Journal of Finance*, 72:1611–1644.

Philips, T. K., R, G., and Capaldi, R. E. (1996). Tactical Asset Allocation: 1977-1994. *Journal of Portfolio Management*, 23(1):57–64.

Rasmussen, M. (2003). *Strategic and Tactical Asset Allocation in Quantitative Portfolio Optimisation, Asset Allocation and Risk Management*. Finance and Capital Markets.

Robert, C. P. (2007). *The Bayesian Choice*. Springer.

Robert, C. P. and Casella, G. (2004). *Monte Carlo Statistical Methods (Second Edition)*. University of Chicago.

Robert, C. P., Celeux, G., and Dielbold, F. X. (1993). Bayesian estimation of hidden Markov models: A stochastic implementation. *Statistics and Probability Letters*, 16:77–83.

Voev, V. (2007). Dynamic modelling of large-dimensional covariance matrices. *High Frequency Financial Econometrics*, pages 293–312.

Wang, H. and West, M. (2009). Bayesian analysis of matrix normal graphical models. *Biometrika*, 96(4):821–834.

Zellner, A. (1971). *An Introduction to Bayesian Inference in Econometrics*. J. Wiley, New York.

Zhang, L., Mykland, P. A., and Ait-Sahalia, Y. (2005). A tale of two time scales: determining

integrated volatility with noisy high-frequency data. *Journal of the American Statistical Association*, 100:1394–1411.

Zhou, X., Nakajima, J., and West, M. (2014). Bayesian forecasting and portfolio decisions using dynamic dependent sparse factor models. *International Journal of Forecasting*, 30:963–980.

Conclusion

Tactical asset allocation (TAA) plays an important role in investment management. In determining portfolio performance attribution, asset allocation policy is shown to be the dominating factor. Well Fargo Asset Management was considered to be the first to introduce TAA products in the 1970s, with an innovative approach to implement dynamic shifts between stock and bond in a systematic way arising from quantitative tools. Since performance of TAA depends on volatility, managing switches in returns variability and modelling volatility spillovers emerge as fundamental steps for a rewarding dynamic portfolio allocation.

Instead of the traditional max-likelihood procedure, in this work I follow a Bayesian approach to make inference about model parameters. Bayesian inference yields great popularity in economic applications since this approach integrates priors about parameters into model estimate. In a Bayesian framework, inference is therefore a learning process based not only on data but also on extra-sample information. The combination of these two sources of inputs is efficient since it accounts for the degree of uncertainty about data and priors.

The augmentation and Bayesian inference allow for generating projections of different market scenarios based on a simulation process arising from posterior distributions. In this work I provide an application of this scheme by evaluating the coherence of the portfolio allocation with the predominant macroeconomic regime implied in the market yield curve.

A brief summary of the main contributions and findings of the thesis is now provided.

Chapter 1 provides an early warning method for tactical asset allocation to deal with volatility clustering and fat-tail distributions of financial returns. The early warning signals are given by a two-state Markov switching model with high-volatility and low-volatility states and time-varying transition probabilities. The transition is driven by exogenous factors namely early-warnings. Using Bayesian inference and Gibbs Sampling for posterior approximation, I apply the model to daily returns of the S&P500 Index sampled from December 2000 up to May 2024. The paper suggests that a measure of the gap between volatility implied in options prices and realised volatility provides a timely warning signal about the risk of a potential shift from a regime of low volatility and positive average returns into a state of high volatility and negative average returns. The paper argues that trading strategies need to be calibrated on the predominant volatility regime. On this, a *Buy* signal in low volatility on the S&P500 Index yields strong and persistent returns over the entire back-testing period. This outcome confirms that volatility is not only a relevant factor for portfolio construction but also a key driver to generate consistent active returns. The application of the model provides evidence that trading strategies deliver significant improvements in terms of IR and portfolio drawdowns if signals are calibrated following a volatility-filtering scheme.

Chapter 2 presents a data-enriched term-structure model for interest rates following a general term-structure architecture based on non-arbitrage arguments. According to the Vasicek's model, the yield curve is completely driven by the unobserved instantaneous spot rate. Nevertheless, many alternative sources of information can be used to estimate it. Our state-space model includes the traditional Vasicek's measurement equation with the spot rate as a state process and it is augmented with further measurement equations on bonds at different maturities. In order to make the evaluation of the yield curve more reactive to market events, the model incorporates additional exogenous variables related to monetary policy, equity market volatility and macroeco-

nomic fundamentals, such as inflation and output gap. All the measurement equations are driven by the state process and the augmentation allows for improving estimation of the latent spot rate. We propose a Bayesian framework for model inference based on an efficient posterior approximation procedure. The computational efficiency follows from the linearity of the model, which allows for Kalman filtering and smoothing recursions. The paper presents an innovative and interpretable way to estimate the risk premium as a combination of explicit sources of market risk. The model is applied to the US yield curve sampled at a monthly frequency from December 2000 up to May 2024. The augmentation and Bayesian inference allow for generating projections of the yield curve fitting market scenarios connected to the economic cycle. Such a simulation provides great support to decisions of tactical asset allocation since it allows for evaluating the coherence of the portfolio allocation with the predominant macroeconomic regime. Warning divergences should raise questions about the opportunity to revise the asset allocation in a more consistent way. On this, the data-enriched approach shows a greater flexibility than a standard modelling without augmentation in determining the proper macro-trading scenario.

Chapter 3 contributes to literature by proposing a methodology for dynamic modelling and forecasting realized variance vectors based on a 2-state Early Warning Markov Switching VAR (EWMSVAR) model. The approach allows for flexible dependence patterns and investigates spillover effects across volatilities of different asset classes. The application of the model to a global portfolio investing in bonds, equities and currencies provides that spillovers follow a regime-based representation, with state transitions driven by the 3-month US T-Bill rate, whose dynamics is strictly connected to market expectations about future monetary policy decisions. The paper suggests to rearrange impulse functions according to a network-based representation. Such a new perspective aims at underling the degree of interconnection across assets in terms of nodes and edges. Under this setup, the $node_i$ is a measure of autocorrelation affecting individual

volatilities, while the $edge_{ij}$ represents the degree of volatility interconnection between assets i and j. Under the *Turbulence* scenario, shocks on individual volatilities are not expected to remain isolated but, rather, they generate a warning leverage effect on volatility of the entire portfolio. On this, the paper underlines the centrality of the 2-year US rate within the network. It implies that volatility shocks on short-term yields make the portfolio diversification a challenging task. The picture is substantially different under the *Low Volatility* scenario since spillovers connect just few nodes. In this environment, volatilities are mainly driven by individual autocorrelation and the leverage effect on portfolio volatility remains quite limited. Diversification and portfolio hedging appear more feasible under this regime. In terms of volatility forecasting, a stationary bootstrap hypothesis testing on equal forecasting accuracy shows that the model proposed in the paper tends to dominate the competing generalised heterogeneous autoregressive approach. The paper provides a trading strategy for the S&P500 Index following the regime-based representation of volatility spillovers. The trading scheme gains relevant advantages over a systematic long position on the US equity market since it provides a timely hedging strategy which achieves a great mitigation of performance drawdowns along episodes of market selloff.

Bibliography

Abiad, A. G. (2003). Early Warning systems: a survey and a regime-switching approach. *IMF Working Paper*, 3(32).

Agudze, K., Billio, M., Casarin, R., and Ravazzolo, F. (2022a). Markov Switching Panel with Eondogenous Synchronization Effects. *Journal of Econometrics*, 230(2):281–298.

Agudze, K. M., Billio, M., Casarin, R., and Ravazzolo, F. (2022b). Markov switching panel with endogenous synchronization effects. *Journal of Econometrics*, 230:281–298.

Albert, J. and Chib, S. (1993). Bayesian analysis of binary and polychotomous response data. *Journal of the American Statistical Association*, 88:669–679.

Amisano, G. and Fagan, G. (2013). Money growth and inflation: A regime switching approach. *Journal of International Money and Finance*, 33(C):118–145.

Andersen, T., Bollerslev, T., Diebold, F., and Labys, P. (2003). Modeling and forecasting realized volatility. *Econometrica*, 71(2):579–625.

Ang, A. and Bekaert, G. (2002). International asset allocation with regime shifts. *Review of Financial Studies*, 15:1137–1187.

Ang, A. and Bekaert, G. (2004). How regimes affect asset allocation. *Financial Analysts Journal*, 60:86–99.

Barndorff-Nielsen, O., Hansen, P., Lunde, A., and Shephard, N. (2011). Multivariate realised kernels: consistent positive semi-definite estimators of the covariation of equity prices with noise end non-synchronous trading. *Journal of Econometrics*, 162(2):149–169.

Barndorff-Nielsen, O. and Shephard, N. (2004). Econometric analysis of realized covariation: high frequency based covariance, regression and correlation in financial economics. *Econometrica*, 72(3):885–925.

Bauer, O. and Vorkink, K. (2011). Forecasting multivariate realized stock market volatility. *Journal of Econometrics*, 160(1):93–101.

Bekaert, G., Engstrom, E., and Grenadier, S. (1989). Stock and Bond Returns with Moody Investors. *Journal of Empirical Finance*, 17:867–894.

Billio, M. and Casarin, R. (2011). Beta Autoregressive Transition Markov Switching Models for Business Cycle Analysis. *Studies in Nonlinear Dynamics and Econometrics*, 15(4):1–32.

Billio, M., Casarin, R., Ravazzolo, F., and van Dijk, H. (2016a). Iinterconnections between Eurozone and US booms and busts using a Bayesian Panel Markov-Switching VAR models. *Journal of Applied Econometrics*, 31(7):1352–1370.

Billio, M., Casarin, R., Ravazzolo, F., and van Dijk, H. (2016b). Interconnections between Eurozone and US booms and busts using a Bayesian Panel Markov-switching VAR model. *Journal of Applied Econometrics*, 7(31):1352–1370.

Blitz, D. and van Vliet, P. (2008). Global tactical cross-asset allocation: Applying value and momentum across asset classes. *Journal of Portfolio Management*, pages 23–28.

Bollen, N. P. B., Gray, S. F., and Whaley, R. E. (2000). Regime switching in foreign exchange rates: evidence from currency option prices. *Journal of Econometrics*, 94:239–276.

Bollerslev, T. (1986). Generalized Autoregressive Conditional Heteroskedasticity. *Journal of Econometrics*, 31:307–327.

Bollerslev, T., Patton, A., and Quaedvlieg, R. (2018). Modeling and forecasting (un)reliable realized covariances for more reliable financial decisions. *Journal of Econometrics*, 207:71–91.

Bonato, M. (2009). Estimating the degrees of freedom of the realized volatility wishart autoregressive model. *SSRN 1357044*.

Bonato, M., Caporin, M., and Ranaldo, A. (2013). Risk spillovers in international equity portfolios. *Journal of Empirical Finance*, 24:121–137.

Bongaerts, D., Kang, X., and van Dijk, M. (2020). Conditional Volatility Targeting. *Financial Analysts Journal*, 76(4):54–71.

Campbell, J. Y. and Ammer, J. (1993). What Moves the Stock and Bond Markets? A Variance Decomposition for Long-Term Asset Returns. *Journal of Finance*, 48:3–37.

Carlin, B. P. and Chib, S. (1995). Bayesian Model Choice via Markov Chain Monte Carlo. *Journal of the Royal Statistical Society, Series B*, B(57):473–484.

Carvalho, C. M., Massam, H., and West, M. (2007). Simulation of hyper-inverse Wishart distributions in graphical models. *Biometrika*, 94(3):647–659.

Carvalho, C. M. and West, M. (2007). Dynamic matrix-variate graphical models. *Bayesian Analysis*, 2(1):69–97.

Casella, G. and George, E. I. (1992). Explaining the Gibbs sampler. *The American Statistician*, 46:167–174.

Casella, G., R. C. P. and Wells, M. T. (2000). Mixture models, latent variables and partitioned importance sampling. *CREST, INSEE*, 15.

Castelnuovo, E., Greco, L., and Raggi, D. (2014). Policy rules, regime switches, and trend inflation: an empirical investigation for the United States. *Macroeconomic Dynamics*, 18:920–942.

Chan, K., Hameed, A., and Tong, W. (2000). Profitability of Momentum Strategies in the International Equity Markets. *The Journal of Financial and Quantitative Analysis*, 35(2):153–172.

Chib, S. and Greenberg, E. (1995). Hierarchical analysis of SUR models with extensions

to correlated serial errors and time-varying parameter models. *Journal of Econometrics*, 68:339–360.

Chiriac, R. and Voev, V. (2011). Modelling and forecasting multivariate realized volatility. *Journal of Applied Econometrics*, 26(6):922–947.

Christensen, J. H. E. and Rudebusch, G. D. (2012). The Response of Interest Rates to US and UK Quantitative Easing. *Economic Journal*, 122:F385–F414.

Ciccarelli, M. and Rebucci, A. (2003). Bayesian VARs: a survey of the recent literature with an application to the European Monetary System. *IMF Working Paper*, pages 2–44.

Clarida, R., Galì, J., and Gertler, M. (2000). Monetary Policy Rules and Macroeconomic Stability: Evidence and Some Theory. *Quarterly Journal of Economics*, 115:147–180.

Commandeur, J. F. and Koopman, S. J. (2007). *An Introduction to State Space Time Series Analysis*. Oxford University Press.

Corsi, F. (2009). A simple approximate long-memory model of realized volatility. *Journal of Financial Econometrics*, 7(2):174–196.

Dai, Q. and Singleton, K. J. (2000). Specification Analysis of Affine Term Structure Models. *Journal of Finance*, 55:1943–1978.

Dempster, A. P., Laird, N. M., and Rubin, D. B. (1977). Maximum Likelihood from Incomplete Data via the EM Algorithm. *Journal of the Royal Statistical Society, Series B*, 39:1–38.

Dielbold, F. X, L. J. H. and Weinbach, G. (1994). *Nonstationary Time Series Analysis and Cointegration*. Oxford University Press.

Dothan, U. L. (1978). On the Term Structure of Interest Rates. *Journal of Financial Economics*, 6:59–69.

Duan, J. and Simonato, J. (1999). Estimating and Testing Exponential-Affine Term Struc-

ture Models by Kalman Filter. *Review of Quantitative Finance and Accounting*, 13:111–135.

Duffee, G. R. (2002). Term premia and interest rate forecasts in affine models. *The Journal of Finance*, 57(1):405–443.

Duffee, G. R. and Stanton, R. H. (2012). Estimation of dynamic term structure models. *The Quarterly Journal of Finance*, 2(02):1250008.

Duffie, D. and Kan, R. (1996). A Yield-Factor Model of Interest Rates. *Mathematical Finance*, 6:379–406.

Elerian, O., Chib, S., and Shephard, N. (2001). Likelihood inference for discretely observed nonlinear diffusions. *Econometrica*, 69(4):959–993.

Engle, R. (2002). Dynamic conditional correlation: a simple class of multivartiate generalized autoregressive conditional heteroskedasticity models. *Journal of Business and Economic Statistics*, 20:339–350.

Engle, R. and Kroner, K. (1995). Multivariate simulataneous generalized arch. *Econometric Theory*, 11:122–150.

Eraker, B. (2001). MCMC analysis of diffusion models with application to finance. *Journal of Business & Economic Statistics*, 19(2):177–191.

Fillardo, A. J. (2004). *Businnes Cycle Phases and Their Transitions*. Springer-Verlag, New Yorks.

Frühwirth-Schnatter, S. (2006). *Finite mixture and Markov switching models*. Springer Science & Business Media.

Frühwirth-Schnatter, S. and Geyer, A. L. J. (1998). Bayesian estimation of econometric multifactor Cox Ingersoll Ross models of the term structure of interest rates via MCMC

methods. *Working Paper, Department of Statistics, Vienna University of Economics and Business Administration*.

Garcia, R. and Perron, P. (1996). An Analysis of the Real Interest Rate under Regime Shifts. *The Review of Economics and Statistics*, 1(78):111–125.

Gelfand, A. E. and Smith, A. F. M. (1990). Sampling-based approaches to calculating marginal densities. *Journal of the American Statistical Association*, 85:398–409.

Geman, S. and Geman, D. (1984). Stochastic relaxation, Gibbs distributions and the Bayesian restoration of images. *IEEE Transactions on Pattern Analysis and Machine Intelligence*, 6:721–740.

Glosten, L. R., Jagannathan, R., and Runkle, D. E. (1993). On the Relation between Expected Value and the Nominal Excess Return on Stocks. *Journal of Finance*, 48:1779–1801.

Gouriéroux, C., Jasiak, J., and Sufana, R. (2009). The Wishart autoregressive process of multivariate stochastic volatility. *Journal of Econometrics*, 150(2):167–181.

Guidolin, M. and Timmermann, A. (2006). An econometric model for nonlinear dynamics in the joint distribution of stock and bond retunrs. *Journal of Applied Econometrics*, 21:1–22.

Gürkaynak, R. S., Sack, B. T., and Swanson, E. P. (2007). Market-Based Measures of Monetary Policy Expectations. *Journal of Business & Economic Statistics*, 25:425–436.

Hall, A. D., Anderson, H. M., and Granger, C. W. J. (1992). A Cointegration Analysis of Treasury Bill Yields. *Review of Economics and Statistics*, 74:116–126.

Hamilton, J. D. (1987). Rational-Expectations Econometric Analysis of Change in Regime. An Investigation of the Term Structure of Interest Rates. *Journal of Economic Dynamics and Controll*, 12:385–423.

Hamilton, J. D. (1989). A New Approach to the Economic Analysis of Nonstationarity Time Series and the Business. *Econometrica*, 57:357–384.

Hamilton, J. D. (1994). *Time Series Analysis*. Princeton University Press.

Harrison, J. and West, M. (1999). *Bayesian forecasting & dynamic models*. Springer.

Hastings, W. K. (1970). Monte Carlo sampling methods using Markov chains and their application. *Biometrika*, 57:97–109.

Hull, J. (2021). *Options, Futures and other Derivatives*. Pearson.

Hördahl, P., Tristani, O., and Vestin, D. (2006). A joint econometric model of macroeconomic and term-structure dynamics. *Journal of Econometrics*, 131:405–444.

Jin, X. and Maheu, J. (2013). Modelling realized covariances and returns. *Journal of Financial Econometrics*, 11(2):359–379.

Jones, C. (1998). Bayesian Estimation of Continuous-Time Finance Models. *Working Paper, Simon School of Business*.

Judd, J. and Rudebush, G. (1999). Taylor's Rules and the Fed: 1970-1997. *Economic Review, Federal Reserve Bank of San Francisco*, 3:3–16.

Kadiyala, K. R. and Karlsson, S. (1997). Numerical methods for estimation and inference in Bayesian VAR-Models. *Journal of Applied Econometrics*, 12:99–132.

Kastner, G. (2019). Sparse bayesian time-varying covariance estimation in many dimensions. *Journal of Econometrics*, 210:98–115.

Kim, C.-J. (1994). Dynamic Linear Models with Markov-switching. *Journal of Econometrics*, 60:1–22.

Kim, C. J. and Nelson, C. R. (1999). *State-Space Models with Regime Switching: Classical and Gibbs-Sampling Approaches with Application*. MIT Press: Cambridge MA.

Kim, C.-J., Piger, J., and Startz, R. (2008). Estimation of Markov regime-switching regression model with endogenous switching. *Journal of Econometrics*, 2(143):263–273.

Kim, H. D. and Wright, J. H. (2005). An Arbitrage-Free Three-Factor Term Structure Model and the Recent Behavior of Long-Term Yields and Distant-Horizon Forward Rates. *Federal Reserve Board, Washinton D.C.*, 33.

Kloeden, P. E. and Platen, E. (2018). Numerical methods for stochastic differential equations. In *Nonlinear dynamics and stochastic mechanics*, pages 437–461. CRC Press.

Koop, G. (2003). *Bayesian Econometrics*. J. Wiley, New York.

Kozicki, S. (1999). How Useful are Taylor Rules for Monetary Policy? *Economic Review, Federal Reserve Bank of Kansas City*, Second Quarter:5–33.

Kuttner, S. P. (2001). Moneatery Policy Surprise and Interest Rates: Evidence from Fed Funds Futures Market. *Journal of Monetary Economics*, 47:523–544.

Lamoureux, C. G. and Witte, M. D. (2002). Empirical analysis of the yield curve: the information in the data viewed through the window of Cox, Ingersoll and Ross. *Journal of Finance*, LVII:1479–1520.

Lee, W. (2000). *Advanced Theory and Methodology of Tactical Asset Allocation*. Wiley.

Lettau, M. and Watcher, J. (2011). The Term Structure of Equity and Interest Rates. *Journal of Financial Economics*, 101:90–113.

Litterman, R. B. (1986). Forecasting with Bayesian Vector Autoregressions-Five Years of Experience. *Journal of Business and Economic Statistics*, 4:25–38.

Lloyd, S. P. (2020). Estimating Nominal Interest Rates Expectations: Overnight Indexed Swaps and the Term Structure. *Journal of Banking & Finance*, 119:105915.

Moreira, A. and Muir, T. (2017). Volatility-managed portfolios. *The Journal of Finance*, 72:1611–1644.

Philips, T. K., R, G., and Capaldi, R. E. (1996). Tactical Asset Allocation: 1977-1994. *Journal of Portfolio Management*, 23(1):57–64.

Piazzesi, M. and Swanson, E. T. (2008). Futures prices as risk-adjusted forecasts of monetary policy. *Journal of Monetary Economics*, 55:677–691.

Polson, N. G., Muller, J. R., and Muller, P. (2002). Affine state-dependent variance models. *Institute of Statistics and Decision Sciences, Duke University*.

Rasmussen, M. (2003). *Strategic and Tactical Asset Allocation in Quantitative Portfolio Optimisation, Asset Allocation and Risk Management*. Finance and Capital Markets.

Robert, C. P. (2007). *The Bayesian Choice*. Springer.

Robert, C. P. and Casella, G. (2004). *Monte Carlo Statistical Methods (Second Edition)*. University of Chicago.

Robert, C. P., Celeux, G., and Dielbold, F. X. (1993). Bayesian estimation of hidden Markov models: A stochastic implementation. *Statistics and Probability Letters*, 16:77–83.

Rudebusch, G. D. and Wu, T. (2008). A Macro-Finance Model of the Term Structure, Monetary Policy and the Economy. *The Economic Journal*, 118:906–926.

Sanford, A. D. and Martin, G. M. (2005). Simulation-based Bayesian estimation of an affine term structure model. *Computational Statistics & Data Analysis*, 49(2):527–554.

Taylor, J. B. (1999). *Monetery Policy Rules*. Chicago University Press.

Turner, C. M., S. R. and Nelson, C. R. (1989). A Markov model of heteroskedasticity, risk and learning in the stock market. *Journal of Financial Economics*, 1(25):3–22.

Vasicek, O. (1977). An Equilibrium Characterization of the Term Structure. *Journal of Financial Economics*, 5:177–188.

Voev, V. (2007). Dynamic modelling of large-dimensional covariance matrices. *High Frequency Financial Econometrics*, pages 293–312.

Wang, H. and West, M. (2009). Bayesian analysis of matrix normal graphical models. *Biometrika*, 96(4):821–834.

Woodford, M. (2012). Methods of Policy Accomodation at the Interest-Rate Lower Bound. *Economic Policy Symposium - Jackson Hole*, 1:185–288.

Zellner, A. (1971). *An Introduction to Bayesian Inference in Econometrics*. J. Wiley, New York.

Zhang, L., Mykland, P. A., and Ait-Sahalia, Y. (2005). A tale of two time scales: determining integrated volatility with noisy high-frequency data. *Journal of the American Statistical Association*, 100:1394–1411.

Zhou, X., Nakajima, J., and West, M. (2014). Bayesian forecasting and portfolio decisions using dynamic dependent sparse factor models. *International Journal of Forecasting*, 30:963–980.